Multi-Dimensional Coupling Mapping to Evaluate the Coupling Factor of Inductive Charging Coils For Electric Vehicles

By

Michael David Abbott

An innovation report submitted in partial fulfilment of requirements for the degree of:

Doctor of Engineering (EngD) International

August 2018

ABSTRACT

Wireless Power Transfer (WPT) technologies have been demonstrated by numerous research groups worldwide. Prototypes, both at small scale, and full sized systems, have been made. Some of these are in active service today, mainly in bus projects such as KAIST's OLEV(Suh, 2015) and Milton Keynes IPT(Bowdler, 2014). Since 2012 the technology has been promised to customers in 1-2 years, however, currently (2018), no WPT systems are available on the market in the UK. So why have WPT technologies stopped just short of mainstream adoption?

Compatibility between the road (GA) and vehicle (VA) parts of a WPT system is has been identified as a barrier to this mainstream adoption. One parameter of interest is the suitability of the magnetic field between the GA-VA, a requirement termed magnetic compatibility. The work of Lin et al.(Lin, Covic and Boys, 2015), has identified that certain GA-VA combinations are intrinsically not compatible.

The work in this document has developed criteria for assessing magnetic compatibility at the early stages of the WPT development process. Coupling factor between the GA and VA is considered the critical criterion for compatibility. This value must exceed a defined minimum across the operational positional range of the WPT system. The value accounts for both the geometry and materials used in the GA/VA as well as some of the field interaction between the GA and VA. Using theory and simulations, it has been shown that coupling factor is independent of the scale of the system.

A set of both finite element (FE) and experimental (EXP) methods have been developed to assess GA-VA magnetic compatibility for small-scale coil prototypes. These are capable of high-resolution measurement in three dimensions, termed Multi-Dimensional Coupling Mapping (MDCM). This method can be used to characterise new GA-VA pairings, consider unusual coupling profiles and perform assessment for the sizing of GA and VA coils to meet alignment tolerances. The coil operational modes of multi-coil GA/VA designs can also be considered.

The draft J2954 standard from the SAE incorporates tests of compatibility with complete GA and VA parts. By using the MDCM method, compliance of a coil design with the J2954 standard can be considered. This assessment can be performed at the early stages of coil development using small scale prototypes without the need for the GA/VA coil electronics. Incorporating MDCM methods into the development process for new WPT designs can standardise assessment and reduce the risk of late stage compliance failure.

ACKNOWLEDGEMENTS

Firstly, I would like to thank my family for supporting me throughout this process. My wife, Teri, has been brilliant at guiding and encouraging me along this journey. Together, we have also welcomed two beautiful children, Rowan and Daphne, who give us so much happiness and a welcome realignment of the work-life balance. I would also like to thank my parents, grandparents and sister who have also helped guide and support me throughout.

Secondly, I must say thank you to my fellow doctoral candidates. Our "Team L.U.N.C.H" discussions, grand ideas, and putting the world-to-rights, made the workplace a fun place to be. I am sure we will all keep in touch, wherever we all end up in the engineering sector.

Next, I must say thank you to Dr Alex Ridge, and Andy Moore who helped me so much in my work. Indeed, without you both my work would have been close to impossible. The help you gave me to source equipment and resources as well as the guidance you provided me in discussions has been crucial in the success of my work.

I would also like to thank a range of WMG and MSU staff who have helped me in both resourcing and fulfilment of requirements of the programme. Dr Nick Mallinson, Professor Dave Greenwood, Dr Andrew McGordon, Dr Andreas Hoffrichter, Nick Little, Professor Stewart Birrell, Gunwant Dhadyalla and many other people who have helped me on my way.

Finally, a thank you to my supervisors who gave me a high degree of independence and broad scope that allowed me to explore freely.

CONTENTS

LIST OF ABBREVIATIONS

3D	Three dimensional. Position existing as a combination of X, Y, and Z.
ADC	Analog to Digital Converter. Used in Oscilloscopes for sampling analogue voltage signals and converting them to digital signals for display on the oscilloscope.
AR	Dr Alex Ridge of the WMG Power Electronics Group, a collaborator on some aspects of this work
BEV	Battery Electric Vehicle. A car which is solely powered from an electric battery. Such as the Nissan Leaf or Tesla Vehicles.
BPP	Bi-Polar Pad, a coil design consisting of two coils with a slight overlap between them
DD	Double-D, a coil design consisting of two coils joined together side by side.
DDQ(P)	Double-D with Quadrature, a modified version of the DD coil with an additional coil above the DD coils.
EMC	Electromagnetic Compliance. Rules and regulations governing electronic systems to ensure they do not produce fields which can interfere with other nearby electronic devices.
EMF	Electromotive Force. This is a voltage generated in a wire when placed in a time-varying magnetic field
FE/FEA	Finite Element (Analysis), computer simulations of the magnetic properties of the coils
EXP	Experimental analysis, direct or calculated results from the coils
GA	Ground Assembly, the part of the WPT that is fixed to the ground/road including all the electronics and control systems
GA coils	Just the coils, ferrite and shielding used inside the GA
HVAC	Heating, Ventilation and Air Conditioning. The system used to control the cabin temperature of the vehicle.
(SAE) J2954	Surface Vehicle Information Report by the SAE international for static wireless charging of light duty vehicles (SAE International, 2017)
KAIST	Korea Advanced Institute of Science and Technology. A research group developing WPT systems (see section 2.3.2)
LC	Inductor (L) Capacitor (C). A type of circuit using these two components, energy resonates between the components.
MDCM	Multi-Dimension Coupling Mapping. A process developed in this work to measure the coupling factor of GA-VA coil pairs (see Chapters 4 for development and 5 for

	application)
OEM/OEMs	Original Equipment Manufacturers. In this scope it refers to automotive manufacturers such as Ford, Jaguar Land Rover, BMW, VW, etc.
PF	Power Factor
RMS	Root mean squared. Averaging method used for measurement of the amplitude of signals with alternating sign
TS	Test Stand, the name given to several reference designs provided in J2954 to ensure the interoperability between different VAs and GAs
VA	Vehicle Assembly, the part of the WPT that is fixed to the vehicle including all the electronics and control systems
VA coils	Just the coils, ferrite and shielding used inside the VA
WMG	Warwick Manufacturing Group, a department of the University of Warwick
WPT	Wireless Power Transfer
X	The direction of travel corresponding to forward and backward from a vehicle's driving position, units are mm
Y	The direction of travel corresponding to left and right from a vehicle's driving position, units are mm
Z	The direction of travel corresponding to up and down from a vehicle's driving position, units are mm

LIST OF FIGURES

LIST OF TABLES

NOTE ON TERMINOLOGY

Wireless charging, Wireless Power Transfer (WPT) and Inductive Power Transfer (IPT) are terms used interchangeably in this work. Strictly IPT is a type of WPT technology. Other WPT technologies exist, Suh (Suh, 2015) lists acoustic, light and capacitive as some alternatives. Suh also considers that only inductive charging can provide both the power level (>500W) and efficiencies (>70%) needed to power vehicles. In more recent work, capacitive power transfer (CPT) has been demonstrated as feasible, but requiring a much smaller gap than IPT (sub millimetre vs 100+ mm) (Dai and Ludois, 2015). Although CPT is an emerging WPT technology, it is still generally accepted that the WPT term still refers to IPT in most published work.

Magnetic resonance coupling (MRC) is also a term found in the literature. It was used initially to differentiate IPT circuit designs that used a capacitor to form a resonance LC circuit with the coils from those that did not. As all proposed designs for WPT now incorporate some sort of resonance circuit, the term is rarely used in recent work.

Coupling factor and coupling coefficient are two terms used in literature for the same parameter. Coupling factor is used here.

1 INTRODUCTION

There is a drive in industry to reduce the environmental impact of all areas of transportation. Of focus has been the reduction of CO_2 tailpipe output from automobiles (Mock, 2014). There have been numerous approaches to reaching this goal including; the downsizing of engine capacity (Ford UK, 2018), clean diesel technologies (Patrick McGee, 2018), and light weighting (Automotive Council UK and Advanced Propulsion Centre UK, 2017). Transportation has an impact also on air quality, and the reduction of other emissions from tailpipes has been the focus of more recent engine standards such as EU6 (Degraeuwe *et al.*, 2017). One method that can reduce and potentially eliminate tailpipe emissions, is electrification (Brook Lyndhurst Ltd., 2015).

The ultimate electrification goal, is a battery electric vehicle (BEV). These vehicles have a fully electric drivetrain and as such have no combustion engine, so the tailpipe emissions are zero. Unfortunately, these vehicles currently have a few compromises (Brook Lyndhurst Ltd., 2015). Some of these compromises are:

- BEVs typically have a limited range, only travelling 70-250 miles on a full charge, vs 300-600 miles for conventional combustion engine vehicles.
- Once depleted, BEVs must be recharged either on domestic supplies (taking multiple hours) or at rapid charging stations (taking 30-90 minutes).
    - Rapid charging stations are less readily available than fuel pumps/fuel stations in most regions as of 2018.
- The initial purchase cost of BEVs is considerably more than comparable combustion engine vehicles, mostly due to the battery costs.
    - Arguably the total cost of ownership is lower for many users, however, the “sticker price” can deter potential customers.

Plug-in or cabled charging of both BEVs and other plug-in hybrids also presents issues:

- Cables are often used outside, meaning they can get wet and dirty.
- Cables can be heavy and cumbersome, particularly an issue for disabled users.
- Cables can be difficult to arrange in a way that will reach the ports whilst avoiding a trip hazard.
- Cables, if not locked in place, can be unplugged either accidentally or with malicious intent and the charge points themselves have been prone to vandalism.

- Charge port flaps and cables locks can also be difficult to use in cold climates, stories of charge flaps freezing shut and difficulty in using charge point screens with gloves have been reported (Plugless Power, 2017).

A solution to these issues has been proposed, it is called wireless charging. Instead of plugging a vehicle in, it is simply parked over a wireless charging enabled bay. The chargers could be in both domestic and commercial environments. Power is then delivered to the vehicle through a pad in the floor and a pad on the underside of the vehicle. This requires minimal additional effort from the user, needing only accurate parking positioning (Suh, 2015). The process works by magnetic induction and can provide power at the same levels as cabled charging, with comparable efficiencies (SAE International, 2017). This application is called static Wireless Power Transfer (WPT).

Other opportunities to apply WPT have also been discussed (Suh, 2015). These are opportunistic WPT, when power is transferred to an idling vehicle, at possibly a taxi rank or a bus stop. The other is dynamic WPT, when a vehicle is powered as it travels along the roadway. Dynamic WPT offers the exciting possibility of unlimited range for BEVs, if the roadway can provide more power than is needed for motion.

Independently of the application, there are typically two sides that make up the whole WPT system. These are the Ground Assembly (GA) and the Vehicle Assembly (VA), corresponding to the parts that sit in the road and on the vehicle respectively. An “assembly” includes all the parts of the WPT system, such as coil windings, ferrite cores, shielding and all the control and power conversion electronics. It is clear, therefore, that ensuring GAs and VAs are compatible with each other in all cases, across different applications and from different suppliers is of paramount importance (FABRIC Consortium, 2015).

Many parameters must be considered for the GA and VA to be compatible (SAE International, 2017). Some of these parameters include the communication link between the coils, frequency of operation, power ratings, control systems, and the electromagnetic field between the coils. If the GA and VA are not compatible across all areas, then issues with power transfer will arise. At best this could mean the efficiency of power transfer is lower, or the power level of the system is compromised. The more likely case, with the current systems, is that no power will be transferred at all (FABRIC Consortium, 2015).

1.1 Scope

The topic of WPT for electric vehicles can be broadly categorised into three key areas:

1. **Wireless System Development:** Encompassing all the components inside a WPT system from the power supplying circuitry to the shape of the coils.
2. **Integration:** This encompasses all the things that are needed to support a WPT system such as the grid power connection, other infrastructure needs as well as payment mechanisms.
3. **Technology Acceptance:** These are the human issues with the technology such as acceptance, business models, and economics.

This work has focused on the area of wireless system development. Within this area, it has developed methods that help to ensure new WPT systems are tested for compatibility at the earliest possible opportunity. By design, the testing performed here is in isolation from power supplies, loads, control systems, and communication methods. This work focuses on investigating the coil assemblies (copper wire, ferrite, shielding etc.) and if the magnetic link between the assembly on the ground and the one on the vehicle is compatible over the range of positions it is expected to function.

As the focus is on how the coupling between GA-VA pairs changes with variations in alignment, many areas of interest are out of scope for this work. This includes detailed consideration of material properties, leakage fields, and thermal issues. Coupling does provide an upper maximum efficiency possible for the overall WPT system, as will be seen in section 3.2.4, and therefore is considered in-scope. It must be noted, however, that the efficiency of the electronics, and the impact of circuit topologies will not be considered in detail.

1.2 Research Questions & Hypotheses

The electromagnetic field between the coils is the heart of wireless power transfer. Without a suitable electromagnetic field link between the GA and VA coils, WPT is not possible. This field, which is typically generated by the GA coil, must be intersected by the VA coil to excite the current needed to provide power to the vehicle. It is also possible to run this process in reverse, with the VA generating the field, for vehicle-to-grid applications (Mohamed and Mohammed, 2018).

Quantifying the electromagnetic link between the GA-VA, is a challenge. The field is affected by the presence of any metallic materials, including the GA and VA themselves. Therefore, if a GA is operating with different VAs then the fields will change. The fields will also change as the relative positions of the coils change. Many methods have been employed in the published work to quantify and present information pertaining to this electromagnetic link. Magnetic field analysis has been shown analytically and in Finite Element (FE) simulations (Joy, Dalal and Kumar, 2014). Experimental (EXP) measurements have been made of flux leakage and power outputs of coils (Lin, Covic and Boys, 2016). Normalised power output of the complete system has also been considered in some work as an

indirect way to assess the link suitability (Su Y Choi *et al.*, 2015). As different groups have assessed the electromagnetic link using different methods, it is not possible to directly compare the coil designs being studied from these published records.

One variable that has been used by a few groups arises from consideration of the GA-VA pair as a conventional transformer. In transformer theory, the ratio of mutual inductance between the GA-VA to the self-inductance of the each of the VA and GA, is an important variable. This is, in effect, the voltage available from the VA for every Ampere of current put into to the GA. The ratio is called the **coupling factor**, and is given the symbol: k.

The coupling factor variable appears to lump together all consideration of magnetic field and the electromagnetic link between the GA-VA. This leads to the first hypothesis of this work:

H1: The coupling factor can be used as a key variable to evaluate if the fields between the GA/VA are magnetically compatible.

However, many factors affect inductance values, including the geometry of the coils, the use of metallic materials like ferrite or aluminium, the polarity of the coils, and the relative position of the VA to the GA. This implies there is a range of inductances and therefore coupling factor for any GA-VA pairing. There does not, however, seem to be any standardised coupling range and researchers are free to choose their own coupling range requirements. Therefore, the following research question arises:

Q1: What is the typical range of coupling factor and what happens outside this range to the operation of the WPT system?

Measuring the coupling factor for a GA-VA combinations is a process that has been addressed in numerous works. Three techniques are commonly applied, these are analytical, simulations and experimental (Joy, Dalal and Kumar, 2014). Some of these works have used small scale coil prototypes, others have used full sized coils. Although it is implied in some small scale work, it is not directly stated and confirmed, why small scale prototypes can be used. This leads to the second hypothesis:

H2: Coupling factor is independent of the scale of the WPT system.

As coupling factor is affected by the relative position of the VA to the GA, the factor must be measured across the expected operational range of positions. Considering operation on a vehicle, three dimensions of linear range exist (vertical – Z, longitudinal – X, and lateral – Y), combined with these, three dimensions of rotation also exist (roll, pitch, and yaw). This means in total, six degrees of freedom can affect the coupling between a GA-VA pair.

Published work has been limited in the assessment over these degrees of freedom. Typically referred to as misalignment studies, WPT systems are considered over one degree of freedom at a time (Prasanth and Bauer, 2013; Joy, Dalal and Kumar, 2014; Su Y Choi *et al.*, 2015). One published work considered two dimensions at once (Lin, Covic and Boys, 2015). In this study, however, comments indicated that experimentally measuring values is unfeasible. The author has been unable to find work that has considered coupling over more degrees of freedom.

Time and technology has moved on since these works were published, and it is now the author's opinion that three dimensional analysis of coupling factor is possible in both simulation and experimental work. Not only that, combined with the hypotheses H1, and H2, small scale systems and innovative methods can be applied to develop high resolution mapping of the coupling. This leads to the third hypothesis of this work:

H3: Multi-dimensional mapping of coupling factor at a high resolution is feasible for both FE and EXP studies.

So why would this be valuable? And why should it be done? Four reasons (shown in *italics*) for creating high resolution multi-dimensional maps of coupling factor have been discussed in this work:

Characterising a new GA-VA coil pairing - The electronics must be designed for specific ranges of coupling and inductance. Outside this range efficiencies and power output can drop (Aldhaher, Luk and Whidborne, 2014; Lin, Covic and Boys, 2015). Therefore, information about how the coupling changes over the range of positions of a GA-VA pair can be fed into the design of the electronics.

Characterise an unusual coupling factor profile – The current low resolution one-dimensional analysis used in the published work could both miss coupling profile features and ignore the way the profile changes in regions of combined dimensional misalignment (such as at the extreme of both lateral and longitudinal offset). This is because published analysis typically only considers single dimensional offset at once (with the other dimensions at zero offset) for less than 10 samples per dimension (see section 4.1.1).

Several different GA/VA coil designs have been proposed by WPT developers over the last decade. From simple circular coils (Tejeda *et al.*, 2016), to square coils (Joy, Dalal and Kumar, 2014), Double-D coils (Budhia *et al.*, 2013), Double-D with Quadrature coils (Zhao and Mieee, 2017), tri-polar coils (Kim *et al.*, 2014), and bi-polar coils (Lin, Covic and Boys, 2015), to name a few. Designs also vary in geometric size of the coils themselves, the ferrite core geometry and material type as well as different shielding employed (Campi, Cruciani and Feliziani, 2014). Also, for designs consisting of multiple coils there is the operational mode of the coils to consider. Selecting the optimum coil design and

operational mode for a GA-VA pair is therefore a significant challenge for a developer of WPT systems. The mapping of coupling factor could enable developers *to find the operational position range of a GA-VA pair* as well as *to find the size needed for a GA-VA to meet a specific operation range.* Both of these insights can then be used to optimise the design.

This leads up to the next research question:

Q2: How can the optimal GA-VA design/operational mode be identified for a particular operational region?

During the process of this work, a draft standard relating to WPT technologies has been released. SAE J2954 introduces some test methods to assess the compatibility of GA/VA coils (SAE International, 2017). The target of this assessment is to ensure the WPT system efficiency and power factor remains above defined limits within the standard. These limits must be met across the defined operational range.

Not only must this be satisfied with the new GA/VA designs being tested, it must also be satisfied when the GA or VA is working with several "Test Stand" reference designs provided. This method, therefore needs not only the full-size versions of any new GA/VA coils but also all their electronics. They also need to be tested with multiple TS GA/VA coils and all their reference electronics.

Leveraging the results from the earlier questions and hypotheses. The opportunity to perform early stage assessment of compliance with J2954 arises. This leads to the following research questions:

Q3: How can multi-dimensional coupling mapping of small scale prototype GA-VA coil pairs, be used to consider compliance with standards?

Q4: How can multi-dimensional coupling mapping be used to consider the operation of a new coil design (GA or VA) with reference coil designs (such as the TS coils in SAE J2954)?

Q5: How can multi-dimensional coupling mapping be integrated into the WPT development process for a new coil design?

For industry, these coupling mapping methods could be a valuable tool to avoid the issue of failing the J2954 compliance tests. J2954 tests must be performed at the final stages of development with the full sized coils and all their electronics. By integrating J2954 compatible compliance tests at the early stages of the design process, the risk of failing the actual compliance tests with the full sized coils should be reduced.

1.3 APPROACH

A literature survey of WPT is covered in Chapter 1.4. This covers the history, fundamentals of operation, and the state of the art of the technology. This survey highlights that development appears to have stalled just short of mainstream adoption. Developers have been saying since 2012 that the technology will be available to consumers in the next 1-2 years (Qualcomm, 2012), however, as of 2018 this is not the case. Barriers to this mainstream adoption are then considered, the most significant barriers are identified in section 2.4. The barrier of magnetic compatibility of coils, particularly coils developed by different research groups, is identified as an area of interest for this work.

Magnetic compatibility of coils is reviewed in Chapter 3. This review covers the significant literature that has considered coil-to-coil compatibility and interoperability. Following this, the requirements for coils to be compatible, the ways that this can be assessed, and how to manage the operation of multi-coil designs is summarized. The first key finding in this chapter are that the coupling factor can be used to indicate if a coil pair are magnetically compatible. The second finding is that the coupling factor itself, is independent of the scale of the system.

Chapter 4 introduces the development of simulations and experimental testing tools to assess magnetic compatibility. This method is named Multi-Dimensional Coupling Mapping (MDCM). Utilising the prior knowledge that coupling factor is scale independent, a small-scale testing rig has been developed to test arbitrary coil designs. High resolution mapping of coupling factor over a range of positions in three-dimensional space has been demonstrated. To ensure confidence in these results, simulations and experimental results have been validated against each other.

Chapter 5 demonstrates how the MDCM method can be used to consider magnetic compatibility for compliance with the SAE J2954 standard. J2954's test methods are evaluated and suitable compatibility criteria are identified. A study is then performed on a DD coil design, which can have its coils independently controlled. Using both the compatibility criteria and the desired operational range, the size the coils needed to satisfy J2954 can be inferred. The optimal mode to operate the coils for both normal operation as well as operation with the other TS designs is also considered. The final section of this chapter considers how the method could be applied to the development of new WPT designs to reduce the risk of late stage compliance issues.

Chapter 6 summarises and discusses the value of the work and how the understanding of WPT technologies have been developed. It discusses how the ideas and knowledge have been exploited to benefit industry and what the next steps should be for this work.

Chapter 7 concludes the document.

1.4 The Engineering Doctorate Portfolio

During the Engineering Doctorate process, six "Submission" documents have been produced and compiled into the overall doctoral portfolio. Some of these submissions loosely correspond to the chapters of this document, and their outcomes are documented here. Others developed skills or demonstrated fulfilment of requirements of the doctorate. These documents are not in the public domain, but copies of Submissions #1 to #5 can be requested from the author[1]. Submission #6 has restrictions on distribution for confidentiality reasons. Although this document has references to this prior work, it can be read in isolation from them.

Submission #1 is not directly related to the scope of the doctorate. An electric vehicle (Nissan Leaf) was used as a platform to collect data from. This involved reverse engineering the signals sent on the CAN bus of the vehicle and developing a telematics platform. The thoughts at the time were that it could be used for data collection related to wireless charging technologies, but this did not happen. Retrospectively, this submission can be considered a skills building exercise as it does not contribute to this innovation report.

Submission #2 aligns with Chapter 1.4. This submission is a survey of the technology, the state of the art and the barriers to adoption. It identified the major groups actively working on WPT technologies as well as government research programmes. This chapter presents some updates to this work and summarises the barriers to adoption that were found.

Submission #3 presents a literature review of work that considers magnetic compatibility. Although at the time, the focus was on dynamic WPT systems, it still presented a review of published work on static WPT compatibility. Chapter 3 updates and summarizes this work.

Submission #4 mostly concerns the development of both the Finite Element (FE) simulations and the experimental (EXP) test rig. It discusses the development process and how various challenges were overcome. This is covered in Chapter 4.

Submission #5 concerns the use of the test rig to assess the compliance of a DD coil design to the SAE J2954 standard. It discusses improvements to the rig, the iterative process of validation between FE and EXP results and how these results can impact the development process for a WPT designer. This work is summarized in Chapter 5.

[1] Correspondence address: michael@abbottastro.com

Submission #6 is another independent piece of work that considers the feasibility of wireless charging in light rail applications. This work was developed in collaboration with researchers from Michigan State University as well as members of the WMG HVM Catapult. Due to the independent nature of this work it is not considered in this innovation report.

The portfolio is summarised in Figure 1.1.

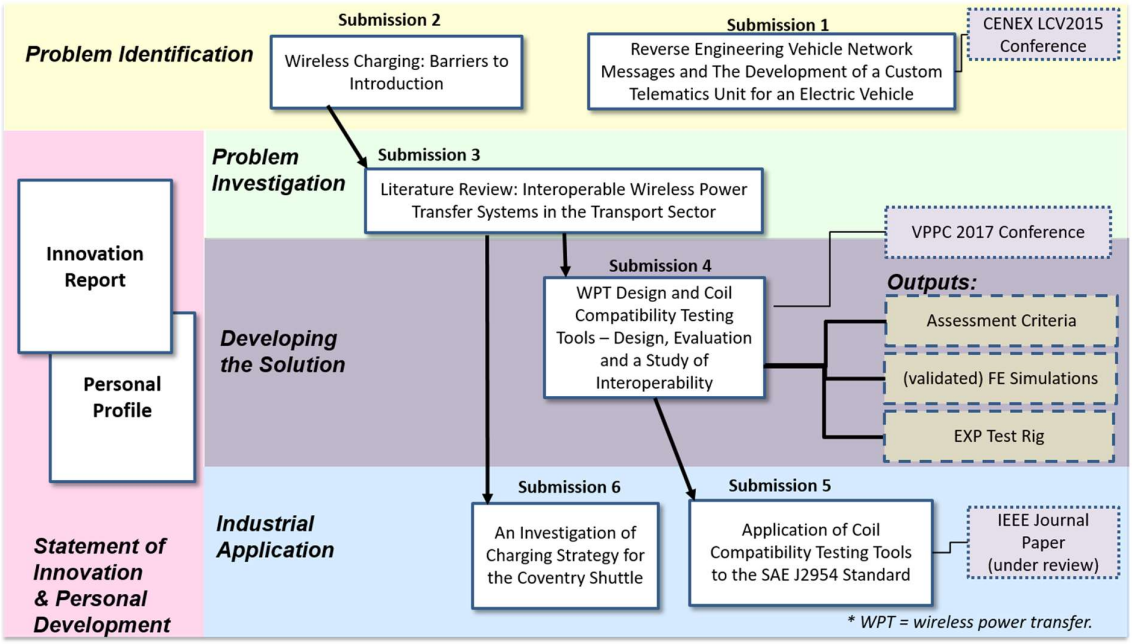

Figure 1.1: Portfolio summary chart. Reports and submissions shown in solid boxes. Published outputs are shown in dotted boxes and developed solutions are shown in dashed boxes.

2 LITERATURE SURVEY FOR WPT TECHNOLOGIES

In this chapter, the history and current state of WPT technologies is considered, and the barriers to mainstream adoption are identified. This chapter closely links to Submission #2 in the portfolio.

This chapter develops background and motivation for the focus of the work. It surveys history and the state of the art of WPT development as of the end of August in 2018.

2.1 HISTORY

Wireless Power Transfer (WPT) is not a new idea, the fundamentals behind it were developed in the 1900s under Nikola Tesla (Suh, 2015). He developed several demonstrators where he powered devices such as light bulbs from an inductive charging coil, later named a Tesla coil. His great vision was a tower to transmit power to a town wirelessly, and he built a prototype at Wardenclyffe in between 1898 and 1901 (Miller *et al.*, 2015). Unfortunately, this experiment failed due to both Tesla's financial issues, as well as the limited understanding of Electromagnetic (EM) waves at the time.

WPT for transport applications were not picked up again until the 1970s when the Lawrence Berkeley National Laboratory and later, the Californian PATH research team, developed a system to wirelessly charge an electric bus (Su Y. Choi *et al.*, 2015). This work was reasonably successful, although a few issues were raised. This was that the overall efficiency of the system was low (circa 60%), the cost was too high (double the estimated cost), the coils had to remain in very close proximity (less than 3 inches, 76 mm), and there were issues with the noise generated by the both the power electronics and vibration from the resonating coils (Bolg*er et al*., 1978; California PATH Program, 1994).

The 1990s saw a resurgence of WPT technology development. The University of Auckland's power electronics department developed a few demonstrators and prototypes for WPT for vehicles and for the manufacturing of computer displays (Boys and Covic, 2015). They spun out the automotive research into Halo IPT which was then acquired by Qualcomm to become Qualcomm Halo.

In the late 2000s, early 2010s, the Korean Institute of Science and Technology (KAIST) rapidly developed what it calls the On-Line Electric Vehicle (OLEV). Five generations of this technology were developed to charge, cars, buses, trams, and a small road train in a few cities across South Korea.

To a large extent, development of WPT systems has only made step change improvements since then. Some other research groups have developed their take on similar technologies, Momentum Dynamics (Miller *et al.*, 2017), Bombardier's Primove (Su Y. Choi *et al.*, 2015), Politechnico di Torino (Transport Research Laboratory, 2015). It is notable that one WPT system became available for public customers

to purchase, this is called Plugless, developed by Evatran (Carlson and Normann, 2014; Plugless, 2016). It is a retrofit solution for a few selected EVs in North America.

2016 marked the first step towards further commercial acceptance of WPT with the publication of a draft standard from the SAE. This document, called J2954, covers static WPT for light duty vehicles (SAE International, 2016, 2017). It was revised in November 2017 and plans to also cover larger vehicles, charging in motion (dynamic WPT), and higher power level applications in the future.

BMW has recently also announced that it will be providing a "wireless charging kit" option to North American buyers of its 530e iPerformance vehicle (TechRadar, 2018). This system, based on Qualcomm Halo's technology, would mark the first time WPT technologies are offered by an OEM to mainstream customers.

Commercially WPT technologies are currently only used in a few niche applications. Recent developments appear to be moving the development towards mainstream commercial applications in the automotive sector. One particularly promising development towards commercialisation is the release of the J2954 draft standard from the SAE.

2.2 FUNDAMENTALS

The aim of automotive power transfer (charging) systems is to transfer energy from the mains (or grid) into the DC bus of the vehicle. Once at the DC bus, the energy can be used by the vehicle to charge the battery, power the inverter and therefore the motors, or power auxiliary devices (HVAC, lights, etc.). Wireless power transfer follows this process, and the functional diagram from the SAE is shown in Figure 2.1.

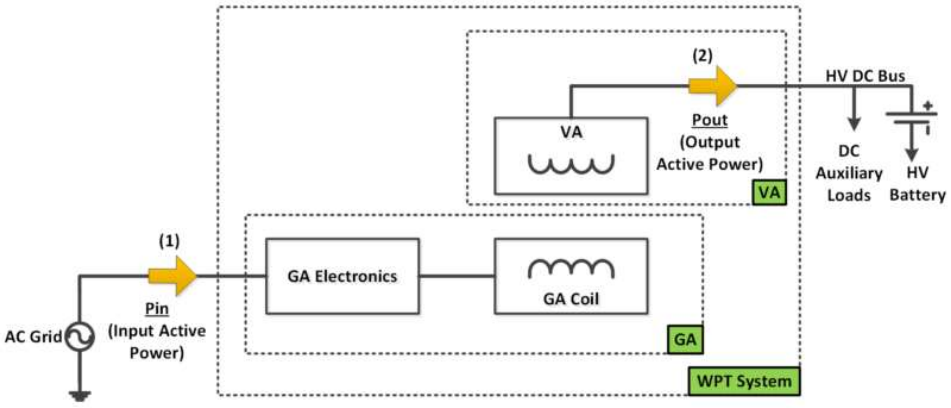

Figure 2.1: Functional Diagram of a WPT system. From (SAE International, 2017).

At the centre of a WPT system are the GA/VA coils. There are coil(s) on the ground and coil(s) on the underside of the vehicle. To transfer power, the coil on the ground is excited with an alternating current. As current travels around the coil, it creates a magnetic field. If the vehicle's coil is in close enough proximity to the ground coil, the vehicle coil will intercept some of this field. As the field is intercepted, it causes a current to be excited in the vehicle coil.

This idea is fundamentally no different to the function of a conventional transformer. Unsurprisingly, many of the equations for conventional transformers are also valid for WPT. There is, however, one significant difference, this is the coupling of the coils. In a conventional transformer the two coils are tightly coupled, because they are either wound around each other, or they are both wound around the same core. In WPT applications the coils are loosely coupled, often separated by a large air gap (100-250 mm) and possibly positional offsets. To quantify this parameter, the coupling factor value is used, this is a quantity going from 0 where there is no magnetic connection between the coils, to 1 where the coils are tightly coupled. A conventional transformer operates with a coupling factor close to 1, whereas WPT applications work with coupling of the order of 0.1 to 0.5 (Boys and Covic, 2013a, 2013b).

The coupling factor is calculated from the ratio of the inductances of the coils. Three inductance values exist in this two-coil system. There is a self-inductance value for each of the coils in the GA and VA, L_1 and, L_2 respectively. Between the coils there is also a mutual inductance, M. The coupling factor, k, is the ratio of these, given in Equation 1.

Equation 1: Coupling Factor

$$k = \frac{M}{\sqrt{L_1 L_2}}$$

2.3 STATE OF THE ART

There are several research groups worldwide, actively developing WPT systems. The publishing activity varies group to group so not all the data to develop a complete picture of their activity is available. Using the published information, a table has been created, shown over the next few pages.

Table 1: (multi-page) Summary of state of the art from the multiple research groups worldwide.

Group	Primary Location	Key Members	Years Actively Developing WPT systems	Commercial Arm
Power Electronics Group, University of Auckland	Auckland, New Zealand	John Talbot Boys, Grant Anthony Covic, Fei Yang Lin, Adeel Zaheer, Michael Neath, Hui Zhi (Zak) Beh, Seho Kim	1989-date	Halo IPT/Qualcomm Halo
Wireless Power Transfer Technology Research Center, Korea Advanced Institute of Science and Technology (KAIST)	Dae-jeon, South Korea	Su Y. Choi, Dong-Ho Cho, Jong-Woo Kim, Beom W. Gu, Seog Y. Jeong, Chun T. Rim	2009-date	OLEV Technologies
Oak Ridge National Laboratory (ORNL)	Knoxville, TN, USA	John M. Miller, P.T.Jones, Jan-Mou Li, Omer C. Onar	2012-Date	Plugless (Evatran) and Momentum Dynamics have links to ORNL
Primove (Bombardier)	Germany		2010-date	Y
Momentum Dynamics	Malvern, PA, USA	Andrew Daga, John Miller (of ORNL), Peter C. Schrafel, Bruce R. Long	(founded 2009) 2013-Date	Y
Utah State Power Electronics	Logan, UT, USA	Zeljko Pantic, Reza Tavakoli, Braden J. Limb, Regan Zane, Jason C. Quinn	2012 - Date	WAVE
INTIS	Lathen, Germany		2011-Date	Y
IPT Technology	Efringen-Kirchen, Germany		1997- Date	Y
Plugless Power (Evatran)	Richmond, VA, USA	Brian Normann	2009 – 2018 Now believed defunct as of 2019	Y
Department of Industrial Engineering, University of Padova	Padova, Italy	Manuele Bertoluzzo, Giuseppe Buja, Hemant Kumar Dashora	2015 - Date	
WiTricity	Watertown, MA, USA		2007-date	Y
PATH (University of California)	Oakland, CA, USA	J.G. Bolger F.A. Kirsten L.S. Ng	1978-1995	N

Group	Static WPT Systems Demonstrated	Opportunistic WPT Systems Demonstrated	Dynamic WPT Systems Demonstrated	Max Demonstrated Power Levels for any WPT System
Power Electronics Group, University of Auckland	Y	Y	Y	22 kW
Wireless Power Transfer Technology Research Center, Korea Advanced Institute of Science and Technology (KAIST)	?	Y	Y	125 kW (25 kW per pickup)
Oak Ridge National Laboratory (ORNL)	Y	Y	Y	20 kW
Primove (Bombardier)	Y	Y	Y	250 kW
Momentum Dynamics	Y	?	?	200 kW
Utah State Power Electronics	Y (50 kW, >90% efficiency)	Y	Y	50 kW
INTIS	Y	?	Y	200 kW
IPT Technology	Y	Y	?	180 kW
Plugless Power (Evatran)	Y	N	N	7.2 kW
Department of Industrial Engineering, University of Padova	?	?	Y	2.8 kW
WiTricity	Y	Y	Y	11 kW +
PATH (University of California)	N	N	Y	60 kW

Group	Highest Operating Frequency	Claimed Efficiency	Vehicles Demonstrated	Special Terminology
Power Electronics Group, University of Auckland	85 kHz (automotive)	90%	Cars	Flux Pipe
Wireless Power Transfer Technology Research Center, Korea Advanced Institute of Science and Technology (KAIST)	20 kHz	80%	Carts, Cars, Buses, Trams	Shaped Magnetic Field in Resonance (SMFIR), On-Line Electric Vehicle (OLEV)
Oak Ridge National Laboratory (ORNL)	48 kHz	70%	Golf Cart, Car (Prius)	
Primove (Bombardier)	20 kHz	>90%	Trams, Buses	
Momentum Dynamics	?	?	Buses	
Utah State Power Electronics	20 kHz	>90%	Cars, Buses	Aggie Bus
INTIS	<35 kHz	>80%	Cars, Vans, Small Buses, Carts	
IPT Technology	?	>90%	Buses, Industrial	
Plugless Power (Evatran)	20 kHz (3.3 kW system)	>80% (tested by Idaho National Lab)	Kits for: Nissan Leaf, Gen 1 Chevrolet Volt, BMW i3 and Tesla Model S	
Department of Industrial Engineering, University of Padova	85 kHz	82%	Cart	
WiTricity	145 kHz	>90%	Cars	
PATH (University of California)	400Hz	60%	bus	

Group	J2954 Task-Force Member	Noted Partnerships	Notes	References
Power Electronics Group, University of Auckland	Y	Qualcomm Halo, Rolls Royce Cars,		(Boys and Covic, 2015; Zaheer *et al*>, 2016)
Wireless Power Transfer Technology Research Center, Korea Advanced Institute of Science and Technology (KAIST)	Y	Korea Railroad Research Institute (KRRI), Endesa		(Park *et al.*, 2015; Su Y Choi *et al.*, 2015; Rim and Mi, 2017)
Oak Ridge National Laboratory (ORNL)		Evatran	Circular coils for a Golf Cart, Interest in the ripples cause by WPT switching	(Ning *et al.*, 2013; Miller and Chinthavali, 2014; Su Y. Choi *et al.*, 2014; Miller *et al.*, 2015)
Primove (Bombardier)			Three phase, very small air gap and alignment tolerance	(Su Y. Choi *et al.*, 2015)
Momentum Dynamics	Y	Advised by Miller of ORNL, CARTA	Details are limited of systems	(Miller and Daga, 2015; Miller *et al.*, 2016)
Utah State Power Electronics			Made a dynamic WPT testing roadway. Details are limited.	(Sorrentino, 2014; Patil *et al.*, 2017; Tavakoli and Pantic, 2017)
INTIS		Fraunhofer Institute	Focuses mostly on testing equipment and integration	(Rim and Mi, 2017)
IPT Technology		Conductix-Wampfler	Very close coils, ~40 mm, lowers the VA. Used in a few cities in UK, eg: Milton Keynes	(Conductix-Wampfler GmbH, 2013; Technology, 2018)
Plugless Power (Evatran)	Y	Bosch, ORNL	Only system available for purchase, ~3000 USD for consumers, 12999/5999 USD for 7.2/3.6 kW lab demo kit	(Jones and Onar, 2014; Cirimele, Freschi and Mitolo, 2016)
Department of Industrial Engineering, University of Padova				(Bertoluzzo, Buja and Dashora, 2017)
WiTricity	Y	MIT, Toyota, TDK, Delphi	Initially also worked on consumer electronics before growth of Qi	(Rakouth *et al.*, 2013; Transport Research Laboratory, 2015; Cirimele, Freschi and Mitolo, 2016; Patil *et al.*, 2017)
PATH (University of California)	N		Very early work, before power electronics in kHz region were available	(Bolger, 1978; Bolger *et al.*, 1978; Zell and Bolger, 1982; Suh and Kim, 2013)

2.3.1 Power Electronics Group, University of Auckland

The oldest and most published group actively developing WPT technologies. Mainly focused on developing static WPT systems. Spun out the Halo IPT commercial arm which was bought up by Qualcomm (EE Times, 2011). One of the most respected groups in the community (Covic and Boys, 2013).

They have investigated many issues surrounding the coil design and layout of coils (Kim *et al.*, 2014; Lin, Covic and Boys, 2015; Zaheer *et al.*, 2015). They are actively involved in the development of the SAE J2954 Standard (SAE International, 2017).

Qualcomm are heavily focused on developing their Halo technology for use in the automotive sector. They are actively engaging with OEMs to bring the system to market (TechRadar, 2018).

2.3.2 Wireless Power Transfer Technology Research Center, Korea Advanced Institute of Science and Technology (KAIST)

Arrived on the scene in the late 2000s and rapidly developed dynamic WPT systems for a range of vehicles in South Korea (Su Y. Choi *et al.*, 2014). Considered the most advanced team in manufacturing and technology readiness for dynamic WPT technologies (Transport Research Laboratory, 2015). Have developed a system in active commercial service and considered the economics of WPT (Lee and Cho, 2015). One of the most respected groups in the community, and contributing to the J2954 task force (Schneider, 2012).

Over the numerous generations of their dynamic WPT technologies they have focused on improving efficiencies, reducing magnetic field intensities, making the systems easier to construct, and improving the longevity of the systems (Su Y. Choi *et al.*, 2015).

2.3.3 Oak Ridge National Laboratory (ORNL)

From the emergence of WPT technologies, particularly that of KAIST, the US Department of Transport was motivated to understand dynamic WPT technologies. ORNL was selected to perform some of this research (Miller *et al.*, 2015). A system consisting of multiple circular coils was developed to power a golf cart along a track as well as some specialist electronics to reduce the impact of switching on the power grid (Miller and Chinthavali, 2014). The group is also involved in the J2954 task force (Schneider, 2012).

2.3.4 Primove (Bombardier)

Primove are a commercial group developing dynamic WPT systems as well as other e-mobility services for buses, trams and other commercial vehicles. Although few published works exist from this group,

other researchers have evaluated their systems (Su Y. Choi *et al.*, 2014, 2015; Transport Research Laboratory, 2015; Bi *et al.*, 2016).

2.3.5 Momentum Dynamics

A US based company working with John Miller (from ORNL). Systems for charging buses at stops have been proposed at 200 kW (Momentum Dynamics Corporation, no date; Maykuth, 2018). Member of J2954 taskforce (Schneider, 2012).

2.3.6 Utah State Power Electronics

Utah State has spun out its commercial arm of WPT development into WAVE Inc. They are developing systems predominantly for buses. A 50 kW static/opportunistic WPT system has been developed and a roadway test-bench is proposed to develop dynamic WPT systems (Bi *et al.*, 2016; Patil *et al.*, 2017).

2.3.7 INTIS

INTIS is a test centre for automotive technologies. They have integrated WPT systems into numerous vehicles and have an indoor test road for dynamic WPT development (INTIS GmbH, 2016d, 2016a, 2016c, 2016b).

2.3.8 IPT Technology

Developed a number of static/opportunistic WPT systems for electric buses. Unique in that the VA is lowered to the GA in operation. This reduces the air gap to circa 40 mm (Conductix-Wampfler GmbH, 2013). Their system is available for commercial use and has been bought for a number of e-Bus projects across Europe.

2.3.9 Plugless Power (Evatran)

Initially a commercial application of the technologies developed by ORNL, Plugless Power has links to Tier 1 suppliers. They have sold retrofit static WPT solutions for a number of electric vehicles including the Nissan Leaf, Chevrolet Volt, Cadillac ELR, BMW i3, and the Tesla Model S (Plugless, 2016). Also sells a laboratory a development kit. Member of J2954 taskforce (Schneider, 2012).

It is noted that the current status of Evatran as an operating business is unknown, some news outlets reported the CEO left the company in July 2018 and there have been limited updates since this point.

2.3.10 Department of Industrial Engineering, University of Padova

Developed a dynamic WPT system for a small electric car/cart (Bertoluzzo, Buja and Dashora, 2017) using DD coils of unequal sizing. Some additional consideration and analysis of coil shapes also has been performed (Dashora *et al.*, 2017).

2.3.11 WiTricity

Spun out from Massachusetts Institute of Technology (MIT), development seems to have focused on static WPT applications. Limited published works. Member of J2954 taskforce (Schneider, 2012).

2.3.12 PATH (University of California)

Early researchers of WPT technologies, ceased work around 1995. Developed a dynamic WPT system for a bus operating at what is now considered very low frequency (400 Hz to 8500 Hz) (Suh, 2015). Low efficiencies reported as were issues with noise (Bolger, 1978; Bolger *et al.*, 1978; Zell and Bolger, 1982).

2.3.13 State of the Art Summary

WPT technologies have been developed into a number of prototypes of dynamic, static and opportunistic applications. Coil designs vary from group to group as different parameters are prioritised.

Across the groups there has been limited commercial uptake of the technologies. The greatest commercial transport application has been in the bus sector where systems have been developed both in research environments as well as in real applications in several cities across the globe. In the automotive sector the aftermarket system from Plugless was made available for a few select EV models, and Qualcomm Halo technology has been reported to be available soon as limited option on a single BMW model.

The WPT research teams that exist today, typically started within larger corporations or spun out from universities. Most of these research teams started working on WPT technologies after 2005.

In terms of the technology capability. Power levels of up to 250 kW have been demonstrated in operation for systems with multiple pickup coils. Efficiencies of 80-90% are typically reported by most research groups in their advertising material for their systems. 20 and 85 kHz are the two most popular maximum operating frequencies that the research groups have developed.

2.4 Identifying Barriers to Adoption

The state-of-the-art summary highlighted that there are several WPT systems that have been developed. The technologies behind them have therefore been proven and demonstrated to work as prototypes. These systems, however, are yet to be successfully commercialised, and thus far are still not available to mainstream consumers.

The reasons why the groups developing WPT systems have yet to achieve mainstream commercialisation were considered in Submission #2. This identified several issues currently

preventing commercialisation and some associated research questions. It also attempted to categorise them in a logical manner. In this process three main categories were identified (note: categories (1) and (3) have been renamed from S#2 for clarity):

1. **Wireless System Development:** Encompassing all the components inside a WPT system from the power supplying circuitry to the shape of the coils.
2. **Integration:** This encompasses all the things that are needed to support a WPT system such as the grid power connection, other infrastructure needs as well as payment mechanisms.
3. **Technology Acceptance:** These are the human issues with the technology such as acceptance, business models, and economics.

A key finding is that it is difficult to consider many research questions in (2) and (3) without knowledge or experience in (1). This is because a lot of (2) & (3) questions require access to, or knowledge of, a functioning WPT system.

One of the subcategories of (1) is the topic of coil design. This is the consideration of the shape of coils, and the surrounding magnetic materials, such as ferrite and shielding. A wide range of different coil designs have been suggested by the various research groups. These designs have been proposed to address different issues and presented in a way that demonstrates their improvements (whether it be in coil design, electronic design or approach changes) over prior work.

These different coil designs are generally considered and developed in isolation and are not typically tested working together with other designs. The way the results are presented can also differ, for instance KAIST has presented results using “normalised output power”(Park *et al.*, 2015; Su Y Choi *et al.*, 2015), whereas Auckland often presents coupling factor values (Lin, Covic and Boys, 2015). This makes direct comparison challenging.

The term interoperability has arisen for mixed operation, when a GA works with a VA that it is not developed to directly work with. Interoperability also reaches further than just coil topology design. Areas such as communication methods, power levels, and resonant frequency must all be considered (see Submission #3).

The barrier of interoperability is a significant concern to many stakeholders behind WPT technologies (UNPLUGGED Project, 2014; FABRIC Consortium, 2015; Transport Research Laboratory, 2015). WPT developers want to ensure maximal interoperability of their systems for competitive advantage. Infrastructure developers want to ensure any systems they use can work for as many consumers as possible. The end users of WPT systems want to ensure that the system fitted on their vehicle will

work in as many places as possible. Finally, OEMs also want to ensure that the expectations of their customers are met.

Published work that has considered interoperability will be discussed in the next sections. This will identify the requirements for interoperability between a GA and a VA and highlight the most significant works.

2.5 Interoperability Between Groups

To ensure WPT systems developed by different groups work together, either the developers of these systems must come together to test and develop their systems with each other, or the systems must all be developed to the same set of standards.

Collaboration between the groups working on these technologies has been limited. There is a large geographic separation of the groups, with them located across the globe. There is also a commercial interest that may hinder collaborative efforts. Collaboration has occurred in Europe under the FP7 FABRIC (FABRIC Consortium, 2014) and UNPLUGGED (UNPLUGGED Project, 2016) programmes, and the findings in these will be discussed in the next section.

Standards have also been in development since at least 2011. SAE J2954 is the most prominent standard currently being developed and in 2016 the first results were published in the May 2016 Technical Innovation Report (SAE International, 2016). It was then revised in November 2017 and is called a Recommended Practice (SAE International, 2017). These documents only currently consider static WPT for Light duty vehicles (e.g. cars and vans).

2.6 Interoperability Parameters

Many factors are needed for the GA and VA to be considered compatible. The work of the FABRIC project (FABRIC Consortium, 2015) attempted to identify and categorise these for dynamic WPT applications. The categories they chose are shown in Figure 2.2. These different parameters and some of the considerations in each category are discussed in detail within Submission #3. In summary, many areas need to be considered to ensure the GA-VA pairing is compatible. If these are not met then the WPT system will not work efficiently or may not work at all.

The parameters needed for static WPT interoperability are almost the same as the parameters needed for dynamic WPT. They only differ in one aspect, which is the vehicle velocity. As the vehicle is travelling along the roadway with a velocity, the tolerance parallel to the roadway (longitudinal) is the length of the WPT enabled segment of the road, which could be many hundreds of meters. In static

WPT the offset tolerance in this direction is over a smaller fixed range, typically less than a meter (SAE International, 2017).

Communication
Communication method (wireless, Bluetooth, etc)
Communication protocol (ISO 15118, IEC 61851 etc)
Position tracking for primary coil activation

Construction and geometry
Coil geometry
Lateral misalignment tolerance
Air gap and tolerances
Achievable vehicle velocity

Electromagnetic
Operational frequency
Magnetic field intensity
Achievable secondary coil voltage
Power rating and power

Conclusion
Charging efficiency
Safety considerations (Shielding, EMC, Heating, etc)
Costs to accomplish interoperability

Figure 2.2: The areas considered for interoperability in the FABRIC project. From (FABRIC Consortium, 2015).

Out of the categories considered in the FABRIC project, "Construction and Geometry" and "Electromagnetic" were of particular interest. This concerns the electromagnetic flux field. If there is an effective flux path between the GA and VA coils, then there is a good electromagnetic link between the circuits in the GA and VA (Budhia, Covic and Boys, 2010). This means power and efficiency requirements can be met. If this path is disrupted or ineffective, then the link between the GA/VA circuits is damaged or broken, and therefore efficiency and power levels will fall.

The consideration of ensuring the flux field between the GA and VA is suitable is termed in this work, the magnetic compatibility. This will be considered further in the next chapter.

2.6.1 Aside on Velocity

It was thought in the early submissions of the doctorate that the velocity would be an important parameter to consider. Investigations into published work, however, found this is only a concern for switching on and off coils as the vehicle passes over. Switching has been considered in the work of both Guo et al. and Zhang et al. (Guo *et al.*, 2016; Zhang *et al.*, 2016) who investigate the issues of transients effects on the coils. McDonough and Fahmi (McDonough and Fahimi, 2012) found that the velocities expected in use on highways have a negligible effect on the magnetic fields between the GA-VA. This is further discussed in Submission #3.

2.7 CHAPTER 2 SUMMARY

This chapter set out to investigate and survey the current state of the art of WPT development as of the end of August 2018.

The key findings in this chapter are:

- WPT technologies have been developed into multiple prototype systems in dynamic, static and opportunistic applications.
- Limited commercial applications have been realised across the groups.
- Research teams are often linked to larger corporations or universities or have spun out the WPT arm into separate businesses.
- Most active research groups started WPT research after 2005.
- Power levels of up to 250 kW have been demonstrated with multiple pickup coils.
- Efficiencies of 80-90% are reported by most research groups.
- 20 and 85 kHz are the two most popular maximum operating frequencies.
- Three key research areas are
    - **(1) Wireless System Development:** Encompassing all the components inside a WPT system from the power supplying circuitry to the shape of the coils.
    - **(2) Communication and Management:** This encompasses all the things that are needed to support a WPT system such as the grid power connection as well as payment mechanisms.
    - **(3) Technology Acceptance:** These are the human issues with the technology such as acceptance, business models and economics.
- Research in (2) and (3) requires knowledge/experience in area (1).
- Interoperability between systems made by different developers is a major concern.
- Collaboration between developers is limited.
- Magnetic compatibility is one of many parameters that must be considered for GA-VA coil pairs to be compatible

3 REVIEW OF MAGNETIC COMPATIBILITY ASSESSMENT FOR WPT

This chapter reviews the literature surrounding GA-VA pair compatibility assessment. It then identifies the requirements for two sides of a WPT system to work together. Coupling factor is then introduced as the sole variable for assessing magnetic compatibility of a GA-VA pairing.

The first half of this chapter forms a review of the published work, the latter half of the chapter considers the methods of assessing the coupling factor. How the scale of the system affects coupling factor values is also considered. Finally, how coupling factor is affected in designs of WPT systems that have multiple coils is introduced.

The term compatibility is used here, rather than interoperability. This is because interoperability is a subset of compatibility, covering the use case of GA-VA pairings where each side is provided by different WPT developers.

The research question and hypotheses being considered here are:

H1: The coupling factor can be used as a key variable to evaluate if the fields between the GA/VA are magnetically compatible.

Q1: What is the typical range of coupling factor and what happens outside this range to the operation of the WPT system?

H2: Coupling factor is independent of the scale of the WPT system.

3.1 COUPLING FACTOR AS AN ASSESSMENT OF FIELD COMPATIBILITY

A significant academic work that has considered the compatibility of different GA and VA coils comes from the University of Auckland's Power Electronics Group. Lin et al. (Lin, Covic and Boys, 2015) published a paper that considered the compatibility of different coil designs. A finite element (FE) simulation tool (JMAG) was used to assess three different coil design types for their compatibility together.

They identified that coupling factor is an "extremely important factor when designing IPT systems", and that maximising the coupling factor is performed in the design process. A suitable coupling factor in this work exceeds 0.1 across the range of operation positions. The position range chosen is ±150 mm in X and Y. Two sets of two dimensional assessment were performed for three different coil designs (giving 9 GA-VA design combinations).

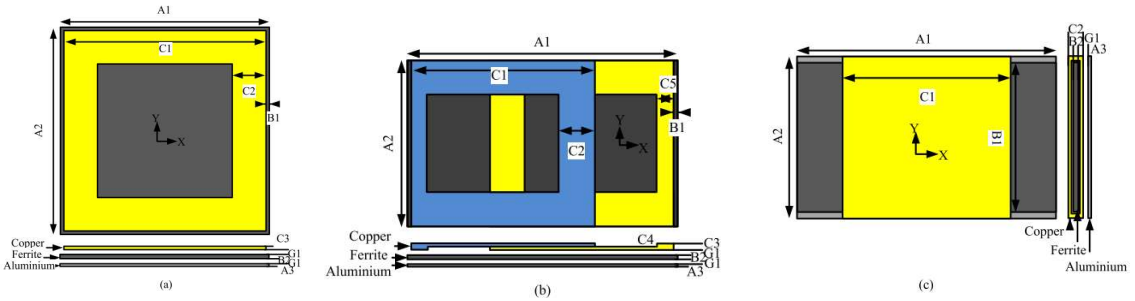

Figure 3.1: The three coil configurations considered from (Lin, Covic and Boys, 2015)*. The coil designs are named a) Circular pad (CP), b) Bi-Polar Pad (BPP), and c) Solenoid Pad (SP).*

The three coil designs investigated are shown in Figure 3.1. The results for the XY analysis at an 80 mm air gap are shown in Figure 3.2. The blue/grey slices mark diagonal cross sections where measurements were taken for Z analysis at 80, 110, 150 and 180 mm air gaps. Different coil sizes, corresponding to the pad surface areas were used, with S1 being the smallest, at 0.07 m^2 and S4 the largest, at 0.3025 m^2. BPP (Bi-Polar Pads) pads as a VA were found to be compatible with all the other GA designs, because they could change the polarization of the coils. SP (Solenoidal Pads) are not compatible with CP (Circular Pads) as they have coupling lower than 0.1 at points across the operational range.

This work assessed the coil compatibility of three coil designs with coupling factor alone. Certain coil design combinations were found to be intrinsically incompatible and others were considered compatible. This supports the (H1) hypothesis introduced.

Evidence is also given for Q1 that a minimum coupling factor value around 0.1 is typical. In the work the argument is made that the power output, P_{out} , is proportional to the square of the coupling factor, k^2. As shown in Equation 2.

Equation 2: Power output from a WPT system. From (Lin, Covic and Boys, 2015).

$$P_{out} = V_1 A_1 k^2 Q_2$$

In a coil design, the quality factor of the secondary coil, Q_2, would be fixed (it's a function of the coil construction geometry and materials). The other terms are, V_1, for the voltage into the GA and, A_1, for the current into the GA.

Lin et al. argue that with $k = 0.038$, if 3.3 kW is required as the output power, then 22 A RMS is needed in the GA coil for parallel tuned circuits. In series tuned circuits the voltage across the GA would reach 4.4 kV. These values approach the maximum current rating of the Litz wire they were using and would require careful electronic design to meet 4.4 kV voltage levels.

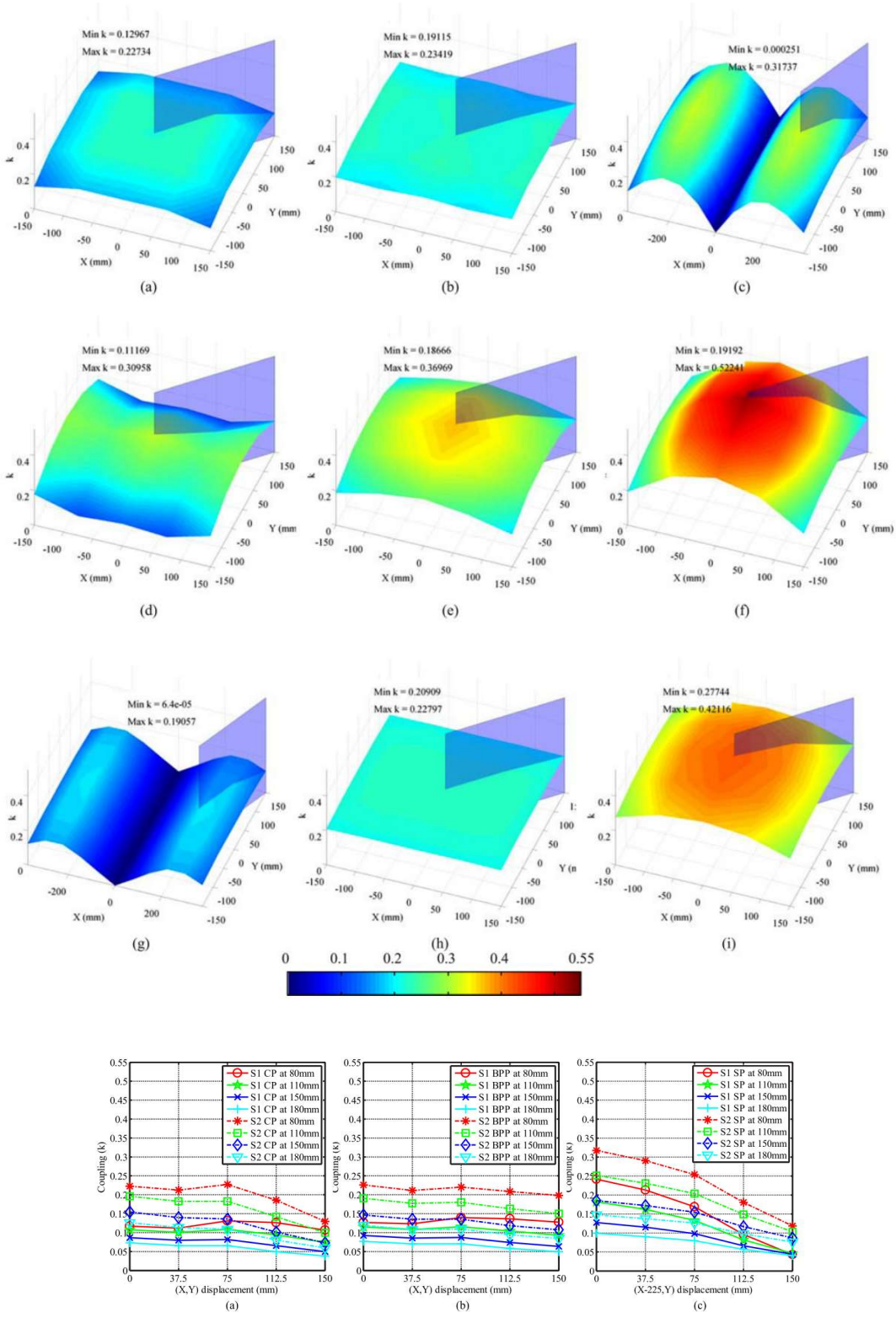

Figure 3.2: Coupling factor comparison of different coil combinations from: (Lin, Covic and Boys, 2015). *Coil combinations were considered suitable if coupling factors exceeded 0.1 across the range. The combinations shown are (a) CP P1- CP S2 (b) CP P1- BPP S2 (c) CP P1- SP S2 (d) BPP P1- CP S2 (e) BPP P1- BPP S2 (f) BPP P1- SP S2 (g) SP P1- CP S2 (h) SP P1- BPP S2 (i) SP*

P1- SP S2. The P1 signifies the use as a primary or GA coil, the S2 signifies the use as a secondary or VA coil. Diagonal analysis, incorporating different Z values was performed for each slice (marked in blue/grey) and is shown at the bottom for (a-c).

Their assessment was made with FE simulations only. This was justified as they had previously used the same software and proven the results to 5-10% accuracy. They also mentioned results from their software tool (JMAG) had been compared against ANSYS Maxwell, an alternative FE simulation tool, in this work. They considered practical (EXP) validations were unfeasible due to the complexity of their study.

This work provides the strongest evidence in the published work that supports the H1 hypothesis. Coupling factor alone has been shown here to be enough to asses if coil combinations are compatible or not. Some consideration is provided too that the coupling factor should be maximised in coil designs and that when it is below 0.1 issues occur in the in the power output of a WPT system.

Zaheer et al. (Zaheer *et al.*, 2015) performed a similar assessment, however, focused their efforts on similar GA designs with different polarization modes of the coils, shown in Figure 3.3. This work used a two VA coil designs, and three GA coil designs. Coupling factors of these different operational modes were measured using both simulations and experimental methods.

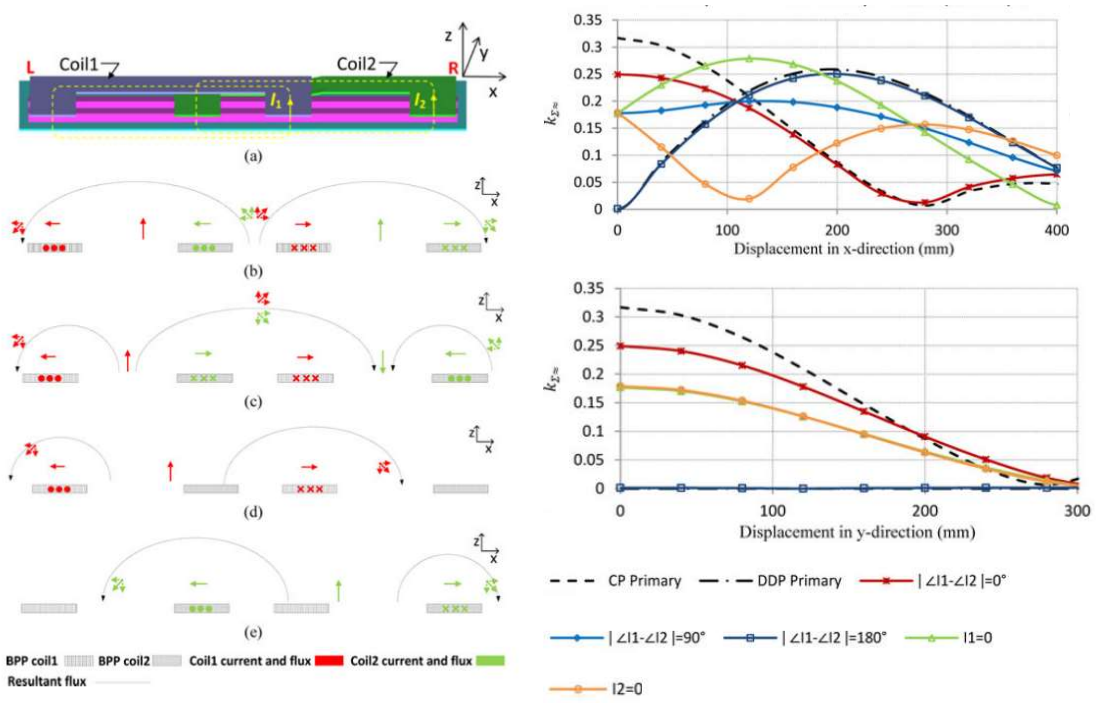

Figure 3.3: Different coil operation modes of the BPP (Bi-Polar Pad) GA coil and the coupling to a CP (Circular Pad) VA coil. (left) shows the different operational modes of the coils, (right) shows the coupling factor to the VA coil for various phase differences, or polarization modes, of the BPP GA coil. From (Zaheer *et al.*, 2015)

The work of Zaheer et al. considers more than just compatibility of GA-VA coil pairings. A significant part of the work is comparing BPP (Bi-Polar Pad) designs to DDQP (Double-D Quadrature Pad) and the leakage flux from these designs. They have gone also as far to consider the uncompensated output power of the WPT system in the same configurations, this shows, in Figure 3.4, where coupling factor is less than 0.1, then power output is at a minimum.

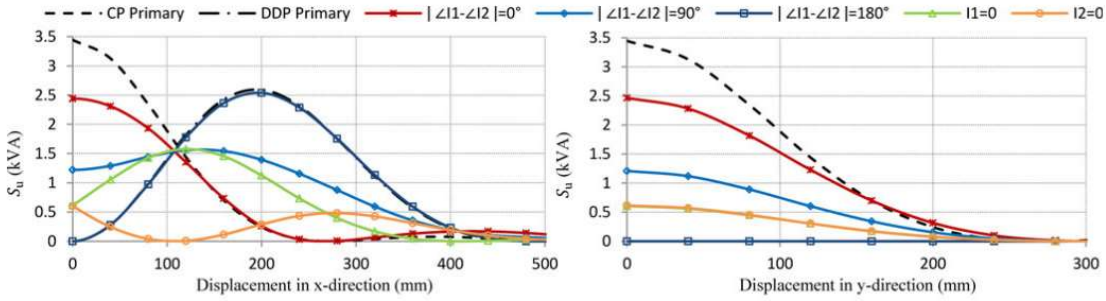

Figure 3.4: Uncompensated power output for the same coil configuration as in Figure 3.3. From (Zaheer *et al.*, 2015).

Coupling has only been considered in one dimension at a time and the air gap (Z direction) is fixed at 125 mm for all measurements. Most of this work is from simulation results, however, experimental analysis has been included in Zaheer et al.'s work.

This work again supports the H1 hypothesis, as it shows how the regions of high coupling correspond to high uncompensated power output. It also provdes further evidence for Q1, that there is a mimumum value of coupling that must be met or the output power is compromised.

Miller et al.(Miller *et al.*, 2016) discussed the whether importance of WPT coils is more important. They considered different circuit compensation techniques and the effects of coupling factor tending to 0 and towards 1. They showed that at low coupling factors the source supply (GA circuit) becomes isolated from the load (VA circuit). They argued the series-series circuit topology (where capacitors are wired in series with the coils in the GA and VA) is best for their application to reduce capacitor voltage stress and maximise efficiency. The most significant finding in their work is that WPT developers should focus on maximising coupling factor rather than quality factor.

These findings relating to coupling factor are supported with network theory analysis. This approach considers the impedance of the circuits of the GA and VA sides of the WPT system. The approach has been applied elsewhere in the literature (Zhu *et al.*, 2016). EXP studies were not performed in Miller et al.'s work and FE simulations are limited to a single dimensional (Z) analysis.

Miller et al.'s work further supports the H1 hypothesis. Their use of network theory to demonstrate the importantce of the coupling factor differs to the other two works, however, the conclusions reached are similar.

In summary, the published work shows some GA and VA coil pairings are fundamentally incompatible. This incompatibility has been found considering just the magnetics through the coupling factor alone. Coupling factor also appears to be the most important parameter to demonstrate a given GA and VA is magnetically compatible.

There is still a need to assess the magnetic fields during the design process. This is to ensure that the fields produced by the GA-VA combination meet the ICNIRP guidelines (International Commission on Non-Ionizing Radiation Protection, 1998, 2010). This assessment should consider the leakage flux limits set in the 2010 guidelines at 27 µT for fields between 10-100 kHz.

Although the field strength is affected by the geometry of the coils, it can only be assessed once the electronics powering the coils are known. This is because it is proportional to the current in the GA coil. As the assessment proposed here is independent from the coil electronics, field assessment is out of scope.

3.2 Coupling Factor

The coupling factor, k, has been shown as a key parameter for assessing if a GA-VA pairing are magnetically compatible (section 3.1). From earlier, it is the ratio of the mutual inductance, M, between the coils to the self-inductance of the pickup (VA) and source (GA) coils, L_2 , L_1.

Equation 1(repeated): Coupling Factor

$$k = \frac{M}{\sqrt{L_1 L_2}}$$

3.2.1 Assessment Methods

Within the published literature, three methods have been used to measure the inductances of coils, and therefore the coupling factor. These are named here as analytical, finite element and experimental.

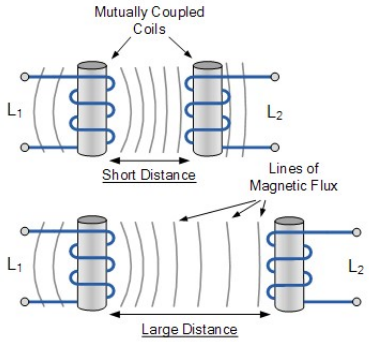

Figure 3.5: An example of performing analytical studies of two solenoids. From (Aspencore, 2018).

Figure 3.5 shows the typical example shown in many textbooks of two solenoids. In this example, analytical methods can be used to evaluate the mutual inductance between two solenoids. The analytical methods in this case work well for simple coil designs, where the cross-sectional area is uniform for both coils, the length is the same and the turns are uniform.

Joy et al. (Joy, Dalal and Kumar, 2014) used analytical methods in the assessment of air core square planar coils, and compared the results to both FE and EXP measurements. Results using analytical methods were in close agreement to the other measured results, as seen in Figure 3.6.

TABLE III
PERFECT ALIGNMENT — VERTICAL AND PLANAR VARIATION

Vertical variation				Planar variation				
Distance (cm)	FEA (μH)	Analytical (μH)	Practical (μH)	Angle θ(degree)	FEA (μH)	Analytical (μH)	Practical θ(degree)	(μH)
2	12.36	18.05	17.31	0	17.4	17.56	0	17.69
3	13.40	13.97	13.66	10	16.9	17.05	15	16.87
4	10.90	11.16	10.61	20	15.9	16.11	30	15.66
5	8.80	9.11	8.83	30	15.3	15.36	45	15.32
6	7.37	7.54	7.23	40	14.9	14.96	60	15.88
7	6.19	6.32	5.81	50	14.9	14.96	75	17.09
8	5.24	5.34	4.84	60	15.3	15.36	90	18.38
9	4.46	4.54	3.91	70	15.9	16.11		
10	3.83	3.89	3.26	80	16.9	17.05		
				90	17.4	17.56		

Figure 3.6: Screenshot of a sample of results for square planar coils from Joy et al. (Joy, Dalal and Kumar, 2014). *Analytical results are close to both FE and EXP (practical) values over a range of air gap distances.*

What characterises this work, however, is that the coils are simple in design. The coils are square with no ferrite or shielding. Offsets are only performed in one degree of freedom at a time, either a single rotational axis or a single direction dimension.

When the simple symmetries of the system are broken, the calculations start to become exponentially more complex. Mutual inductance expressions for thin co-axial disk coils are shown in Figure 3.7 and the same for thick co-axial disks are shown in Figure 3.8. R_{11}, R_{12}, R_{21}, R_{22}, are corresponding radii, z_{11}, z_{12}, z_{21}, z_{22}, are corresponding heights, it is advised to refer to (Babic, Salon and Akyel, 2004) for the full definition.

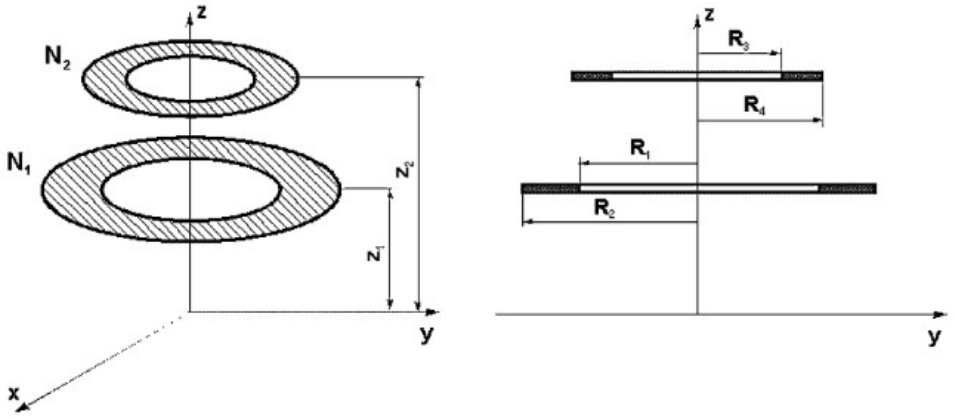

$$M = \frac{\mu_0 N_1 N_2 \int_0^{\pi} \int_{R_{11}}^{R_{12}} \int_{R_{21}}^{R_{22}} \int_{z_{11}}^{z_{12}} \int_{z_{21}}^{z_{22}} \frac{\cos\theta r_I r_{II} \mathrm{d}r_I \mathrm{d}r_{II} \mathrm{d}z_I \mathrm{d}z_{II} \mathrm{d}\theta}{r}}{(R_{12} - R_{11})(R_{22} - R_{21})(z_{12} - z_{11})(z_{22} - z_{21})}$$

$$r = \sqrt{(z_{II} - z_I)^2 + r_I^2 + r_{II}^2 - 2 r_I r_{II} \cos\vartheta}$$

Figure 3.7: Diagram and equation for mutual inductance for thin co-axial disk coils. From (Babic, Salon and Akyel, 2004).

These examples are shown to illustrate the complexity of analysis once basic symmetries are broken. Further complexities also exist in the real WPT systems being proposed by research groups. These designs introduce materials such as ferrite and aluminium, which in an analytical method means the magnetic permeability term, μ, can no longer be treated as fixed, and therefore must be integrated over the system geometry. They also are not symmetrical and must operate over a range of positions in three dimensional space, this means the r term can no longer use the co-axial symmetry of the system, and must be considered in the three dimensional region of space.

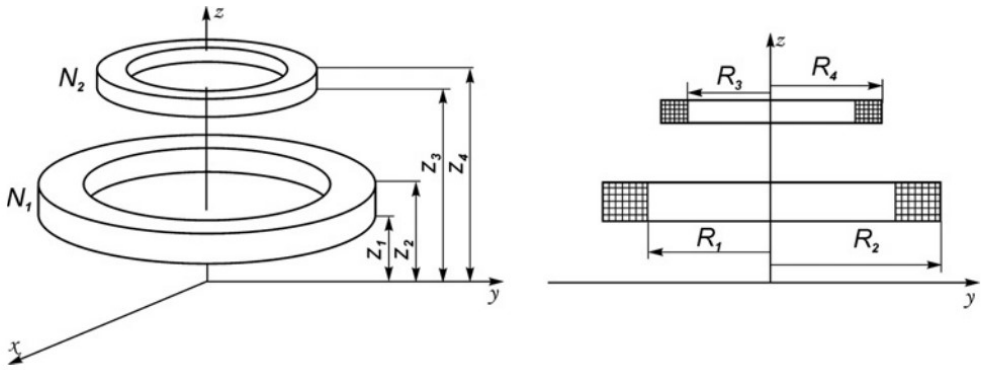

$$M_{\mathrm{B}} = \frac{\mu_0 N_1 N_2 \int_0^{\pi} \int_{R_1}^{R_2} \int_{R_3}^{R_4} \int_{z_1}^{z_2} \int_{z_3}^{z_4} (\cos\theta \mathrm{d}r_{\mathrm{I}} \mathrm{d}r_{\mathrm{II}} \mathrm{d}z_{\mathrm{I}} \mathrm{d}z_{\mathrm{II}} \mathrm{d}\theta / r)}{(z_4 - z_3)(z_2 - z_1) \ln(R_2/R_1) \ln(R_4/R_3)}$$

$$r = \sqrt{(z_{\mathrm{II}} - z_{\mathrm{I}})^2 + r_{\mathrm{I}}^2 + r_{\mathrm{II}}^2 - 2 r_{\mathrm{I}} r_{\mathrm{II}} \cos\theta}$$

Figure 3.8: Diagram and equation for mutual inductance for thick co-axial disk coils. From (Babic and Akyel, 2017).

For these reasons, analytical methods are not practical for studying the complex coil geometries being proposed in the current generation of WPT systems. It is therefore understandable no published work has attempted to perform analytical assessment of inductances of these complex coil geometries.

Finite Element (FE) methods take the rules of physics and apply them to thousands of nodes in a given volume. At each node a set of differential equations are configured which are then simultaneously solved using a computer. This method is widely used in engineering to model various effects such as fluid flow, structural analysis, heat transfer, and electromagnetic effects. FE simulations been validated to be accurate to between 5-10% of experimentally measured values for WPT applications (Lin, Covic and Boys, 2015). They do not offer information regarding how this accuracy can be improved further as it was acceptable for their purposes. In this document the factors that may affect accuracy are discussed in Section 4.5.

Within the published works, many have applied FE simulations to calculate inductances and coupling factors of the coil designs they are developing. Lin and others at Auckland University have used JMAG and ANSYS Maxwell tools to assess their coil designs (discussed in 3.1) (Kim *et al.*, 2014; Lin, Covic and Boys, 2015; Zaheer *et al.*, 2015). KAIST have used ANSYS Maxwell to verify their designs and look into

the fields within the ferrite cores (S Y Choi *et al.*, 2014; Su Y Choi *et al.*, 2015). Zhang et al. also use ANSYS Maxwell in their assessment (Zhang *et al.*, 2015).

Like a calculator, FE simulation results are only as accurate as the data put in. This means the model, typically a Computer Aided Design (CAD) of the real coils that are being used, must be suitably accurate. The simulation parameters, and the simulation tools used must also be suitable to the effect(s) being studied. Finally, the mesh, which is the arrangement of the nodes within the simulation volume, needs to be suitable. "Suitable" in these cases must be carefully considered by the users of FE simulations and ultimately depends on the desired accuracy, computational resources and time needed. This is further discussed in Submission #4 and chapter 4.

Experimental (EXP) methods can also be employed to measure inductances. This involves building prototypes of the coil design and directly measuring the inductances. Specialist tools are needed for accurate measurement of mutual and self-inductance (detailed in section 4.3).

3.2.2 Coupling Factor and Magnetic Field

H1: The coupling factor can be used as a key variable to evaluate if the fields between the GA/VA are magnetically compatible.

H1 claims that the coupling factor is all that is needed to assess the magnetic compatibility of coils. However, in the introduction, the electromagnetic field link between the GA-VA is stated to be the important factor. Therefore, coupling factor must relate in some way to these electromagnetic fields.

The inductance terms that calculate the coupling factor do indeed account for the magnitude and direction of the flux fields, $\vec{\boldsymbol{B}}$. This can be shown using Faraday's Law of Induction. Inductance, L, multiplied by the rate of change of current, $\frac{di(t)}{dt}$, equals the amount of EMF, v, produced by in the VA coil by the changing magnetic flux field, ϕ. The surface, $\vec{\boldsymbol{A}}$, in this case is the cross-sectional area of the GA/VA coil and N is the number of turns. This calculation can be used to evaluate the self-inductance, where the induced EMF causes the voltage to lag in the coils, and the mutual inductance, where the induced EMF from the current in the GA coil powers up the VA coil.

Equation 3: Induced EMF from Faraday's Laws of Induction

$$\phi = \iint \vec{\boldsymbol{B}} \cdot d\vec{\boldsymbol{A}}$$

$$v(t) = L\frac{di(t)}{dt} = -\mathrm{N}\frac{d\phi(t)}{dt}$$

The terms in Equation 3 use in a double integral around the coil geometry. In this step both the geometry of the coils, and the relative positioning of the coils is accounted for.

This shows how the inductance values, and therefore coupling factor, relate to the electromagnetic fields. From this consideration it is clear that the coupling factor is therefore an indirect method to assess the field compatibility.

3.2.3 Typical Coupling Factor Ranges

Q1: What is the typical range of coupling factor and what happens outside this range to the operation of the WPT system?

The first part of this question can be considered from a direct survey of published literature.

Lin et al. (Lin, Covic and Boys, 2015) considered a suitable coupling factor must exceed 0.1. No maximum value was discussed.

The TS coil designs in SAE J2954 (SAE International, 2017) have minimum coupling values reported as 0.088, 0.126, 0.087 and 0.136 for the normal GA-VA combinations in the standard's appendices C.2, D.1, E.1.1 and E.2.1.1 respectively. The maximum coupling factors for these coils are 0.245, 0.344, 0.232 and 0.397 respectively.

The WPT system developed by ORNL reported coupling between 0.075 to 0.35 (Ning *et al.*, 2013).

The prototype coils considered by Ibrahim et al. (Ibrahim *et al.*, 2016) had a coupling factor range between 0.1 and 0.8.

Coupling factor values ranges for the other WPT systems discussed in the state of the art (section 2.3) are not openly available. So cannot be considered here.

Of the coupling factors identified here, the mean minimum coupling factor is 0.106 and the mean maximum coupling factor is 0.404 from a sample of six minimum coupling factors and five maximum coupling factors. Operation outside of these ranges will be considered in the following sections.

3.2.4 Minimum Coupling Value

In this section, research question Q1 is further considered:

Q1: What is the typical range of coupling factor and what happens outside this range to the operation of the WPT system?

There is unfortunately no one-size-fits-all coupling value minimum that must be met to consider coils compatible. There is, however, a value that appears in the literature as a common target value. This value is 0.1.

Work from the University of Auckland has discussed why 0.1 is the target they use (Boys and Covic, 2013b). This was briefly discussed in section 3.1, and Equation 2 was introduced.

Equation 2(repeated): Power output from a WPT system. From (Lin, Covic and Boys, 2015).

$$P_{out} = V_1 A_1 k^2 Q_2$$

As the power output relates to the VA (VA here being the Volt-Ampere rating rather than Vehicle Assembly) rating of the source side coils by a factor of k^2, a coupling factor of 0.1 would mean the VA rating needs to be 100 times the desired power output. Increasing the VA rating means either increasing either the voltage or current into the GA coils. Increasing the voltage is not always possible due to electronic limitations and safety regulations. Increasing the current into the coils is limited by the rating of the coil wires, power supply limitations, and thermal limits.

The efficiency of WPT systems can fall at very low coupling values. There is a theoretical maximum efficiency for coil-to-coil transfer that has been discussed in the literature. This is shown for a Series-Series (SS) compensation topology in Figure 3.9. This theoretical maximum efficiency is the ceiling value for the efficiency of the WPT system as there will be other losses from the powering and rectification circuitry. Other compensation topologies exhibit similar theoretical maximum efficiencies.

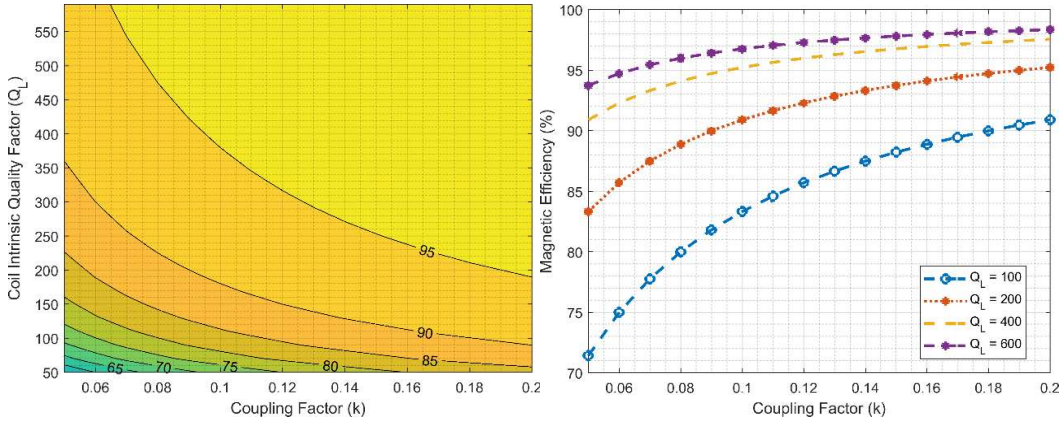

Figure 3.9: Magnetic Efficiency % as a function of coil intrinsic quality factor ($Q_L = Q_1 = Q_2$) and coupling factor, (k). This shows the profile of Equation 4.

Equation 4: Maximum magnetic efficiency for coil-to-coil transfer (Lin, Covic and Boys, 2015)

$$\eta_{max} = \frac{1}{1 + \frac{2}{k\sqrt{Q_1 Q_2}}}$$

This means that for given intrinsic coil quality factors where $Q_1 = \frac{\omega L_1}{R_1}$ and $Q_2 = \frac{\omega L_2}{R_2}$ there is a maximal efficiency possible from the point of view of magnetic power transfer between coils. $Q_1$and Q_2 are intrinsic values limited by the construction of the coils. R_1, and R_2 are the ohmic resistances of the wire used to make the coils.

Plotting the magnetic efficiency onto a surface with coil intrinsic Q factor and coupling, shown in Figure 3.9, highlights the need for the coupling factor to exceed 0.1. There is a steep decline in efficiency at values lower than 0.1. Similar trends are noted for the other compensation topologies. Kalwar et al. have shown similar results (Kalwar, Aamir and Mekhilef, 2015).

Demonstrated in this way, the effect of improved intrinsic coil quality factors can be seen. To some extent the coil's quality factor can be increased to balance out the effect of low coupling factor. This solution, however, has its limitations as coils can only be built to a certain maximum quality factor. Intrinsic coil quality factors of 100 to 500 are found in typical WPT coils (Kamineni *et al.*, 2015). The work of Miller et al. discusses the balance of coupling and quality factors further (Miller *et al.*, 2016). Note that the use of superconducting materials is not considered in the scope of this work, there are many practical issues with implementing such a system as discussed by Machura and Li (Machura and Li, 2019).

This assessment makes use of the calculations from Lin, Covic and Boys (Lin, Covic and Boys, 2015) and therefore has the assumption that the losses on both sides of the WPT are equal. This assumption is reasonable to make as it true when the system is perfectly tuned, with the optimal energy transfer between the coils. This assumption typically also holds true for asymmetrical coil designs (when the primary and secondary sides are of different sizes), as the coils in this case are likely to use different wire thicknesses.

Practically, real WPT systems also may have to de-rate to operate at low coupling values. KAIST discusses how their system has a normalized output power that changes with the alignment (Su Y Choi *et al.*, 2015). This change in output power is by design in their electronics and can be seen in Figure 3.10. Other systems, such as those used by Auckland (Boys and Covic, 2013a, 2013b) choose to compensate low coupling by increasing the primary side current, maintaining the same output power.

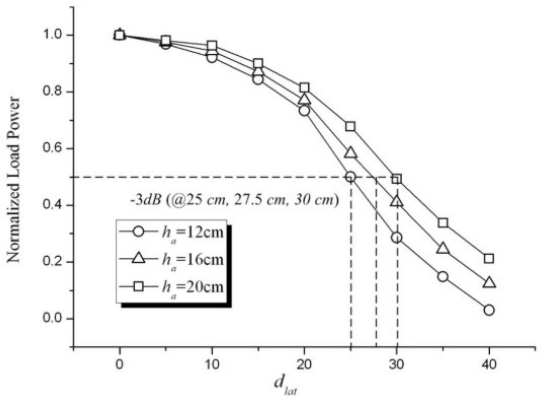

Figure 3.10: Normalised load power against lateral offset of KAIST's 5th Generation OLEV system (Su Y Choi *et al.*, 2015)*. Rather than compensating for low coupling factor by increasing the current in the GA, the VA output power is reduced.*

Because of these two issues at very low coupling, there needs to be a minimum coupling limit that a WPT system is designed for. Below this value, the system should shut down (or not switch on), and request user intervention. The limit could be set by standards (such as SAE J2954's >80% efficiency requirement), or by other system specific limitations, such as limits based around overheating the coils, damaging the power supplies, exceeding the ICNIRP field limits, etc.

3.2.5 Maximum Coupling Factor

In this section research question Q1 is further considered:

Q1: What is the typical range of coupling factor and what happens outside this range to the operation of the WPT system?

Lin et al. (Lin, Covic and Boys, 2015) discusses that WPT designers are typically aiming to maximise coupling values, this leads to the question are high coupling values an issue?

From the consideration of WPT systems as a loosely coupled transformer ($k < 0.5$), a high coupling factor means is that the WPT system then becomes a tightly coupled transformer ($k > 0.5$) according to the definitions from Kalwar et al. (Kalwar, Aamir and Mekhilef, 2015). A tightly coupled transformer, or just a conventional transformer, is an electronic component that has been used for decades in electronics. There is no issue from an electronics standpoint in developing circuitry to transfer power efficiently across a convnetional transformer.

There are, however, limitations with the real circuits used for WPT. This arises because the circuit design will be optimised for a particular coupling range. Diekhans and De Doncker (Diekhans and De

Doncker, 2015) discuss that the electronics they have employed can work with coupling up to 0.45. Above this the nominal power cannot be transferred.

The WPT system developed by IPT Technologies (section 2.3.8), probably uses a much higher coupling factor than other WPT designs. The system drops the VA down onto the GA to reduce the gap between the coils to approximately 40 mm. This is likely to result in the GA-VA being tightly coupled. As the electronics in this system are designed to work this way, even though the coupling factor is very high, efficient power transfer is still demonstrated (Conductix-Wampfler GmbH, 2013).

3.3 Scale Independence of Coupling Factor

In this section, H2 Hypothesis is considered:

H2: Coupling factor is independent of the scale of the WPT system.

This is explained further below:

> *If a coil design is proposed, and all the dimensions of this design are scaled up/down by a factor. Including the gap between the coils. Then the value of coupling will remain unchanged.*

This point is interesting, at first glance it could be considered trivial, coil design is unchanged so one might just assume that the coupling factor between them would therefore simply be the same. But then considered further, why this should be the case is unclear. After all it is known many of the variables such as field strength and inductance will change as the scale factor changes.

In the published work, a number of researchers have used small scale prototypes (Prasanth, Bauer and Ferreira, 2015; Bandyopadhyay *et al.*, 2016; Bertoluzzo, Buja and Dashora, 2017). None have directly considered how coupling is affected by scale, although there is some mention that magnetics scale linearly.

There are three ways the author considered to approach the consideration of H2. The first is investigating the theoretical equations for inductances, and show from these, how the scaling impacts the coupling factor. This approach is covered in 3.3.1. The second approach is to demonstrate scaling using a FE simulation of the coils, this is shown in 3.3.2. The third way would be to build a set of identical coil designs at different scales and perform an EXP study. This third method is not performed here due to the cost and time needed for this assessment.

3.3.1 Analytical Consideration of Scaling

The mutual, self-inductance, and coupling factor can be considered for scaling properties analytically. Starting with Neumann's formula in Equation 5. Where $\mu_0$is the permeability of free space, N_1 and N_2 the number of turns in each coil, dl and dl' a small increment along each wire, and r is the separation between each wire increment.

Equation 5: Neumann formula (Babic, Salon and Akyel, 2004)(Chan, 2000)

$$L = \frac{\mu_0}{4\pi} N_1 N_2 \oint \oint \frac{d\vec{\boldsymbol{l}} \cdot d\vec{\boldsymbol{l}}'}{\vec{\boldsymbol{r}}}$$

Now if the geometry is altered such that all dimensions are scaled by a factor, A, then the new inductance L_{scaled} can be considered by multiplying all spatial variables by the scale factor. This is shown in Equation 6.

Equation 6: Scaled Neumann formula (Babic, Salon and Akyel, 2004)

$$L_{scaled} = \frac{\mu_0}{4\pi} N_1 N_2 \oint \oint \frac{A d\vec{l} \cdot A d\vec{l}'}{A\vec{\boldsymbol{r}}}$$

$$= \frac{\mu_0}{4\pi} N_1 N_2 \oint \oint \frac{A \cdot A}{A} \frac{d\vec{l} \cdot d\vec{l}'}{\vec{\boldsymbol{r}}} = \frac{\mu_0}{4\pi} N_1 N_2 \frac{A \cdot A}{A} \oint \oint \frac{d\vec{l} \cdot d\vec{l}'}{\vec{\boldsymbol{r}}} = AL$$

Therefore, the inductance values are proportional to this scaling factor. Coupling factor, however, is independent, as shown in Equation 7.

Equation 7: Scaled Coupling Factor

$$k_{scaled} = \frac{M_{scaled}}{\sqrt{L_{1(scaled)}\, L_{2(scaled)}}} = \frac{AM}{\sqrt{AL_1\, AL_2}} = \frac{M}{\sqrt{L_1\, L_2}} = k$$

The Neumann formula does make the assumption in the double integral that the wires are infinitely thin and geometrically smooth. This geometrically smooth assumption is acceptable in the coils being studied for WPT. To consider non-thin coils, the equations discussed in section 3.2.1 can be used, such as those in Figure 3.8. In this case the same scale factor relation for inductance is found, see Equation 8.

Equation 8: Scaled Inductance for non-thin coils

$$M_{\mathrm{B}} = \frac{\mu_0 N_1 N_2 \int_0^{\pi} \int_{R_1}^{R_2} \int_{R_3}^{R_4} \int_{z_1}^{z_2} \int_{z_3}^{z_4} (\cos\theta \mathrm{d}r_{\mathrm{I}} \mathrm{d}r_{\mathrm{II}} \mathrm{d}z_{\mathrm{I}} \mathrm{d}z_{\mathrm{II}} \mathrm{d}\theta / r)}{(z_4 - z_3)(z_2 - z_1) \ln(R_2/R_1) \ln(R_4/R_3)}$$

$$M_{scaled} = \frac{\mu_0 N_1 N_2 \int_0^{\pi} \int_{R_1}^{R_2} \int_{R_3}^{R_4} \int_{z_3}^{z_4} (cos\theta . Adr_I . Adr_{II} . Adz_I . Adz_{II} . d\theta / Ar)}{(Az_4 - Az_3).(Az_2 - Az_1).\ln\left(\frac{AR_2}{AR_1}\right).\ln\left(\frac{AR_4}{AR_3}\right)}$$

$$M_{scaled} = \frac{\mu_0 N_1 N_2 \int_0^{\pi} \int_{R_1}^{R_2} \int_{R_3}^{R_4} \int_{z_3}^{z_4} \frac{A.A.A.A}{A} (cos\theta . dr_I . dr_{II} . dz_I . dz_{II} . d\theta / r)}{A.A.(z_4 - z_3).(z_2 - z_1).\ln\left(\frac{R_2}{R_1}\right).\ln\left(\frac{R_4}{R_3}\right)}$$

$$= \frac{A.A.A.A}{A.A.A} \frac{\mu_0 N_1 N_2 \int_0^{\pi} \int_{R_1}^{R_2} \int_{R_3}^{R_4} \int_{z_3}^{z_4} (cos\theta . dr_I . dr_{II} . dz_I . dz_{II} . d\theta / r)}{(z_4 - z_3).(z_2 - z_1).\ln\left(\frac{R_2}{R_1}\right).\ln\left(\frac{R_4}{R_3}\right)} = AM_B$$

These equations for the coils do not have any ferrite or shielding materials. For considering more complex coil designs that do have ferrite and shielding, FE simulations are needed.

3.3.2 Simulation Consideration of Scaling

A complex GA/VA coil design, which has ferrite has been developed in ANSYS Maxwell. This model has been validated against experimental prototype coils to 10% accuracy (discussed further in section 4.5 and 5.6.1). Figure 3.11 shows both the coil design and the results from the studies. Coils are in nominal position (0,0,45) mm at a scale factor of 1, and operating in polarized mode.

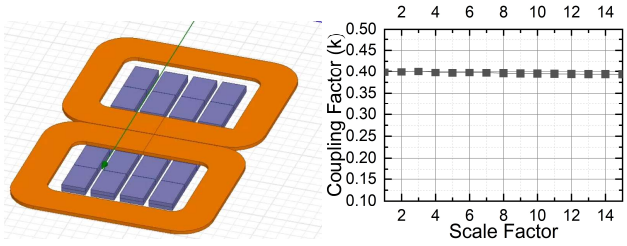

Figure 3.11: Finite Element CAD (left), Inductances (centre), and coupling factor (right) for the DD coil design from finite element simulation at different scale factors.

As expected from the analytical study, and Equation 7, coupling factor remains constant with scale. There is a slight decline of the value at the highest scale values, but this difference remains less than the 3% convergence criteria used in the simulations.

These simulations, combined with the analytical considerations in the previous section demonstrates that coupling factor is independent of the scale of the system. Therefore the evidence shown here supports the hypothesis H2:

H2: Coupling factor is independent of the scale of the WPT system.

3.3.3 Aside: Coupling Factor and Number of Turns

Although, not directly related to the core of this work, it is useful to understand how coupling factor is affected by the change of the number of turns in a WPT design.

With the assumption that the number of turns does not significantly affect the geometry of the coils, it can be considered in the same way as scale factor. Analytically, the number of turns is a multiplier added to the front of the inductance equation (Equation 5). Therefore, mutual inductance will scale linearly with number of turns. Self-inductance will scale to the square of number of turns. As the coupling factor is proportional to the mutual over the square-root of the self-inductances is therefore not affected by the changing number of turns.

In the ANSYS Maxwell software itself, when turns of the coils are modelled as a single block, the number of turns is not part of the FE simulation at all. The number of turns becomes a multiplier added to the results of a single turn coil in post processing. The configuration screen for this is shown in Figure 3.12. In real-world applications, changing the number of turns does inevitably affect the coil geometry, however, it is acceptable in this simplification to use this multiplier method only.

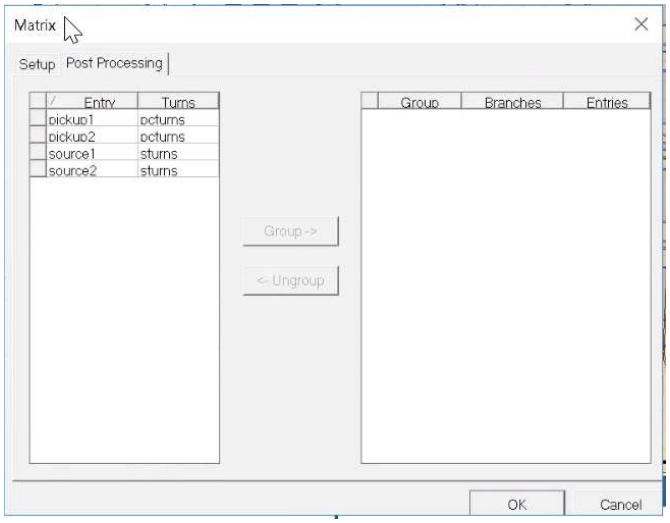

Figure 3.12: Configuration of the number of turns in ANSYS Maxwell. It is part of the post-processing step.

3.4 Multi-Coil Operation Mode

So far, the GA and VA have mainly been discussed as if they consist of single coils. This, however, is probably not the case, as many WPT designers have proposed multi-coil designs. The most popular multi-coil design in the literature is the Double-D or DD coil design.

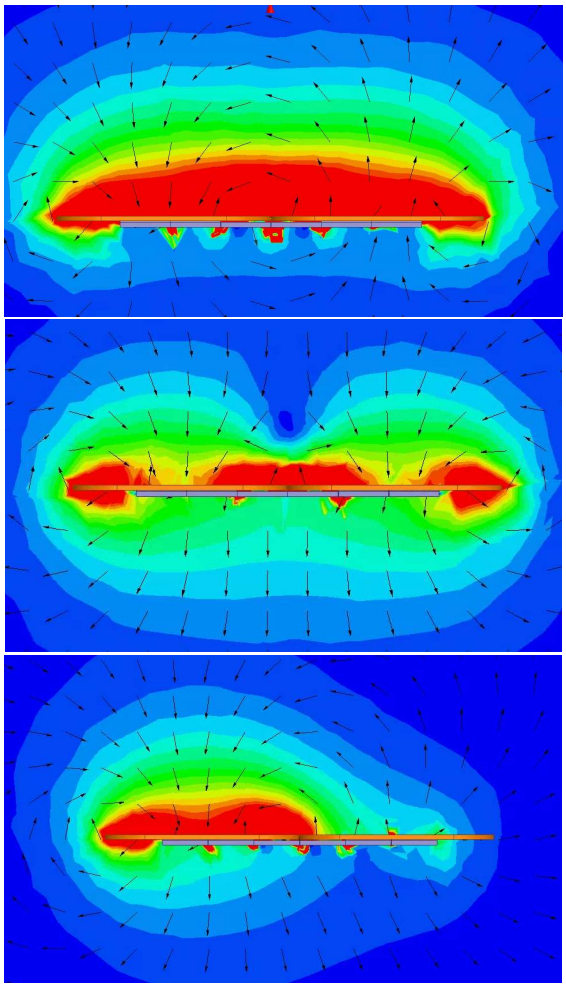

Figure 3.13: The three operational modes of the DD coil, polarized (top), non-polarized (centre) and single coil (bottom). Arrows denote magnetic field direction. Colours indicates field magnitude.

By introducing more than one coil to a GA or VA, an option arises in how these can be operated. Assuming that coils are driven at the same frequency from a single supply (typical of most WPT designs) then these two coils can be operated in three different modes. This difference in relative phase is also termed polarization. The first mode is polarized, where the flux path exits one coil into the other(Budhia *et al.*, 2013). The second mode is non-polarized, where a flux path leaves both coils. The final mode is single, where only one coil is active. These are shown in Figure 3.13. Care must be taken to ensure the VA is operating in the correct mode for the GA, else there is a risk the excitations will be cancelled out by each other (Abbott, Yang and Jennings, 2017).

Another opportunity offered by multi-coil designs is the option to selectively disable coils. This could be used to ensure flux leakage limits are met or to reduce the self-inductance of a GA/VA to improve the overall coupling factor. This is particularly important in dynamic WPT operation, where GA coil arrays need to be switched as the VA moves over them (Zaheer *et al.*, 2017).

What is important about these configuration options is that they affect all the inductance values. Therefore, the coupling factor must be considered for each mode. Coupling factor is not, however, the only consideration. Using part of GA/VA coil could also result in a reduction of the power rating of the WPT system, this is because only part of the conducting material is being used.

3.5 CHAPTER 3 SUMMARY

This chapter has reviewed the published work and introduced some theory and assessment to consider magnetic compatibility. This has provided evidence and information to help support the research questions and hypotheses.

H1: The coupling factor can be used as a key variable to evaluate if the fields between the GA/VA are magnetically compatible.

Two significant works have been reviewed that considered coupling factor as a measure of magnetic compatibility. Using coupling factor alone, certain coil design combinations were identified as fundamentally incompatible as the coupling factor was considered unsuitable (too low). How coupling factor links to the magnetic fields has also been considered in section 3.2.2. With this evidence, in the scope of this work, coupling factor can now be used as the only variable to consider the link between the GA-VA for magnetic compatibility.

Q1: What is the typical range of coupling factor and what happens outside this range to the operation of the WPT system?

Only a few WPT systems have shared the range of coupling factors in the published work. The mean range from an admittedly small sample size is 0.106 to 0.404.

Outside this coupling factor range two issues have been identified. The first is that in order to maintain the desired power output at low coupling values, the voltage and current applied to the GA must be increased. At a coupling factor of less than 0.1, the high currents and voltages required into the GA coil start to become unmanageable from a safety and power supply perspective. High coupling factor values also result in issues for the electronics used within WPT systems, as they are typically designed to operate in a limited range of coupling. High coupling values, however, do not prevent power transfer between a GA-VA pair, as in this case the WPT system is electronically similar to a conventional transformer.

Coupling factor contributes to a fundamental efficiency limit. The magnetic efficiency, which is the maximum efficiency of transfer between the GA-VA coils, ignoring any losses in the electronics, is limited by both the quality and coupling factors. Quality factor is a fixed variable based on the coil

construction and their intrinsic resistance. It has been shown for a series compensated WPT topologies (other topologies produce similar results) that there is a steep decline in efficiency below coupling factors of 0.1 in typical WPT systems.

H2: Coupling factor is independent of the scale of the WPT system.

This chapter has shown evidence to support the second hypothesis (H2) in section 3.3. Analytical and FE simulations were used to demonstrate this property. This hypothesis can therefore be accepted as true in the scope of this work.

The property of scale independence means small scale prototypes of coil designs will exhibit the same coupling factors as the full-scale designs (assuming all dimensions scale). Therefore, small scale prototypes can be used to investigate the magnetic compatibility of coil designs. For a researcher this is a valuable way to simplify the process of experimental methods. Small scale coils are cheaper to manufacture, safer to use (drop hazards), and require significantly less space resources.

4 Development of Multi-Dimensional Coupling Mapping (MDCM) Methods for WPT

This chapter details the process of development of an assessment method for coupling factor. It follows the work undertaken in Submission #4 and some of the refinements performed in #5.

This tackles the hypothesis H3:

H3: Multi-dimensional mapping of coupling factor at a high resolution is feasible for both FE and EXP studies.

At first, the design of coupling mapping assessment is considered. This defines the range and resolution of the study region, and the need for validation of Finite Element (FE) results with experimental (EXP) measurements.

The development of both the Finite Element (FE) and Experimental (EXP) methods are then discussed. Some of the challenges and the solutions employed are highlighted.

Section 4.6 discusses how the developed methods can be applied to research question Q2:

Q2: How can the optimal GA-VA design/operational mode be identified for a particular operational region?

4.1 Design of Assessment

Previous sections highlighted that the coupling factor is a key parameter when considering magnetic compatibility. To calculate this value, the self-inductance and mutual inductance between GA and VA coils must be measured.

To perform these assessments both the region where measurements are taken should be defined, as well as the requirements on the accuracy of the measured results. This is detailed in this section.

4.1.1 Study Region

In a vehicular application there are six degrees of motional freedom. For the purpose of this work they are defined here, with their associated explanation:

- X Direction – From the driver's seat of a vehicle this is forward/backward.
    - Longitudinal
- Y Direction – From the driver's seat this is left/right direction.
    - Lateral
- Z Direction – From the driver's seat this is up/down direction.
    - Vertical
- Yaw Rotation – Rotation around the Z axis
    - Controlled by turning the steering left/right
- Pitch Rotation – Rotation around the Y axis
    - Raising or lowing the front or rear of the vehicle
- Roll Rotation – Rotation around the X axis
    - Raising or lowering the left/right side of the vehicle

To select the study region, the application and scale must be considered. At full scale in automotive applications, vehicle ground clearance varies between 100-300 mm (Submission #4). Previous automotive studies have found drivers position themselves laterally with an accuracy of ±150 mm within a lane whilst driving along a simulated UK motorway (Naberezhnykh *et al.*, 2014). Parking studies have shown a lateral range of ±120 mm (Birrell *et al.*, 2014). Longitudinally, whilst parking, the tolerance can be up to ±740 mm (Birrell *et al.*, 2014). Rail applications have a lateral offset of a few millimetres (Armstrong, 2008). Systems that guide the driver into alignment are not considered here.

The draft J2954 standard (SAE International, 2017) has chosen a study region of ±100 mm laterally, ±75 mm longitudinally and Z classes of 100-250 mm (ignoring the GA thickness). These ranges are lower than discussed in the above literature as J2954 does include methods of guidance to the driver to ensure accurate parking alignment.

These ranges must be scaled based on the size of the prototype coils being studied. For instance a $1/10^{th}$ scale prototype should have a region with dimensions $1/10^{th}$ of the size of the full scale system.

4.1.2 Published Work

Published work, typically performs assessment in one dimension at a time.

KAIST in the development of their 5^{th} Generation OLEV system only considered Y direction offset, at 50 mm intervals up to 400 mm (Su Y Cho*i et al*., 2015). This can be seen in Figure 3.10.

Zhang et al. (Zhang *et al.*, 2015) used circular coil designs, and therefore because of the inherent symmetry only considered one dimensional position range. Intervals of 25 mm were used up to 150 mm offset laterally/longitudinally.

Prasanth and Bauer (Prasanth and Bauer, 2014) performed both lateral and longitudinal misalignment analysis separately. Simulations were employed alongside experimental measurements at intervals of 20 mm over a 40 mm range laterally, and 250 mm interval over a 1000 mm range longitudinally.

Joy et al. (Joy, Dalal and Kumar, 2014) considered lateral and vertical variations, longitudinal was not necessary due to coil symmetry. Intervals of 10 mm were used over a 100 and a 110 mm range (Z and X respectively). This study also included consideration of rotational variation.

Some work has considered two dimensions at once (Lin, Covic and Boys, 2015). Lin et al. used a 75 mm interval over ±150 mm range laterally and longitudinally. A vertical range of 80 to 180 mm was used at 30 mm intervals. To assess three dimensional properties, a diagonal slice was taken across the profile, shown as the shaded region in Figure 3.2. A comment was made in this work that initially a 25 mm interval was used, but they found it could be increased to 30 mm, and still capture the coupling profiles.

Considering the resolution as the number of samples per dimension, 10 is the highest in these published works (from Joy et al.). Other studies only use around five points. The author is not aware of any published work that has assessed three linear dimensions together in a single study in either experimental or simulation studies.

4.1.3 Scale

The fact that coupling factor is independent of the scale of the system (findings from H2, discussed in section 3.4), means that there is no need to work with full scale systems. As small-scale prototypes will produce the same results. Therefore, to reduce the cost of constructing prototypes a small scale is employed in this work.

At first, 1/10th scale was considered, due to the convenience of scale calculations. Whilst constructing coils, however, it was found to be too difficult to wind the coils tight enough for this small-scale. Therefore, the scale target was doubled to 1/5th scale. With the study in chapter 5, the prototype coils had already been made, independently to this work, so were not designed to a scale.

4.1.4 Study Region

GA/VA pairs operate in three-dimensional linear space in automotive applications, the gap between the floor and the underside of the vehicle can change (vertical, Z-direction) as well as the position of the vehicle both laterally (left-right - Y direction) as well as longitudinally (forward-backward – X direction). For dynamic WPT systems, longitudinal motion is essentially infinite. In rail applications, the lateral position is highly constrained, as the vehicle is fixed to rails. Because of these degrees of freedom, magnetic compatibility cannot be considered at a single point.

There are also three rotational axes to consider. Yaw is rotation around the Z axis. For static WPT it depends on how aligned the vehicle is within the designated bay. The range of yaw in dynamic and opportunistic scenarios is much lower, as the vehicle will be travelling in the direction of the roadway. The other rotational axes are roll and pitch. Roll rotation could occur on very uneven road surfaces where one side of the road is higher than the other, another occurrence in normal use could be when buses lower one side of their suspension to aid kerbside access. Pitch rotation can occur in heavy acceleration or braking, or at significant changes in gradient on the roadway.

At first, the design of the multi-dimensional mapping methods will only consider linear motion. This is to simplify the process of development. Once linear mapping has been demonstrated then efforts can be made to include rotational mapping into the assessment.

4.1.5 Challenge of Multi-Dimensional Studies

Each additional dimension or variant being studied exponentially increases the number of measurements. Consider 10 positional points are sampled in a single direction, which is a reasonable quantity of data points to capture the trend of the coupling profile. 100 samples are needed in two dimensions. In three dimension this increases to 1,000 samples.

1,000 samples are not practically possible if the GA-VA are being manually positioned. It would take too much time to perform this type of study.

1,000 positional points are also a challenge in many FE simulation studies. Each simulation requires an amount of computing resource and time to complete.

Of course, if this was increased further, with for instance 5 values of rotation, and three modes of coil operation, a 15-fold increase in the number of measurements is needed.

It is therefore understandable that the in published literature (section 4.1.2), care has been taken to reduce the number of samples. Measurements have been taken at large intervals, using typically only one dimension or direction at a time. "Slices" of measurements are used, to assess three dimensional properties, and rotation is rarely considered.

4.1.6 Opportunities From "High Resolution" Sampling

In the previous chapter, coupling factor is identified as a key variable relating to the compatibility of a GA-VA pairing. If a GA-VA pairing cannot satisfy the minimum coupling factor value at all points within its operational position range, then it cannot be considered magnetically compatible.

The aim in H3 was to perform "**mapping of coupling factor at a high resolution**". Up to 10 points per linear direction, which is typical of the studies in published literature (section 4.1.2), the author does not consider high resolution. But what could be the benefits of performing high resolution mapping? A few points were considered as justification for developing such methods:

- **Characterising a new GA-VA pairing –** In this case some new coils or a new pairing of coils has been considered, but their characteristics are unknown. Finding out the coupling factor at a high resolution in three dimensions could be used to identify and benchmark the potential operation of coil pairings. This could then be used to inform the designers of the suitability of the pairing and the tolerances needed for the WPT system electronics.
- **To find the operational position range of a GA-VA pair** - Given a coupling factor range, the positional point where coupling factor falls outside this range can be known. This can be used to set the limit of the operation range of the pairing.
- **To find the size needed for a GA-VA to meet a specific operation range** – Given both a coupling factor range, and an operational position range, the GA-VA design can be assessed. This will find where (position) the coupling factor limits are met. Due to the scaling property (H2), the scaling of the coils needed to meet both coupling factor and operational range can be inferred.

- **Characterise an unusual surface profile** – As the coupling profiles employed in the published works typically only consider one dimension at a time. It is conceivable that they may miss unusual profile characteristics. In Figure 4.1 an example of how one-dimensional plotting could miss the actual coupling profile is shown. Here 4 different surface plots are shown that have identical one-dimensional characteristics along the axes, but differ greatly in other parts of the region. A three-dimensional high-resolution coupling map would not have this issue and help give designers confidence that the property of a given pairing is known across the region.

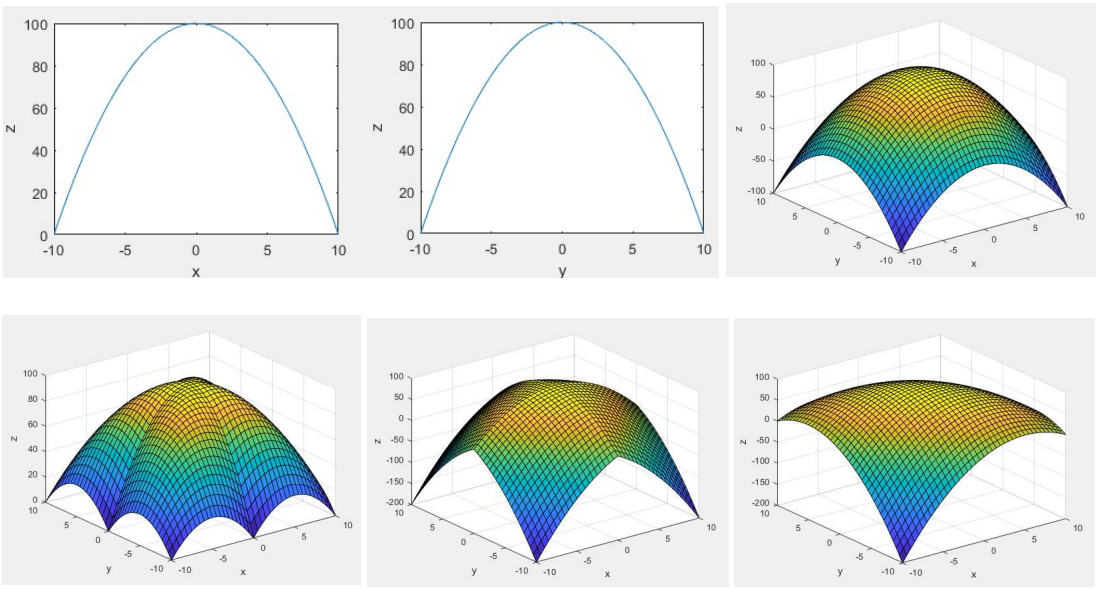

Figure 4.1: Demonstration of 4 different surface plots that produce the same X=0, Y=0 2D line plots. The function in all plots is: $z = 100 - x^2 - y^2 + f(x,y)$. (Top-left) X-Z plot for Y=0. (top-centre) Y-Z plot for X = 0. (Top-Right) Surface plot for: $f(x,y) = 0$. (Bottom-Left) Surface plot for: $f(x,y) = |xy|$. (Bottom-centre) Surface plot for: $f(x,y) = -|xy|$. (Bottom-right) Surface plot for: $f(x,y) = xy$. All these plots exhibit identical X-Z and Y-Z plots but the surface plots differ.

- **Coupling profiles as a standardised metric** – For WPT developers, there is an interest in optimising the design of the coils. Coupling factor offers an opportunity to compare coil designs directly for how well each GA-VA pairing works. Comparisons could either be made around the limits of each design's operation range or the average coupling factor in a defined region. Developers can then select preferred designs or even perform design optimisation based around these metrics.

4.1.7 Sampling Interval

The previous section motivated the reasons why multi-dimensional high-resolution mapping should be used; this section will consider the practicality of doing so. There is a desire to create the highest

possible number of sampling points in the study region. This means the interval between points is smaller so the positions of interest (i.e. where the coupling limits are reached) can be known to a greater precision and accuracy. Unfortunately, taking each sample requires time. Time is needed for a computer to calculate the results for FE simulations, and time is needed to position and take measurements from EXP coils. Therefore, a compromise must be met.

As this work is the first of its kind, to attempt these multi-dimensional coupling factor measurements, an element of trial and error is needed to see what the optimal sampling interval is for a given application. The interval will be dictated by how fast samples can be taken and how long one is willing to wait for the results. It could also be limited by other factors such as computational memory limits or other hardware limitations (a particular concern for FE simulation work).

4.1.8 Validation of FE simulations

There is substantial value in combining both FE and EXP methods. The merits of FE methods are that that modifications to the coil design or construction can be rapidly tested, at a low cost. FE methods are also well suited to visualising magnetic field shapes and measuring field in regions that cannot be measured experimentally. The drawback of FE methods is that they can easily produce inaccurate results, through errors or simplification of the CAD or simulation configuration changes. For this reason, FE results must be validated, by showing they agree with EXP values.

The level of agreement must be considered carefully. In the published work, 5-10% differences in values are discussed by other researchers (Lin, Covic and Boys, 2015). A compromise must be met, between the time and effort available and the acceptable difference. For instance, if a FE CAD is designed to represent the detail of the coils down to individual coil turns, it is likely to be closer to the experimental values than a CAD which simplifies the coil turns to a solid block. However, this detailed CAD will require a more complex mesh, and therefore simulations will take longer to complete.

In this work, 10% was chosen as the validation target. At this level, any significant mistakes made in the FE simulation configuration should be highlighted. Simplifications can still be employed in the FE CAD to ensure the mesh is not too complex. This validation level has been used by others in the published work (Lin, Covic and Boys, 2015).

4.2 Development of Finite Element (FE) Simulations

4.2.1 FE Software Package Selection

In this work two FE simulation packages were considered. These were chosen as they were available to the author, due to previously purchased licenses and that they are commercial packages that had been demonstrated to work by other researchers in published work.

The first package is COMSOL Multiphysics. This package can combine simulations of many different physical phenomena depending on which modules are licenced. These can include fluid modelling, battery and fuel cell effects and heat transfer. The module of interest for studying WPT magnetic compatibility is the AC/DC module. Simulations of the coils can include different electrical connections and configurations, and inductance values can be simply extracted.

COMSOL, however, had a few critical limitations for use in the high-resolution studies:

- **Meshing:** COMSOL gives full control of meshing to the user. These meshes were often rejected by COMSOL, particularly if the CAD had any geometric entities in close proximity (such as Copper coils resting on ferrite blocks). To overcome this, the meshes had to be increased in complexity.
- **Simulation Time:** Simulation time of 3D CAD models was of the order of 30 minutes to 2 hours.
- **Computational Resources:** COMSOL performed many calculations using the volatile RAM (Random Access Memory). This meant complex 3D meshes required upwards of 16 GB of RAM in order for the simulation to not run out of memory. This prevented the possibility of multi-threaded simulations on the available computer hardware.

The other package used is ANSYS Electromagnetics Suite 16.2, particularly the program ANSYS Maxwell. This software tool was found to be far better suited to the studies for this assessment. Simulations completed in the order of a minute, and due to optimisation in the software code, the computational resources (RAM use) was much lower (of the order of 2 GB per simulation). One of the reasons for this is that the software itself controlled the meshing.

ANSYS was not without its faults, but the author found ways these could be overcome:

- At simulations with > 9,000 positional samples, the simulation rate slowed significantly as it progressed. Initial simulation rates were around 200 per hour, by around the 2500th simulation this had dropped to 130 per hour, above 3000 simulations there was a significant decline, to

around 50-70 per hour. To overcome this, study ranges were split into multiple runs of <3,000 positional points.

- There was significant confusion about how to deal with GA/VA designs with more than one coil. This is discussed further in the next section.

4.2.2 Calculation of Inductance for Multi Coil Operation

Where a GA or VA consists of multiple coils that can be independently controlled, as discussed in Section 3.4, then this must be accounted for in FE simulations. The three coil operational modes can be analysed with one simulation run by considering the addition of the inductance values given by ANSYS. These calculations are needed due to the way the ANSYS software reports inductance values.

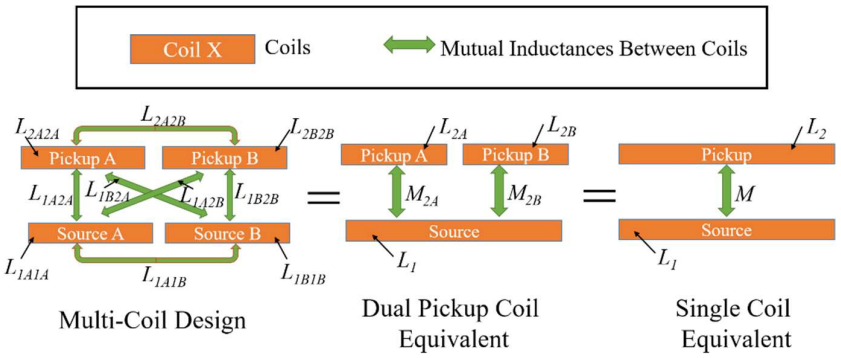

Figure 4.2: Multi-coil inductance values from ANSYS to the equivalent single coil values. L_{XXXX} Values are exported from ANSYS and combined in MATLAB using the grouping calculations shown in Table 2.

Self-inductance of the GA coils, L_1, is calculated with the addition of the two-single coil (A and B) self-inductances L_{1A1A} and L_{1B1B} as well as the mutual inductance between the separate coils L_{1A1B}. Similar additions can be performed with the pickup inductances, L_2. A diagram of this is shown in Figure 4.2, and the calculations are shown in Table 2.

Table 2: Multi-Coil grouping calculations for inductances from ANSYS. These give GA/VA inductance values for different operational modes.

Mode	Inductance Value	Grouping
Polar	Source Self (L_1)	$L_{1A1A} + L_{1B1B} + 2L_{1A1B}$
	Pickup 1 Mutual (M_{2A})	$L_{1A2A} + L_{1B2A}$
	Pickup 2 Mutual (M_{2B})	$L_{1A2B} + L_{1B2B}$
	Pickup Self (L_2)	$L_{2A2A} + L_{2B2B} + 2L_{2A2B}$
	Mutual (M)	$L_{1A2A} + L_{1B2A} + L_{1A2B} + L_{1B2B} = M_{2A} + M_{2B}$
Non-Polar	Source Self (L_1)	$L_{1A1A} + L_{1B1B} - 2L_{1A1B}$
	Pickup 1 Mutual (M_{2A})	$L_{1A2A} - L_{1B2A}$
	Pickup 2 Mutual (M_{2B})	$L_{1B2B} - L_{1A2B}$
	Pickup Self (L_2)	$L_{2A2A} + L_{2B2B} - 2L_{2A2B}$
	Mutual (M)	$L_{1A2A} - L_{1B2A} - L_{1A2B} + L_{1B2B} = M_{2A} + M_{2B}$
Single	Source Self (L_1)	L_{1A1A}
	Pickup 1 Mutual (M_{2A})	L_{1A2A}
	Pickup 2 Mutual (M_{2B})	L_{1A2B}
	Pickup Self (L_2)[a]	L_{2A2A} or L_{2B2B}
	Mutual (M)	$L_{1A2A} + L_{1A2B} = M_{2A} + M_{2B}$

[a] Assumes only one pickup coil is active at a time and is connected independently, if this is not the case then Non-Polar values must be used

After developing these calculations, the coil grouping function was found in ANSYS Maxwell. This allows WPT designers to combine coils in this manner inside the ANSYS Maxwell simulation configuration. The results for inductances using the grouping function was found to be identical to the manually calculated values here. The advantage of not grouping the coils in ANSYS simulations is that a single simulation run can be used. Then in data processing, the inductance values for all three operational modes can be calculated. This takes less time than three separate simulation runs.

Similar additions will exist if there is more than two coils in the GA or VA. The calculations will need to be extended to accommodate the extra coil terms. Care must be taken to choose a single coil as the reference point in polarisation. Alternatively the above calculations could be used for each of the coil pairings and a summation performed. I.e. in a GA or VA with coils *A,B,* and *C*. Coils *A* and *B* could be combined to give a grouped coil, *D*, this could then be combined with coil *C*.

4.3 Development of Experimental (EXP) Methods

The experimental (EXP) test methods went through several revisions and changes before getting to the test rig that is available now. Here the methods to measure coupling factor, construct coils, and position them accurately in an automated manner are discussed.

4.3.1 Measuring Coupling Factor

Specialist devices exist to measure self-inductance of coils. In this work a Rohde & Schwarz, Model HM8118 LCR Meter was employed. This device is connected to the terminals of the coils and will give a reading directly. These devices are temperature sensitive and must be calibrated before every use once the device has thermally settled to avoid drift in readings.

Measuring mutual inductance, M, is possible using a simple relation between the current in the GA to the voltage across the VA. Exciting the source coil with an alternating current will result in an EMF or voltage generated in the pickup coil. The open circuit voltage on this pickup coil is related to the current in the source, I_1, as follows:

Equation 9: *Open Circuit Voltage on the Pickup Coil* (Boys and Covic, 2013a)

$$V_{oc} = j\omega M I_1$$

The user controls the alternating current's frequency, ω, and the complex term, j , can be cancelled out by using RMS values for voltage and current. This means mutual inductance can be simply extracted, from the values being measured and controlled.

Although the mutual inductance could be measured on the LCR meter, the oscilloscope method was preferred for both he interface into MATLAB as well as the reduction in thermal sensitivity.

4.3.2 Early Experimental Work

Before the focus on multi-dimensional coupling mapping was considered, a WPT system for a 1/10th radio controlled car was developed. The target was to provide 40 Watts of power to the car whilst it travelled along the track. The initial aim of this work was to investigate the challenges of designing a WPT system for a real application.

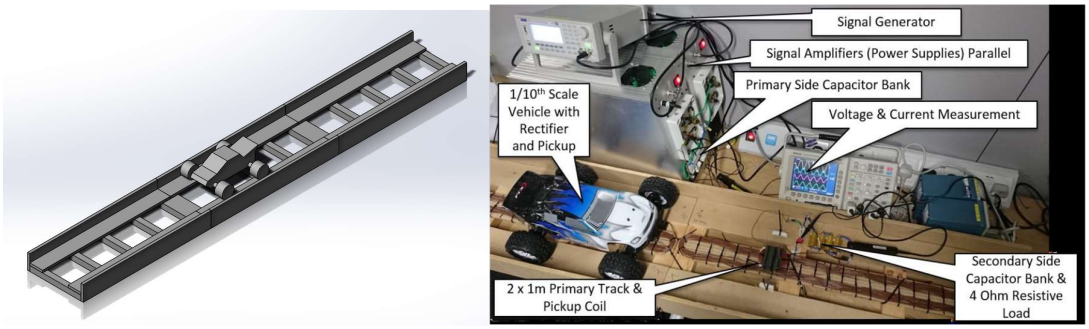

Figure 4.3: Early experimental work to construct a dynamic WPT for a 1/10th scale radio controlled car.

A budget of circa £500 was requested to build this equipment (shown in Figure 4.3) and help within the department was asked for to source a suitable power supply to power the coils. With the help of Andrew Moore, a suitable supply was found. These devices are signal amplifiers, initially designed to produce ripples on a battery's terminals. With some minor modifications, they are now used as power supplies for the various coils being tested on the rig. These devices can provide an arbitrary signal output with a frequency of up to 100 kHz and an amplitude of up to ±15 V and ±8 A. Two amplifiers can be wired in parallel to double the current to ±16 A. These supplies have been used in every revision of the test rig since.

A few lessons were learnt from this first experimental work:

- The resonant frequency of 85 kHz was initially targeted, this would typically necessitate the use of Litz wire. Litz wire is a specialist type of wire in which the individual strands are isolated from each other. It is particularly difficult to get hold of Litz wire suited to this application, only two suppliers could be found. The first, OSCO, could custom make wire for this use but required a large minimum order quantity. The other supplier, RMCybernetics, had some wire in stock. In all cases the wire was at least five times the cost of comparable standard wire (£270 vs £50, as of 14/11/2017). The wire must also be soldered using a solder-pot technique (rather than traditional soldering) to remove the enamel on each strand.
- Winding the wires into the shape of the coil design is particularly difficult. The wire cannot be held easily around turns. Various ways of holding the coils in place were trialled. These included hot-melt glue, electrical tape and zip ties, shown in Figure 4.4. These methods, however, were not able to construct the coils to an accuracy the author was satisfied with. The coil windings would spread out and overlap and the CAD designs had to be revisited to account for changes in dimensions, in some cases over a 10% difference, from the original design.

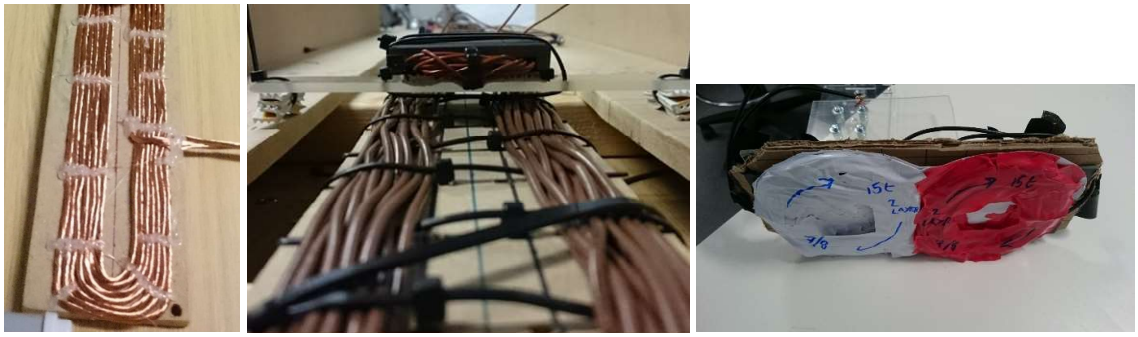

Figure 4.4: Different coil construction methods trialled, hot glue (left), zip ties (centre) and electrical tape (right). These methods were unable to construct the coils to satisfactory accuracy.

- Although Litz wire is needed for overall efficiency of a WPT system it is not actually important for the assessment performed here. This is because there is no need for significant power to be transferred. The pickup coils are in open circuit condition. In later work, standard wire was used to reduce costs.
- Development of the circuitry needed to integrate the WPT system into the vehicle was particularly challenging. A wide range of voltages (0-45 V RMS) is possible on the pickup coils that could damage the battery charging circuity (rated to 36 V). Also, the high frequency of the oscillations (initially 85 kHz, later 20 kHz) necessitated the need for diodes that could switch fast enough to rectify the power. A specialist circuit had to be designed that could both rectify and protect the vehicle's electronics. This is seen in Figure 4.5.

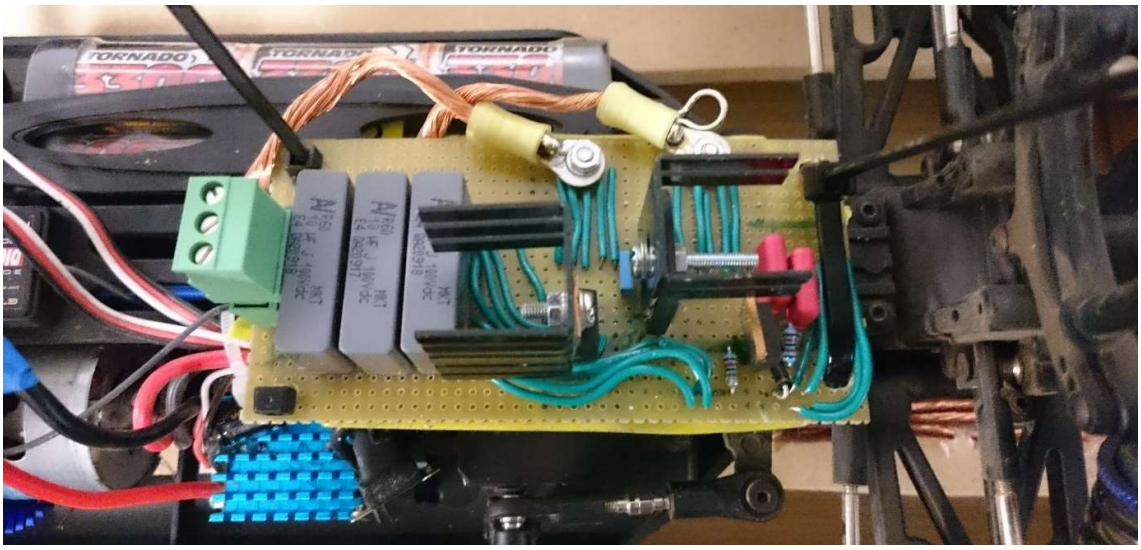

Figure 4.5: Specialist circuit designed to rectify the current from the VA coil and to protect the radio controlled car's charging circuit if the voltage got too high.

- Positioning the coils in an accurate and repeatable manner was not possible on the vehicle. The suspension system and soft tyres meant that the car would move around too freely to stay in position long enough to take a reading. A manual mount was also made, which can be seen in Figure 4.6. This stayed in position better than the car, but accurately positioning the coils was time consuming, and the range this mount could move over was limited as the feet would fall into the gap between the track and the coil.

Figure 4.6: Manual mount used to position the coils. Accurate positioning was difficult to attain using this method.

4.3.3 Automated Coil Positioning and Measurement

From this work, it was clear improvements of coil positioning and coil construction were needed to perform the type of mapping discussed in H3 and section 0. Ideally millimetre level accuracy with a system that can position coils quickly (in the order of <10 s) would be used. Therefore manual positioning methods had to be ruled out.

Electronic systems using linear or servo motors are ideal for this type of application. Therefore, it was decided to investigate the option of an XYZ positioning table or stage. These are typically expensive (>£500) for specialised scientific work (ZABER, 2018), this is because they can be able to go to micron level accuracy (far more than the accuracy needed in this work). Recently an inexpensive option was discovered, whereby a DIY Laser cutter kit could be repurposed as a XY table.

The DIY laser cutter kit chosen, comes with two directions of motion (XY) it was then easily modified into an XYZ motion base with the addition of a screwball actuator. It consists of an aluminium frame, acrylic pieces, three stepper motors (2 for Y motion and 1 for X), and a control board, all for circa £250. With an additional servo driver and screwball linear motor, circa £50, it is possible to have a £300 XYZ motion table. Control of the position is performed by serial communication from a USB port and MATLAB code has been written to do this. This code has been made open source (MIT Licence) and shared via GitHub (Abbott, 2018b). The complete rig can be seen in Figure 4.7.

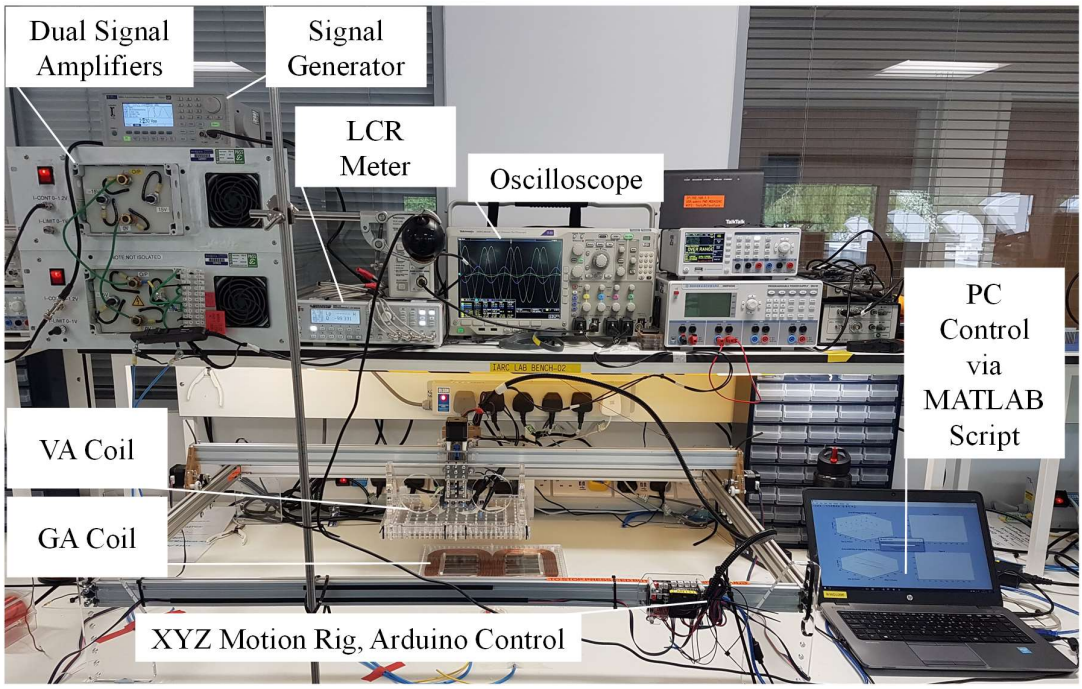

Figure 4.7: Complete test rig experimental setup with key components labelled.

Coil construction improvements were realised with the design of a pegboard. This enabled the ability to wind GA coil designs around a 20x20 mm interspaced grid. All the components of this board are plastic based so do not affect the magnetic fields, it can be seen in Figure 4.8.

Figure 4.8: Pegboard for the winding of different GA coil designs. The Board is a Poly-Ether-Ether Ketone (PEEK) plastic. Screws and fixings are nylon.

The final part of developing a rig that can perform the experimental assessment is incorporating automated measurements. This was achieved via a TCP/IP socket connection to the oscilloscope. This

meant serial commands could be sent from MATLAB to request measurement values. A slight time delay (~0.35s) is needed for each query to prevent the queries clashing with the received data.

4.3.4 Mutual Inductance

Overall the test rig can both position and measure the mutual inductance of coil designs in a repeatable manner. The XYZ range of the motion is approximately 750 mm in X, 600 mm in Y, and 54 mm in Z (the whole rig also can be raised or lowered in 20 mm steps to change the Z range). 8 measurements can be taken from the oscilloscope for each position (maximum number of measurements on most Tektronics oscilloscopes) and approximately 720 positions can be recorded per hour (dependant on number of measurements and interval spacing). Actual position accuracy is ±2mm in X and Y and ±1 mm in Z, relative position accuracy (between positions) is sub-millimetre.

4.3.5 Self-Inductance

Although self-inductance values change less than mutual over the positional ranges, the change is not necessarily negligible and must be accounted for in some configurations. Unfortunately, due to time constraints, measurements of self-inductances are yet to be automated. The self-inductances were measured using a Rhode and Schwarz HM8118 LCR meter at both the point of maximum coupling (or perfect alignment at the closest point) and at the maximum position of the range (or minimum coupling). Positioning was performed using the experimental rig so share the positional accuracy of the mutual inductance measurements. If the self-inductance values differed at the extremes by less than 10% from the value measured at nominal alignment (perfect alignment at the normal height), then the nominal value was assumed for all points.

If, however, the self-inductance values varied by more than 10% from nominal over the position range, then a profile had to be generated. As this profile must be made with manually recorded data-points it had a limited number of samples. These samples were taken for each Z value at the nominal position, the (diagonal) midpoint and the (diagonal) maximum position. Using the property of symmetry, these values were mirrored across the profile. Using interpolation of the points the complete profile was generated. An example is shown below in Figure 4.9.

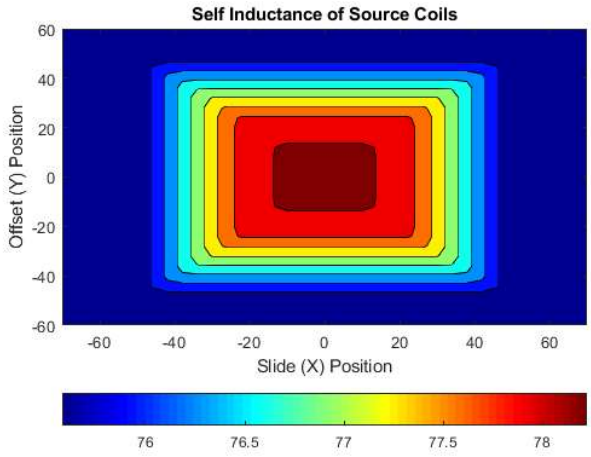

Figure 4.9: Source coil self-inductance profile for the DD coils used in Chapter 5 at Z = 45 mm, units are µH. These profiles were only generated when the self-inductance values varied more than ±10% from nominal, otherwise, the nominal value was used across the whole range. The cause of these variations is the proximity of the second coil which acts to increase the self-inductance of the coil under test.

4.4 Data Processing

MATLAB scripts have been developed to extract the data from both the EXP and FEA results. These scripts also normalise datasets, plot graphs and perform difference analysis. All these scripts have been made open source (MIT license) and are available on GitHub (Abbott, 2018a).

FEA results must be read into MATLAB as <.csv> files, an example can be seen in Figure 4.10. The MATLAB script automatically reads them in as a table and then extracts the information in the header of the files to work out what the values correspond to. The script is capable of reading in and joining the split FEA results (where simulation ranges are broken up) as well as interpreting the correct scale (nH, µH, mH). EXP results are already in a convenient <.mat> file which can be directly read.

	A	B	C	D
1	slide [mm]	Matrix1.L(pickup1,pickup1) [uH] - gap='25mm' offset='0mm'	Matrix1.L(pickup1,pickup1) [uH] - gap='25mm' offset='2mm'	Matrix1.L(pickup1,pickup1) [uH] - gap='25mm' off
2	-50	32.18817	32.07005	
3	-46	32.40202	32.23217	
4	-42	32.41991	32.41371	
5	-38	32.5267	32.60685	
6	-34	32.67193	32.54698	
7	-30	32.6983	32.61039	
8	-26	32.70916	32.79435	
9	-22	32.82533	32.84424	

Figure 4.10: An example of the <.csv> files produced from ANSYS Maxwell simulations. Contents of the column headers and first row must be extracted to get values of position (slide, gap, offset) and inductance unit (nano-, micro-, or milli-Henrys).

The script then begins to calculate the inductances. It uses a command line interface to request from the user the fixed and semi fixed values for the experimental self-inductances. It calculates the mutual inductance for experimental values using the open circuit voltage relationship (Equation 9). It also

then can calculate the mutual inductances for the three operational modes of the FE results for DD coils.

Once all the inductance values are known, the coupling factor is calculated for each position, and then plotting begins. To make the XY plots, the "griddata" function is used. This interpolates the data points and averages where needed to produce a uniform surface. This must be done for every Z value. An example of the resultant plots from the FE study are shown in Figure 4.11.

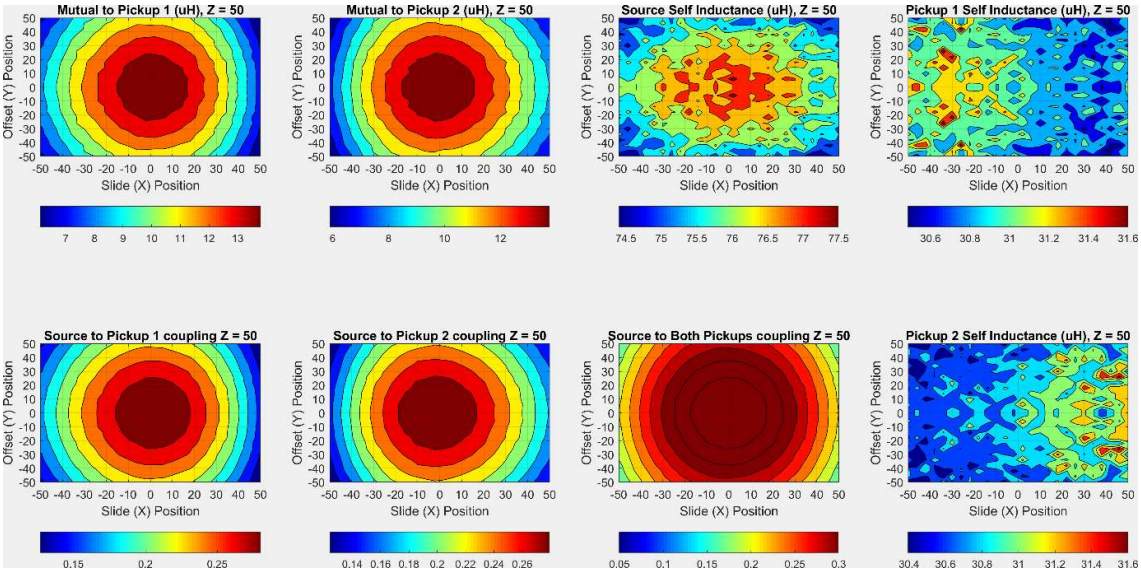

Figure 4.11: Example of the plots produced for every Z value for a FE study.

4.5 FE VALIDATION

The target for validation, as discussed in section 4.1.8 is to have Finite Element (FE) and experimental (EXP) results within ±10% of each other. Once this is achieved, the FE simulations can be considered validated and then they can be used in isolation from EXP. This is particularly useful in studies that would otherwise be difficult to perform experimentally, such as rotational analysis and field measurements.

It is not practical to expect the validation target to be met for every single one of the over 9000 positional point that are being measured. It is more useful instead to consider the overall differences across the measurement range and identify regions where there are significant deviations of the FE and EXP values. By doing this any mistakes or oversimplifications in the FE or EXP methods should be highlighted.

To calculate the differences between FE and EXP results a multi-step process is used. This is because the actual range and sampling interval of the two datasets can differ. First the range is set using the

smaller dataset, the larger dataset is then trimmed to this size. Secondly the shared Z values for both sets are identified. For each dataset and each Z value a uniform surface is generated. These surfaces are then compared to each other at every point and the percentage difference is stored into a third surface. The mean value of this third surface is used for the difference trends (for validation) and the surface itself is plotted to highlight regions where the results differ. This whole process is repeated for each of the mutual and self-inductances as well as the coupling to both individual pickup coils. Some example results are shown in Figure 4.12.

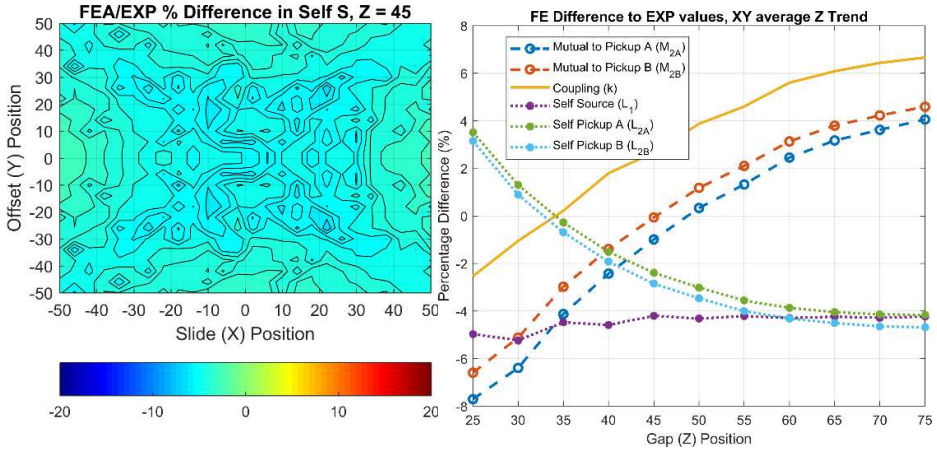

Figure 4.12: (Left) Percentage difference profile between Finite Element (FE) and Experimental (EXP) results for the source coil self-inductance. This shows the self-inductance profile (previously shown in Figure 4.9) is in close agreement to the FE values. (Right) shows the difference average trends over each Z value. It is worth noting that this FE model consistently underestimated self-inductance values, and over-estimated mutual inductance values. The reasons for this are discussed in section 5.6.1.

Other ways to consider the differences between FE/EXP values exist. The process here treats all data points as equal and regions where the values are lower than expected can be cancelled out by regions that are higher than expected, this can result in a net-zero difference. It may be relevant in the future to weight error values in positional space and the magnitude of the readings (for instance, an error at the edge of the range may be less significant than an error at the centre, and a 0.01 µH error has a much bigger % difference on a 0.1 µH value than a 10 µH value). Also, it may be useful to consider absolute error values rather than mean values, thereby preventing underestimated regions being cancelled out by overestimated regions. For this work, however, the method currently employed is well suited to identifying areas where the results differ greatly, and therefore highlighting potential mistakes in either experimental or simulation methods.

4.5.1 Lessons Learnt From Validation

There is no straightforward way to identify what is causing the differences between FE and EXP results. The differences can be introduced from many factors used in both methods. Some of the factors met during this work are listed below and are discussed in more detail in Submission #5. These factors may be of use to developers who find that their FE and EXP results are not meeting the desired validation target.

- **Mistakes** in FE simulation configuration. There are many ways to configure FE simulations, there are also many options that can be controlled. If these are set incorrectly, the results from FE simulations can be wrong. Mistakes were common in the early simulation work, due to a limited understanding of what impact many of the configurations options had. Some of these mistakes included setting distance parameters incorrectly, and missing out some ferrite bars in the CAD of the coil design.
- **Assumptions** in FE calculations for multi-coil grouping. This issue has been largely overcome now, however, in the earlier work (Submission #4) it was a considerable factor. Assumptions that the mutual inductance between multiple coils on a single side (GA or VA) could be ignored generated a difference in FF/EXP results. Later work in Submission #5, showed this was not the case and demonstrated the correct way to calculate the inductance for grouped coils. It also showed the calculations needed to get these results, shown here in Section 4.2.2. After this, the coil grouping function was found in ANSYS that could perform the same calculation. Before the assumption was corrected, it led to a large difference in FE results (discussed in Submission 5).
- **Oversimplification** of the FE CAD model. Some simplifications were made on the CAD so that simulations could be completed quickly, but some of these resulted in great variation in the results. Identifying which simplifications are acceptable, and which are not has been a significant part of the learning process. It has been found that simplifying coil turns as a solid block is acceptable within the 10% validation, however the simplification of multiple ferrite blocks as a single bar does not produce results that are within the 10% target.
- **Material Parameters.** The materials used in construction of the coils must be configured in the FE simulation. Of interest is the ferrite material, which can have a large bearing on the inductance values. The key parameter for ferrite is the magnetic permeability. This is only defined in datasheets to ±20% accuracy.
- **Coil Construction** variations. Normally the coil design would be first modelled in FE and then constructed as an EXP prototype. When the coils are constructed it was common to find that the design could not be built in the same manner, typically the wires could not be wound tight

enough, or they would spread out more than desired. This meant the results differed and the design had to be revised in the FE simulation.

- **Invisible Parameters** in the FE CAD. These are very small geometric gaps in the FE CAD design, of the order of 0.1 mm. One parameter in particular occurs when multiple ferrite blocks are employed to build a ferrite bar, shown in Figure 4.13. In the CAD the blocks must be separated by a defined distance, and it was found changing this value by "invisible" amounts can result in large changes to inductance values. Trial and error was needed to find what value of this invisible parameter produces results that agree with EXP values.

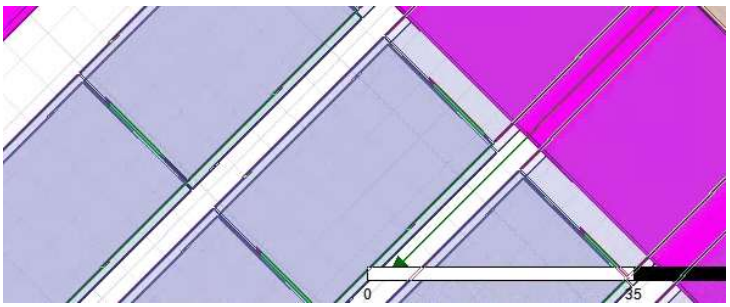

Figure 4.13: Screenshot illustrating the "invisible parameters". Here the separation of the ferrite blocks can be altered by amounts of the order of 0.1 mm. It is not easily visible in the CAD, however the value makes a large difference in the inductance values.

- **Equipment Nuances** with the EXP rig. Overloading the power supplies could occur if the amplitude was set too high. This resulted in the sine wave output becoming distorted or fluctuating greatly, impacting the measured readings. Therefore, care must be taken to ensure this did not occur as the coils moved over the position range. Another issue that created a large problem, is the ADC on the Oscilloscope. It was found at low amplitudes the reported measurements could be 10-15% lower than the actual values (at very low amplitudes there was also a warning displayed on the oscilloscope). If the amplitude was too high, the oscilloscope reported clipping of the signals and the measured values were also inaccurate. Therefore, care had to be taken to ensure the signal amplitudes were kept in the right range. The best way found to do this was to tune the frequency of the supplies to maximum resonance amplitude at the extreme limit of position. This meant as the coils came closer together, the increase in coupling was balanced by the decrease in resonance, meaning the overall signal amplitude remained relatively constant.

4.5.2 Use of the Validated FE

Once the FE simulations have been validated, they can be used in isolation from EXP work with confidence that the results are accurate (within 10% of the experimental values). This means they are particularly valuable for considering rotational operation ranges.

Care should be taken, however, with confidence in the validated FE models once changes to the CAD are introduced. For instance, rotational changes are a relatively small alteration to the CAD so in this case there is high confidence in the accuracy of the results. Larger alterations to things like the coil geometry or material properties can mean the validation is no longer valid. In this case, re-validation must be performed with the desired alterations. It is beyond the scope of this work to consider how various modification of the FE simulations affects the validation accuracy.

4.6 Using MDCM for Coil Design/Mode Optimisation

A two dimensional study was performed by the author that looked into the optimum design of coils (Abbott, Yang and Jennings, 2017). In this work the operation of three GA coil designs (named TST, DD, and ST) operating with one VA coil design (of a DD type) were considered. The coil designs are shown in Figure 4.14.

These coil designs were selected as they shared similar characteristics to the designs proposed by the research teams in KAIST (Su Y. Choi *et al.*, 2014) and Auckland (Zaheer *et al.*, 2016). The TST design is similar to the previous OLEV generations (Park *et al.*, 2015)(Su Y Choi *et al.*, 2015). The lumped DD design is similar to the layout proposed by the research team in Auckland university (Zaheer *et al.*, 2016). The ST design is similar to the proposed layout of the sixth generation On-Line Electric Vehicle (OLEV) from KAIST (Thai *et al.*, 2015).

The sizing of the source coils has been chosen to ensure fair comparison across the designs. The road side track size is 720 mm length and 80 mm in width. Where the tracks are segmented this happens at 80 mm intervals. Track coils are constructed with 6 turns of AWG 20 multi-core non-Litz wire.

In this study the coils were compared over a 200 mm by 200 mm operational region selected in the centre of the range. This region was considered as it would represent an integer number of coil units in the DD and TST designs. As the GA designs are all envisaged for dynamic WPT application, the region would be repeated infinitely along the roadway.

The assessment included both FE and EXP results, however, only EXP values were considered for the comparison. At the time of the study, the FE results had not been validated.

Over the operational region, the mean values of coupling were calculated. TST has an average of 0.066, DD 0.051 and ST 0.076. This is the first way that designers could consider the optimal coil design by selecting the design with the highest average coupling factor.

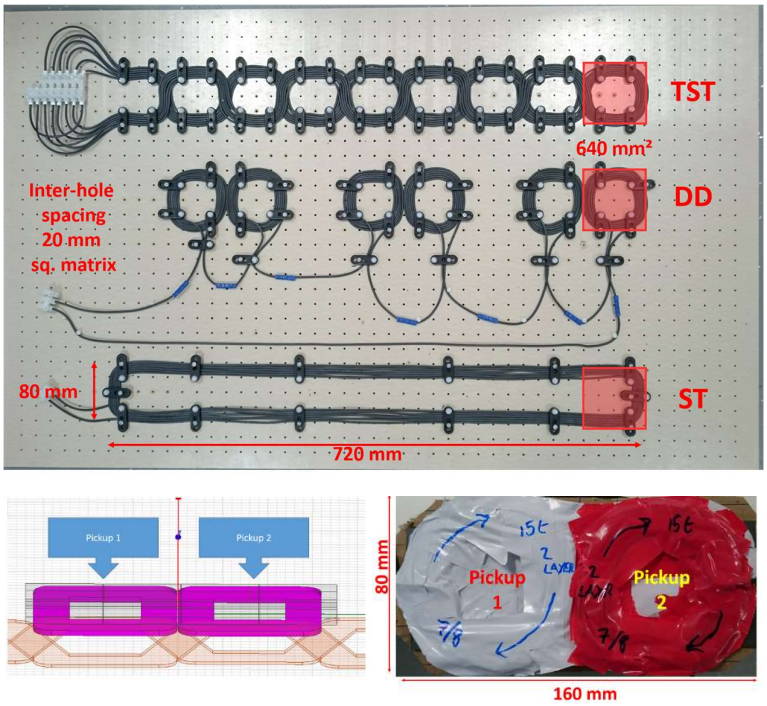

Figure 4.14: Three GA coil designs (top) and one VA design (FE CAD - left, Actual Coils - Right). The three GA coils were named Twisted Stretched Track (TST), Lumped DD (DD) designs and Stretched Track (ST).

Alternatively, the optimal design could be found by considering the proportion of the region that exceeds the minimum coupling value. In this case, across this range, the coupling exceeds 0.1 for 38.4% of the measurements on the ST, 29.3% for TST and 18.0% for the DD. These areas are illustrated in Figure 4.15. This is the second way that a developer could select the optimal coupling design.

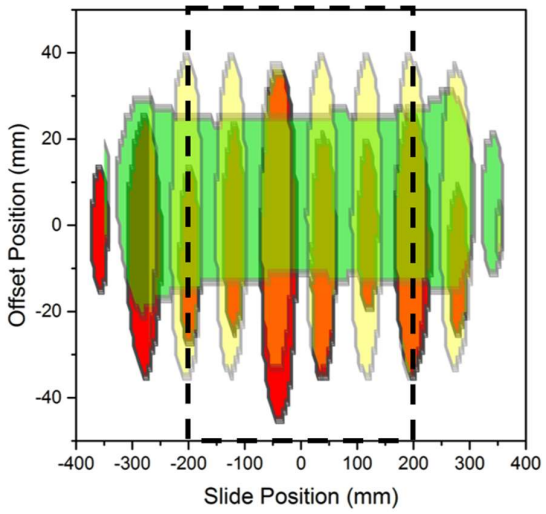

Figure 4.15: Regions with coupling factor greater than 0.1. TST – Yellow, DD – Red and ST – Green. Dashed box represents the operational region considered.

The two options to select the optimal coil design, either average coupling or maximal operational range, produce different results in this example. The TST GA has the highest coupling average, but the ST has the greatest operational range. The choice between either of the options depends on the desired application of the WPT system. Coil designs for compliance to the SAE J2954 standard (as discussed in the next chapter) will not realise significant benefit from higher coupling than the defined minimum. This is because the power output is fixed by the rating of the system, and the efficiencies must be high (>80%) even at the minimum coupling values (SAE International, 2017). Coil electronics similar to those proposed by KAIST, realise a higher power output at greater coupling values (Su Y Choi *et al.*, 2015). These therefore would realise a benefit from the higher average coupling over the position range.

Considering the optimal operational mode is also possible with the MCDM method. The DD GA design on the pegboard had each of the three coil pairs wired into different operational modes. The first and last were non-polarised (but in opposing directions to each other), and the middle pair were polarised. Both polarised and non-polarised operational modes of the VA were then analysed. This is shown in Figure 4.16. This shows that for the polarised GA coil pair, the polarised VA is the optimal operation mode. For the non-polarised GA pairs, the non-polarised VA operation is the optimal operation mode.

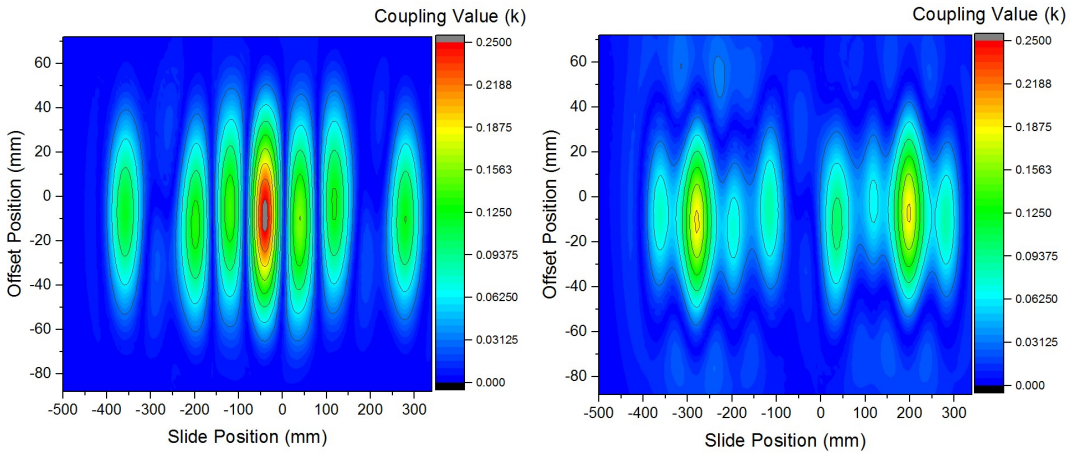

Figure 4.16: Polarised (left) and non-polarised operational modes for the VA coil operating with the DD GA. The three DD GA coil pairs are wired in different modes.

These show how the MDCM method can be used towards assessment of research question Q2:

Q2: How can the optimal GA-VA design/operational mode be identified for a particular operational region?

4.7 Chapter 4 Summary

This chapter considered hypothesis H3:

H3: Multi-dimensional mapping of coupling factor at a high resolution is feasible for both FE and EXP studies.

There are no examples of multi-dimensional mapping of coupling factor in the published works. Most studies have considered single dimensions at a time and only up to 10 readings were taken over the regions. The challenges of performing multi-dimension mapping were considered in this work and the region of operation of WPT systems discussed.

Four reasons to perform high resolution mapping were identified:

- **Characterising a new GA-VA coil pair**
- **To find the operational position range of a GA-VA pair**
- **To find the size needed for a GA-VA to meet a specific operational range**
- **Characterise an unusual coupling factor profile**

To perform multi-dimensional mapping, both FE and EXP methods were needed. FE methods can be used to perform a wide variety of assessments not feasible in EXP studies, however, the results from FE can be inaccurate. By comparing them with EXP results, FE methods can then be validated.

FE simulations and an automated coil positioning and measurement system has been developed for EXP studies. Up to 200 FE simulations per hour (per computer) can be completed, and 720 EXP positional points per hour, can be measured using the discussed equipment. The EXP test rig is has a range of 750 mm in X, 600 mm in Y, and 54 mm in Z. The accuracy of positioning is ±2mm in X and Y and ±1 mm in Z, positional accuracy between measurements is <1 mm in all directions. Methods to process and display the data and perform validation between EXP and FE results were also introduced.

This chapter has shown it is possible to develop methods to study coupling factor over three linear directions of motion (X, Y and Z) for both FE and EXP studies. Rotational studies can be performed also in FE. Due to the high rate of both FE simulations and EXP measurements, and the low cost of the EXP test rig (<£300) it is therefore feasible to perform high resolution Multi-Dimensional Coupling Mapping (MDCM), the hypothesis H3 is therefore proven.

The selection of optimal operation modes and the optimal coil design was then considered for three GA designs operating with a single VA design. This showed that either the highest average coupling or the greatest region where coupling exceeds a minimum value can be used as an optimisation target. The VA operational modes were also considered. This demonstrates how the MDCM method can be used to answer research question Q2:

Q2: How can the optimal GA-VA design/operational mode be identified for a particular operational region?

Note that the assessment of operational modes and optimal designs ignores all effects of real-world electronics and current losses inside the coils. The optimisation shown here is of the coil design in isolation of these factors. The MDCM method could, however, include these considerations in the practical case, as the method can include these limiting factors in the optimisation parameters. For instance, if it is known from circuit simulation that power transfer is only possible in the coupling region of 0.3 to 0.5, then the optimisation could focus on maximising the positional range of these limits.

5 MDCM APPLICATION – SAE J2954 WPT STANDARD

This chapter closely follows the work undertaken in Submission #5. In this chapter the final research questions are considered:

Q2: How can the optimal GA-VA design/operational mode be identified for a particular operational region?

Q3: How can multi-dimensional coupling mapping of small scale prototype GA-VA coil pairs, be used to consider compliance with standards?

Q4: How can multi-dimensional coupling mapping be used to consider the operation of a new coil design (GA or VA) with reference coil designs (such as the TS coils in SAE J2954)?

Q5: How can multi-dimensional coupling mapping be integrated into the WPT development process for a new coil design?

The chapter details an application of the MDCM method that could be highly industry relevant. This is because it is likely, in the future, that designers of WPT systems will have to develop their systems to comply with standards (Transport Research Laboratory, 2015). Here, the only standard currently available, the draft J2954 standard from the SAE (SAE International, 2017), is considered and the methods used to test compatibility are identified. Following on from this, the criteria that must be applied to the MDCM assessment tools to match the J2954 methods are considered.

To demonstrate the process, an example GA and VA coil design, is tested both for compliance with the operational range of SAE J2954 (Q3) and compatibility with the other coil designs provided in the standard (Q4). As the coil design being considered is a scale prototype, the minimum sizing needed for the coils to meet the J2954 operational range at full-scale is identified (Q3). The coil design also has independent coil control of the two coils, this means the different operational modes can be considered. Because of this, the optimal operational mode for the DD coils when they are operating together, and inter-operating with other coil designs is considered (Q3).

Section 5.7 of this chapter considers the process WPT developers use to bring a new coil design from a concept into a SAE J2954 compliant GA or VA coil design. The modification of this process is considered to include the MDCM method and the potential benefits of doing this are identified (Q5).

Although, this chapter focuses on the test methods in the draft SAE J2954 standard, it is likely that all WPT standards will employ similar requirements to ensure interoperation. This means that the

assessment tools are likely to remain valid for consideration of both future revisions of SAE J2954 and for any other standards that may arise in the future. This is discussed further in section 5.8.

5.1 Review of J2954

The SAE J2954 draft standard (SAE International, 2017) discusses the requirements WPT developers must meet to produce a compliant GA or VA for use in static WPT for light duty vehicles. A number of tests must be performed and requirements met before for any new GA or VA can be used in this application. These tests ensure safety, efficiency, and interoperation.

5.1.1 Summary of J2954 Requirements

The first requirement for the GA and VA to work together is that the power ratings of the systems must be compatible. For instance, a 3 kVA rated GA would not satisfy the power desired by a 20 kVA rated VA. The maximum ratings are typically fixed for a coil design, however, it is possible to de-rate the GA to support multiple VA power levels. In SAE J2954 the power rating is signified by the WPT1/2/3/4 value at 3.7/7.7/11.1 and 22 kVA respectively. GAs are expected to be rated to WPT3 or higher and work with all VAs at or below the GA's level. These power levels are similar to the systems demonstrated by the research groups in section 2.3.

The second requirement, once the power level has been satisfied, is that the efficiency of the system is acceptable. For a static WPT, SAE J2954 requires efficiencies >80%. If the efficiency is lower than this, then users may prefer to plug-in to reduce the charge cost. There are also issues with the heat generated, an 11 kVA system at 80% efficiency produces potentially 2 kW of waste energy, predominantly as heat. This could cause the pads to get excessively hot or require significant cooling systems. The required value of efficiency in SAE J2954 is similar to the reported efficiencies from the various research groups studied in the state of the art (section 2.3).

The third requirement for WPT to operate is the proximity of the VA to the GA. The relative position of the coils, or alignment, must be within the operational region of the coils. Outside of the operational region either the coupling between the coils is too low (extreme misalignment, discussed in section 3.2.4) or the electronics powering the coils are unable to accommodate the change in inductance values (extremely close alignment, discussed in section 3.2.5). In both cases, outside the operational region the power levels and efficiency requirements cannot be satisfied. GA/VA proximity is defined in three linear directions and three rotational axes. In J2954 these are specified as follows:

- X Direction – From the driver's seat of a vehicle this is forward/backward.
    - X = 0 is defined as the centre-point of the GA (or can be specified by GA manufacturer).
    - X range is ±75 mm

- Y Direction – From the driver's seat this is left/right direction.
    - Y = 0 is defined as the centre-point of the GA (or can be specified by GA manufacturer).
    - Y range is ±100 mm
- Z Direction – From the driver's seat this is up/down direction. A few definitions of Z are used:
    - SAE J2954's standard Z definition is that Z = 0 when the lowest point of the VA is touching the ground, i.e. the ground clearance of the VA. See Figure 5.1.

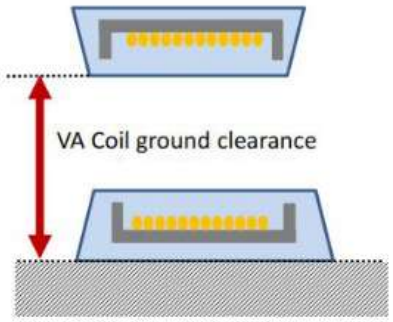

Figure 5.1: SAE J2954's standard definition of Z classification. From (SAE International, 2017).

        - Z classifications are Z1 (100-150 mm), Z2 (140-210 mm), and Z3 (170-250 mm)
    - Magnetic Z gap is that Z = 0 when the magnetically active points (the extreme points ferrite and coils) of the GA are touching the VA. See Figure 5.2.

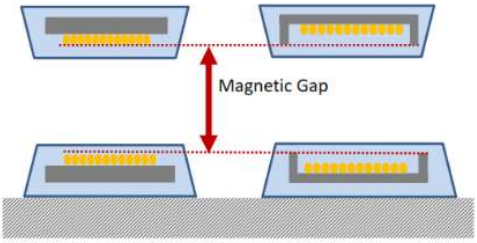

Figure 5.2: Definition of Z magnetic gap. From (SAE International, 2017).

    - Air gap Z is that Z = 0 when the GA casing is touching the VA casing. See Figure 5.3.

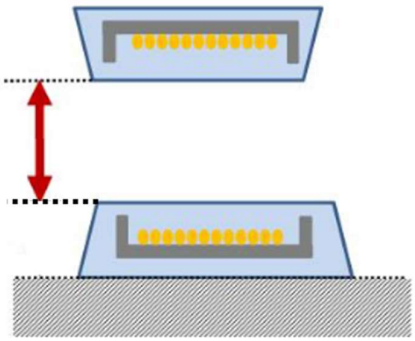

Figure 5.3: Definition of Z air gap. Modified From (SAE International, 2017)

- Yaw Rotation – Rotation around the Z axis
  - ±10 Degrees range
- Pitch Rotation – Rotation around the Y axis
  - ±2 Degrees range
- Roll Rotation – Rotation around the X axis
  - ±2 Degrees range

The next requirement is that the GA and VA have a compatible resonant frequency. This is because efficient WPT relies on the frequency of resonant oscillations between the induction coils and resonant capacitors within both the GA and VA to closely match. The range of frequencies in SAE J2954 are from 81.38 to 90 kHz. To ensure this across the operational range of proximity some tuning of the electronics is employed. This can account for small changes in frequency, within this range, if the GA or VA resonant frequency lies outside this range efficiencies will be very low or the system will not function at all (Kamineni, Covic and Boys, 2016).

The frequency band proposed is higher than most groups have demonstrated in systems in the state of the art, section 2.3. By increasing the frequency, from the commonly demonstrated 20 kHz, to the 85 kHz frequency potentially offers higher efficiency. The agreement on this band is based on experiences from people in the automotive sector whom work with the global standards and agreements such as those from the IEC, CISPR, and ICNIRP (Obayashi and Ev, 2014), so help to ensure the final WPT devices should meet EMC requirements.

5.1.2 Aside on Z Classification

The SAE has made the decision to classify WPT systems based on the ground clearance of the VA coil, rather than the GA to VA spacing (shown in Figure 5.1). This means the thickness of the GA is ignored. Therefore if a GA is designed to be thicker, and therefore the position of its coil(s) is closer to the VA,

it could potentially claim a greater Z classification. This means, for WPT developers, there can be benefits to designing thick GAs.

5.1.3 J2954 Test Stand Designs

SAE J2954 (SAE International, 2017) proposes two test methods to ensure different coil designs are compatible. The first is to test complete GAs or VAs together with a set of "Test Stand" (TS) GA/VA designs. The second method is to test GAs only and measure the flux through two probes.

20 Test Stand (TS) designs are given in J2954 in the form of engineering diagrams of the coils and circuit diagrams of their powering electronics. These are provided in various appendices at the end of the document. An example of the information provided is shown in Figure 5.4.

The details included for the TS coil designs in J2954 are very useful to WPT developers as they can provide inspiration for new WPT concepts. These TS designs have been demonstrated as functional by the members of the standard. The details are more engineering focused than those available in other published work so should be easier to reproduce.

There are, however, some details missing. Missing details include the ferrite material used in all the designs, the number of turns in one of the coil designs, the circuit diagrams do not specify component suppliers or product codes, and some of the engineering drawings lack enough detail for accurate reproduction. An example of these issues is shown in Figure 5.5. A developer, therefore, may need to make an educated guess at numerous parameters to build the complete TS assembly.

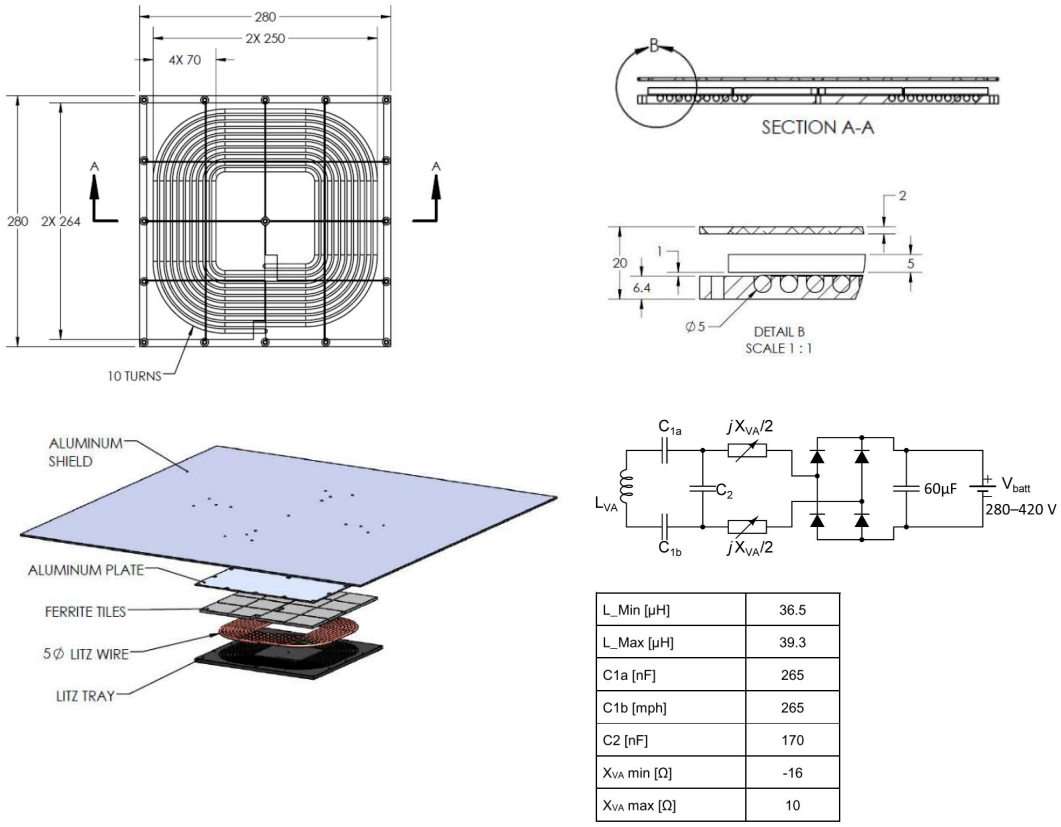

L_Min [µH]	36.5
L_Max [µH]	39.3
C1a [nF]	265
C1b [mph]	265
C2 [nF]	170
X_{VA} min [Ω]	-16
X_{VA} max [Ω]	10

Figure 5.4: Information given for the J2954 TS design in appendix A.4 of the standard. This is a VA TS design for a WPT2 level Z1 classification.

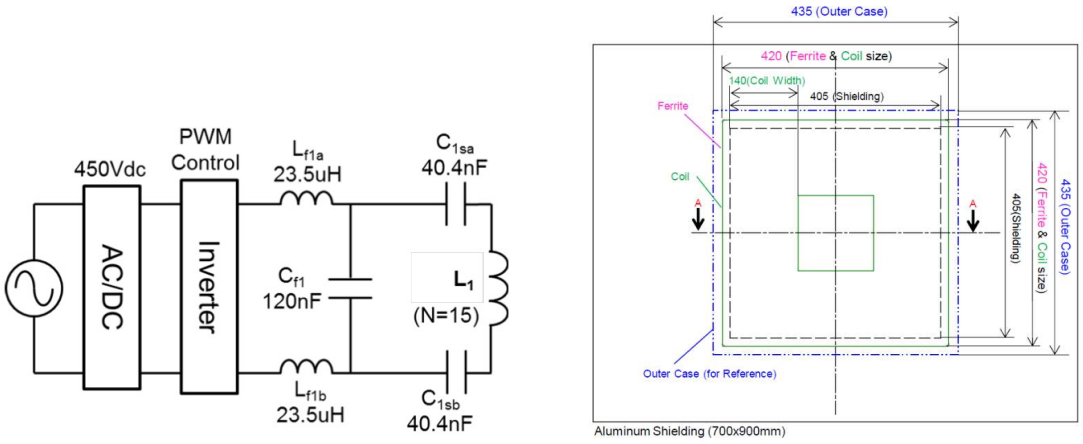

Figure 5.5: An example of some of the less detailed information in J2954. Developers are left to fill in the gaps in the electronic design of the inverters and electronic components in the GA-TS design from appendix C.1.2 (left). The TS design from appendix A.3 is missing the number of turns in the coil design.

The TS designs are still only provided in an "informative" basis, this means designs are still subject to change in later revisions of J2954. There are currently no TS designs given for the highest power level category (WPT4) or for "flush mount" GA. Flush mount is where the GA would be built into the floor and not protrude above the roadway. These shortcomings are considered in appendix R.1.2 of J2954 and are noted to be covered in later revisions of the standard.

5.1.4 First Test Method

The first method applies the hypothesis that if all GAs and VAs work with their defined set of GA/VA TS designs, then they should all work with each other. A diagram of what this means is shown in Figure 5.6.

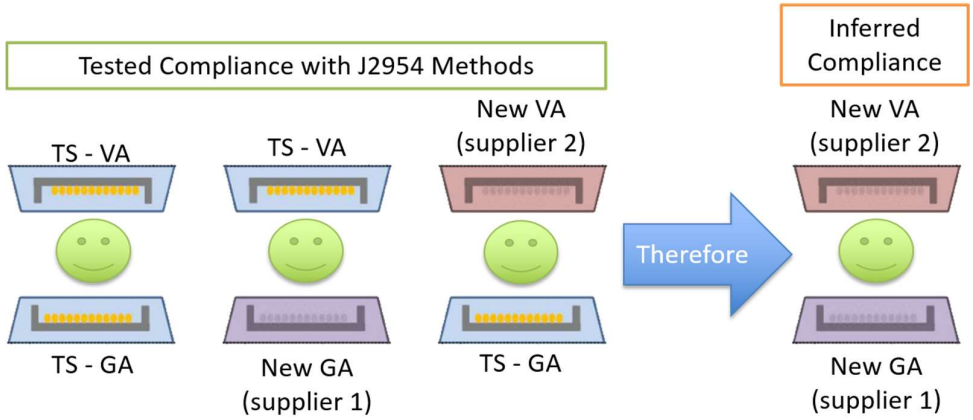

Figure 5.6: The hypothesis of the first test method in J2954. Modified from (SAE International, 2017). *TS-TS testing has been performed within the standard, and the standard requires any new GA or VA to be tested and compliant (using J2954's method) with the TS designs it should work with. The assumption is that as long as any new GA or VA passes the compliance tests with the TS coils, they should therefore work together.*

SAE J2954 states this about the validation of their method (from appendix R.1.1):

"During testing in mid 2016, extensive data was taken on …three GAs and eight VAs for WPT1 and WPT2 to determine performance in configurations that included only devices from one manufacturer (matched systems) and in configurations which included devices from two manufacturers (interoperable configurations). Data was recorded on input power, output power and power factor at optimal positions, as well as minimum and maximum offsets in X, Y, and Z for output voltages of 280 V, 350 V and 420 V. Additional informative "sniff" data was taken for B field and E field, and in some cases, temperature. Efficiency was calculated. This data was tabulated and one system for each WPT class was selected as the Normative Test Stand GA and VAs shown in Appendices A and C. The other system is given in Appendices B and D."

They go on further to state WPT3 level systems and flush mount GA (not protruding from road surface) validation will be performed in subsequent revisions of the standard, pending the collection of results.

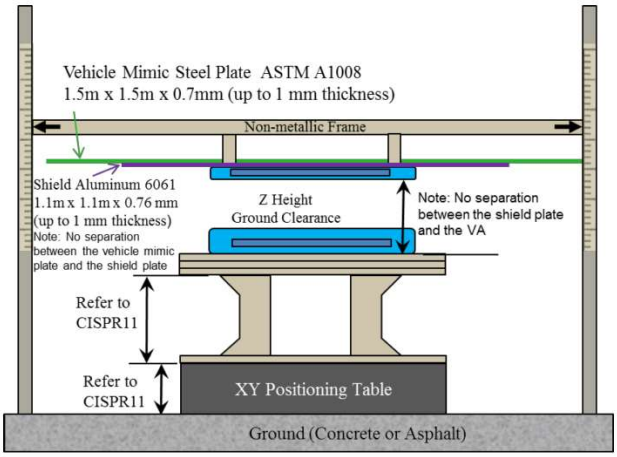

Figure 5.7: Test Stand experimental design diagram showing the stage and mount to position the GA and VA for testing. From (SAE International, 2017).

Figure 5.7 shows the advised experimental setup to perform assessment of coil compliance with the standard. This should be able to position coils to ±1 mm, and servo motor control via a computerised system is recommended. The GA-VA pairing being tested is expected to operate at nominal position and at the extreme limits of operation (±75, ±100, Z_{range}). Efficiency at nominal must exceed 85%, measured as the power into the DC bus of the vehicle compared to the power in at the mains. Efficiency at the extreme operational limit points should exceed 80%. Rated power output should also be met, as well as communication, thermal tolerances, EMC compliance, electromagnetic field limits, foreign object detections and power factor.

The testing processes within SAE J2954 are well supported and documented. The research groups involved in developing the standard include many of the groups discussed in the state of the art (Section 2.3). Although there is no evidence directly supporting the claim that compliance of new GA-VA pairings can be inferred from their previous compliance with the TS GA/VA (shown in Figure 5.6), the SAE is confident in their approach. Once a number of J2954 compliant GAs and VAs have been developed it will be possible to test the assumption further.

5.1.5 Second Test Method (J2954 -Appendix H)

The second method is in the early stages of development and many details are yet to be formalised. It tests GA designs with two flux measurement probes. These probes measure the co-axial and longitudinal flux fields. Assuming the values are within defined ranges, then the flux from the GA

should be compatible with the required VAs. The ranges given in this method are noted to be subject to change and the method itself is not finalised.

The second method in J2954 potentially offers a simpler way to test GA designs, however, this method is currently for “informative” purposes only, and many parts and values are “subject to further investigation”. This could mean any testing could be nullified with the release of the future revisions of J2954.

5.1.6 Component Level Testing

SAE J2954 expresses support for component level testing, this means individual functional units of WPT systems can be assessed independently of each other. By doing this, components can be assessed earlier on in the development process, as a complete system is not needed. For developers, it also makes tracking down issues causing non-compliance easier to find as there are fewer functions present.

Currently J2954 offers component level testing down to separation of the GA and VA. This means GAs and VAs can be tested independently for compliance. This requires both the complete coils and electronics for testing. There is currently no way to test GA/VA coils at a lower component level in J2954. This means complete GA and VA units must be produced before they can be tested, these must include the powering and control circuitry. Also, all the TS assemblies, that the GA/VA should be compatible with, must also be constructed. This means testing a coil design for compatibility with J2954 is only possible at the late stages of development of new coil designs.

J2954 discusses the re-use of the TS electronic designs for the component level testing of new coil designs (section 14.2.3). This could be possible to perform, depending on the flexibility of the electronics chosen by the WPT developer. As mentioned previously, J2954 only specifies the circuit diagram and suggest some component values. The WPT developer must design the PCB and select suitable components for the GA or VA of interest..

5.1.7 Coupling Factors

Coupling factors are not specified as a requirement in the J2954 standard. However, for informative purposes the maximum and minimum coupling factors have been included for the TS reference coil designs.

Minimum coupling values are reported as 0.088, 0.126, 0.087 and 0.136 for the GA coils in J2954 appendices C.2, D.1, E.1.1 and E.2.1.1 respectively. The maximum coupling factors for these coils are 0.245, 0.344, 0.232 and 0.397 respectively.

5.2 Traffic Light Assessment

Q3: How can multi-dimensional coupling mapping of small scale prototype GA-VA coil pairs, be used to consider compliance with standards?

As discussed and evidenced in Chapter 3, coupling factor can be used as the sole measurement to consider if a GA-VA pairing are magnetically compatible (H1). This hypothesis can therefore be used here to asses a GA-VA coil pair for compliance. Based on other findings in Chapter 3, only the minimum coupling factor needs to be considered. As the TS designs are validated in J2954 into complete WPT systems, it can be assumed that the efficiency requirements of J2954, and therefore the electronics to power the GA/VA coils, have been made to work at these coupling values.

To make the assessment clear a traffic light colour system is used in this work. These values are rounded to the nearest 0.01 from the values of coupling reported in the TS designs in J2954, discussed in the previous section:

- **RED** - Where coupling values are less than 0.09, the system is considered magnetically incompatible as the GA/VA electronics will have difficulty satisfying the efficiency requirements of J2954. This is evidenced by the fact no TS designs are compliant in this range of coupling. For this reason, these regions are shown in red.
- **YELLOW** - When the coupling is between 0.09 and 0.11, the compatibility is not guaranteed, but it is possible to develop the electronics in the GA/VA to satisfy J2954. This is evidenced by the fact some TS designs are compliant in this range of coupling. These regions are shown in yellow.
- **GREEN** - Above 0.11, electronics for the GA/VAs that satisfy J2954's efficiency requirements are assumed to be readily available. This is evidenced by the fact all TS designs are compliant in this range of coupling. So, these regions are shown in green.

The values used for the traffic light colour system could be subject to change in future revisions of J2954.

5.3 Example GA-VA Pair

To further the assessment process an example small scale GA and VA coil was needed. Ideally the GA/VA would have independent control of the coils, to look at the differences caused by the changing operational modes. Fortunately, another researcher at WMG, Alex Ridge (AR) of the Power Electronics group, had designed and constructed a suitable coil set that could be used for this study. It is a

symmetric Double-D (DD) design. This design includes both a GA and VA coil that are identical to each other. The design is shown in Figure 5.8.

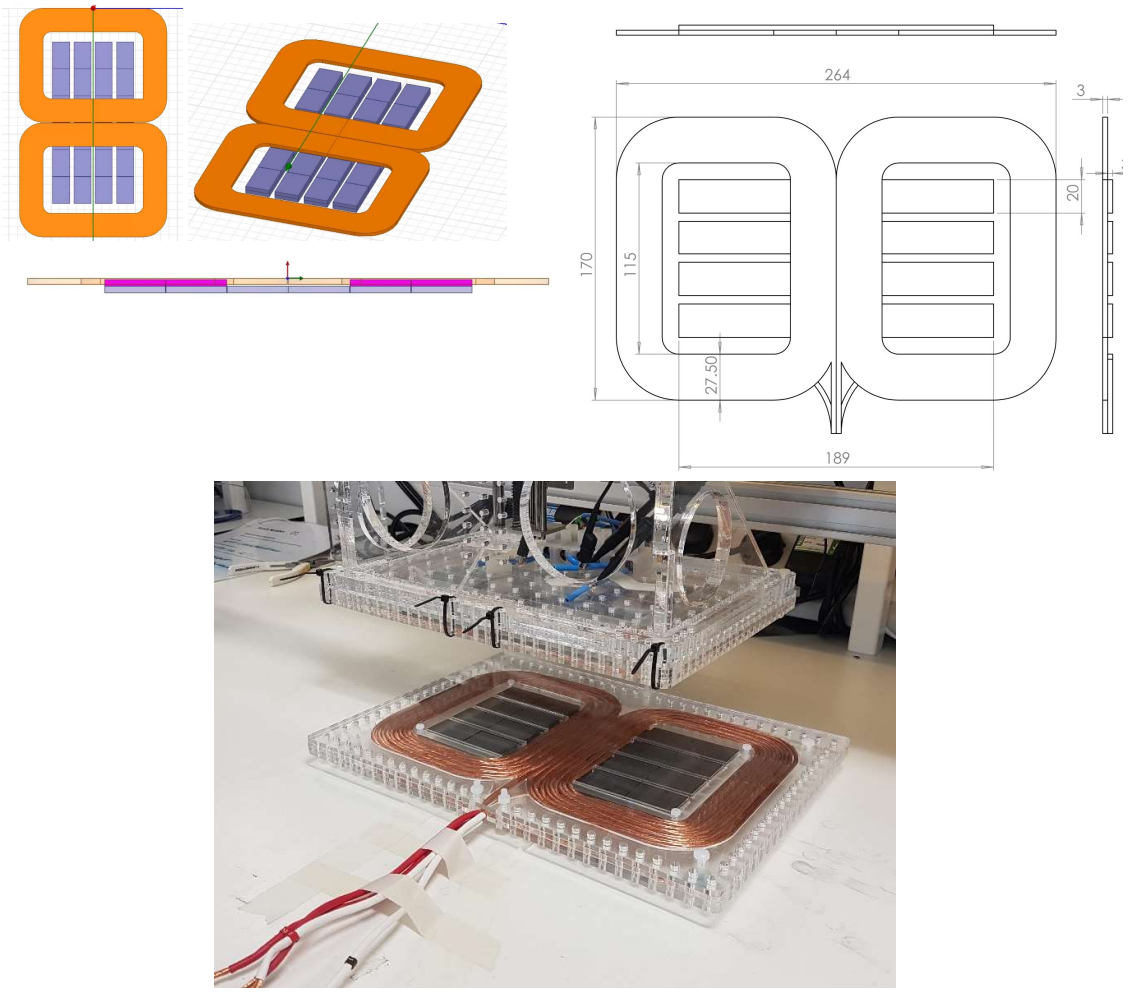

Figure 5.8: Screenshot of the finite element 3D CAD design (top left), Engineering drawings (top right), and a photo (bottom), of the DD coil design studied. Dimensions are shown in mm, note that there is a small variation in constructed coil dimension compared to original design. Coils were designed and constructed by AR.

The assembly for the coils is acrylic and fastened with nylon screws. No shielding is used in this assembly for simplicity. 4 acrylic sheets of 3mm thickness were used to hold the ferrite and coils in position for each assembly.

The coils consist of 10 turns of copper Litz wire. The wire is 100 strands of 0.2 mm diameter enamelled copper wire. 4 Ferrite bars are used, consisting of 10 N87 PLT32/20/3.2 blocks in each bar. These blocks are double stacked within the area inside the coils.

The coil terminals can be connected independently, so they can be operated in three operational modes depending on their connection to the power supply. As the DD coil is symmetrical, only one of the two coils need to be considered for the single coil mode.

The dimension of the constructed coils (minus casing) is 273 mm by 173 mm in the XY plane.

5.3.1 Scale of Example Coils

Table 3 compares the example DD coil's dimensions to each of the TS designs. Compared to the mean of GA TS design discussed in the appendices of J2954, the DD coil is 0.34 the scale. Compared to VA TS average dimensions it is 0.68 scale.

Table 3: Summary of the 20 TS designs proposed in the appendices of J2954. This includes approximate external coil dimensions. Scale is compared to the size of the DD coils proposed in this work.

Appendix	VA/ GA	No. of Coils	WPT Class	Z Class	Style[a]	Coil External Dimension in X (mm)	Coil External Dimension in Y (mm)	X Scale to DD[c]	Y Scale to DD[c]	Mean Scale to DD[c]
A.1[b]	VA	1	WPT1	Z1	A	300	300	0.91	0.58	0.74
A.2	VA	1	WPT1	Z2	A	355	355	0.77	0.49	0.63
A.3	VA	1	WPT1	Z3	A	435	435	0.63	0.40	0.51
A.4	VA	1	WPT2	Z1	B	280	280	0.98	0.62	0.80
A.5	VA	1	WPT2	Z2	B	350	350	0.78	0.49	0.64
A.6	VA	1	WPT2	Z3	B	420	420	0.65	0.41	0.53
B.1	VA	2	WPT2	Z1	C	240	250	1.14	0.69	0.91
B.2	VA	2	WPT2	Z2	C	330	250	0.83	0.69	0.76
B.3[b]	VA	2	WPT2	Z3	C	390	350	0.70	0.49	0.60
C.1	GA	1	WPT1	Z3	D	675	591	0.40	0.29	0.35
C.2[b]	GA	1	WPT2	Z3	E	750	600	0.36	0.29	0.33
D.1	GA	2	WPT2	Z3	F	650	635	0.42	0.27	0.35
E.1.1	GA	1	WPT3	Z3	G	750	600	0.36	0.29	0.33
E.1.2	VA	1	WPT3	Z1	B	300	300	0.91	0.58	0.74
E.1.3	VA	1	WPT3	Z2	B	350	350	0.78	0.49	0.64
E.1.4	VA	1	WPT3	Z3	B	420	420	0.65	0.41	0.53
E.2.1.1[b]	GA	2	WPT3	Z3	F	650	635	0.42	0.27	0.35
E.2.1.2	VA	2	WPT3	Z1	C	310	210	0.88	0.82	0.85
E.2.1.3	VA	2	WPT3	Z2	C	380	260	0.72	0.67	0.69
E.2.1.4	VA	2	WPT3	Z3	C	460	330	0.59	0.52	0.56
DD Coil[c]	VA/GA	2	-	-	-	273	173	1	1	1

[a] Style denotes coil designs that are similar, differing only in dimensions and/or number of coil turns
[b] Denotes coil designs have been selected for FE interoperability study with the DD coil design
[c] The DD coil design of interest in this work used for scale comparison.

5.3.2 Aside: Is the example coil a Bi-Polar Pad (BPP) or DD coil design

It has been discussed that the example coils in this work are actually Bi-Polar Pads (BPP) rather than DD coils. This argument arises because the coil's operational mode can be independently controlled (hence BI-polar), whereas DD coils typically would be wired in a fixed polarised mode and therefore cannot.

The author has decided to continue to use the DD coil name for the example coil design in this chapter. This is because in the published works BPP designs typically overlap the two coils, see Figure 3.1. The

coil example here does not have the coils overlapped. The other reason is that AR, the designer of the coils, referred to the design as DD coils. Ultimately, it makes no difference to the study what the coils are named.

5.4 Intervals for High Resolution Mapping

The standard study area selected for this work is ±50 mm in X and Y and 25-75 mm in Z. This is 0.5 the full-sized J2954 range in Y and 0.67 the full-sized range in X. Where necessary, this standard range has been extended in this work to accommodate a number of different studies.

Based on the rate of FE simulations (200 per hour per computer) and EXP measurements (720 per hour) from Chapter 4. The sampling interval could be selected. The author decided that three days (72 hours) should be the maximum acceptable time to complete the study. A few factors guided this decision:

- If the simulation or experimental setup is to fail due to unexpected factors, such as a power cut, or a computer running out of memory and crashing, then the data loss of three days' work is not too critical.
- Studies can be configured on a Friday to complete over the weekend, reducing the risk of the equipment being knocked or tampered with in the laboratory.
- Although ANSYS could cope with larger studies by splitting them up into regions consisting of ~3000 positional points, the completed datasets still needed storage of the order of 100-200 GB. Hard disk space started to become a significant concern, particularly on computers with Solid State Disks (SSDs) which have less storage capacity (200-500 GB). Therefore to avoid the issue of running out of storage space, the total number of sample points should be limited to around about the same number of points possible in three days of simulation time.
- The experimental studies would need to be repeated three times, for each operational mode. This means, a three day study would need nine days to collect a complete dataset for the three operational modes.
- The validation process was still not complete at the time of the experimental design, therefore a number of simulation and experimental runs could be needed. As discussed in Submission #5, it actually took nine runs to meet the validation target. This had to be considered in the timescale of the doctorate.

With 72 hours to complete a study, 14,400 FE simulations or circa 52,000 EXP positional points can be recorded. Through some trial and error in interval selection the final configuration of interval measurements was developed as shown in Table 4.

*Table 4: Range and interval chosen for three dimensional study for compliance with J2954. *For FE studies, due to the symmetry of the CAD, data was only collected for positive Y values and mirrored into the negative Y range.*

Variable	Range (mm)	Interval (mm)	Data Points - EXP	Data Points - FE
X (±50 mm)	100	2	51	51
Y (±50 mm)	100	2	51	26*
Z (25-75 mm)	50	5	11	11
		Total	28,611	14,586

5.5 EXAMPLE GA-VA PAIRING RESULTS

In this section the results from the studies for the three operational modes are considered. Only the EXP coupling profiles are shown, as these look identical to the FE coupling profiles (as expected with a 10% validation target). The coupling results have also been summarised in section 5.5.4.

An FE study was performed for both rotational and TS interoperability consideration.

5.5.1 Polarized Mode

The self-inductance of the series-connected source coils were measured as 78.61±0.03 µH at (0,0,45), 90.18±0.03 µH at (0,0,25) and 72.97±0.03 µH at (50,50,75). Because these vary by more than 10%, a self-inductance profile was generated, as discussed in section 4.3.5, for the experimental results. The self-inductance of pickup A was 31.08±0.03 µH and pickup B was 31.07±0.03 µH at (0,0,45), and did not vary by more than 10% over the range, so a constant value was used.

For validating the FE model, the average difference of key parameters across the range of Z slices is shown in Figure 5.9. This will highlight if FE values significantly deviate from the experimental values. The target is for the percentage difference to remain less than ±10%.

The experimental coupling values for three Z slices are shown in Figure 5.10. These map the coupling of the coils in the XY plane for each Z slice. Table 5 summarizes the maximum and minimum experimental coupling values found in the ±50 mm range of X and Y.

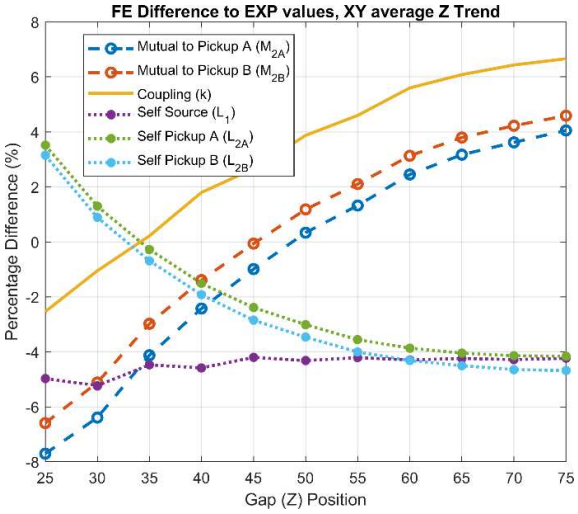

Figure 5.9: The difference trends of finite element results against the experimental values for the polarized operational mode, mean difference value for the ±50 mm XY range.

Table 5: Polarized EXP Coupling factor limits for ±50 mm XY Contours.

Z Value (mm)	Coupling Max	Coupling Min
25	0.641	0.213
35	0.507	0.180
45	0.398	0.152
55	0.314	0.129
65	0.250	0.110
75	0.200	0.093

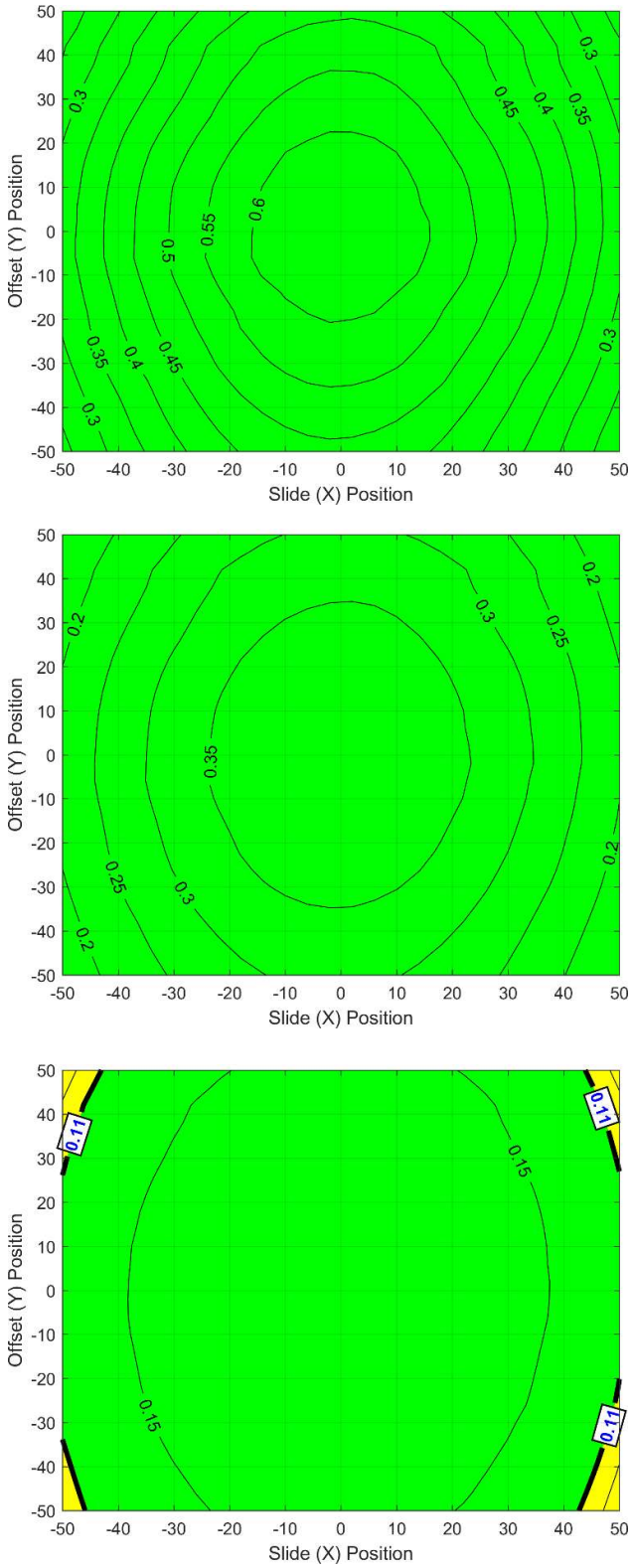

Figure 5.10: Experimental coupling values for polarized operational mode at three Z positions, 25 mm (top), 45 mm (centre) and 75 mm (bottom). Coupling factor values are recorded on contours at 0.05 intervals. Colours indicate magnetic compatibility as discussed in section 5.2.

5.5.2 Non-Polarized Mode

In non-polarized mode, the self-inductance of the source coils was measured as 43.98±0.03 µH at (0,0,45), and did not vary by more than 10%. The self-inductance of pickup A is 31.08±0.03 µH and pickup B was 31.07±0.03 µH at (0,0,45), these did not vary by more than 10% over the range. Therefore, all self-inductances of this mode were fixed for experimental measurements.

The differences between the simulated and experimental results across every Z slice are shown in Figure 5.11. The experimental coupling contours for three slices are shown in Figure 5.12 and are summarized in Table 6.

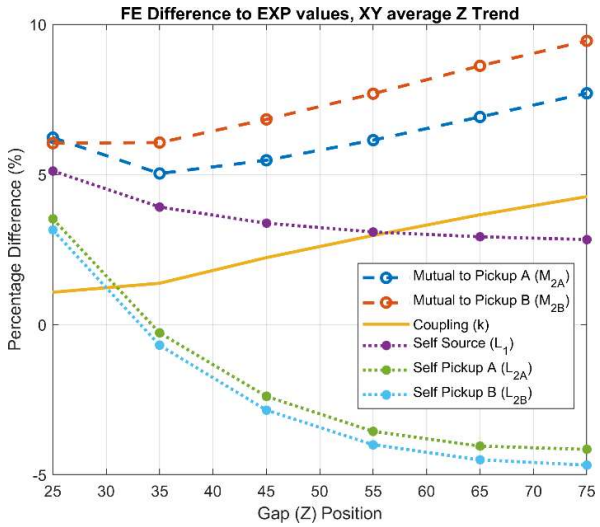

Figure 5.11: The difference trends of finite element results against the experimental values for the non-polarized operational mode, mean difference value for the ±50 mm XY range.

Table 6: Non-Polarized EXP coupling factor limits for ±50 mm XY Contours.

Z Value (mm)	Coupling Max	Coupling Min
25	0.256	0.063
35	0.191	0.051
45	0.147	0.043
55	0.118	0.036
65	0.096	0.030
75	0.082	0.026

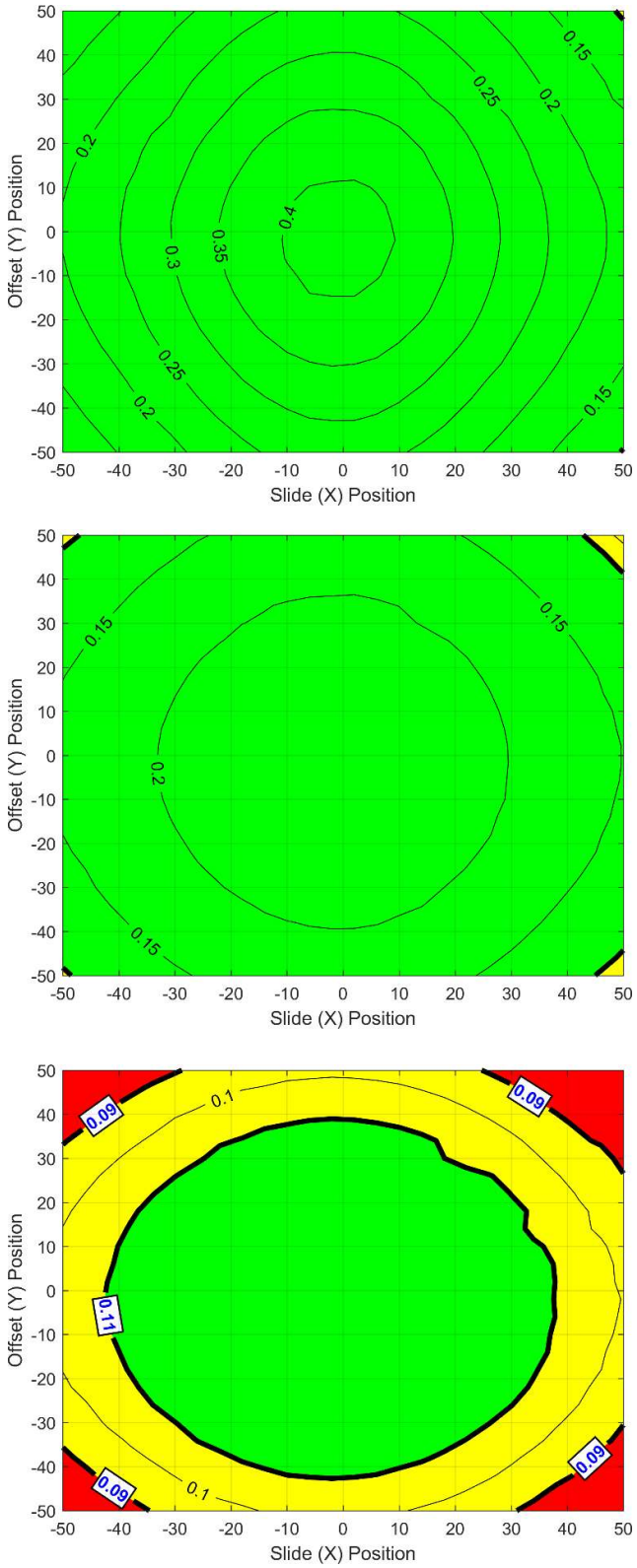

Figure 5.12: Experimental coupling values for non-polarized operational mode at three Z positions, 25 mm (top), 45 mm (centre) and 75 mm (bottom). Coupling factor values are recorded on contours at 0.05 intervals. Colours indicate magnetic compatibility as discussed in section 5.2.

5.5.3 Single Coil Mode

The self-inductance of the source coils in this mode was measured as 30.80±0.03 µH at (0,0,45), and did not vary by more than 10%. The self-inductance of pickup A is 31.08±0.03 µH and pickup B is 31.07±0.03 µH at (0,0,45), these values do not vary by more than 10% over the range. Therefore, all experimental self-inductances are fixed.

The differences between the simulated and experimental results across every Z slice are shown in Figure 5.13. Note, that although the mutual inductance to pick up B is shown here and is outside the ±10% target, the actual values of mutual inductance for this pickup are negligible as only pickup 1 is over an active source coil.

The experimental coupling contours for three slices are shown in Figure 5.14 and are summarized in Table 7. Figure 5.15 shows an extended range in X for the Z = 45 mm contour.

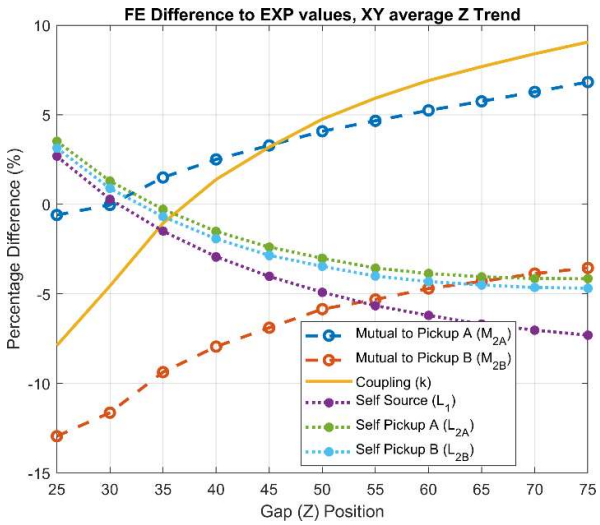

Figure 5.13: The difference trends of finite element results against the experimental values for the single coil operational mode, mean difference value for the ±50 mm XY range.

Table 7: Single Coil EXP Coupling factor Limits for ±50 mm XY Contours.

Z Value (mm)	Coupling Max	Coupling Min
25	0.906	0.276
35	0.663	0.215
45	0.498	0.170
55	0.385	0.136
65	0.302	0.110
75	0.241	0.090

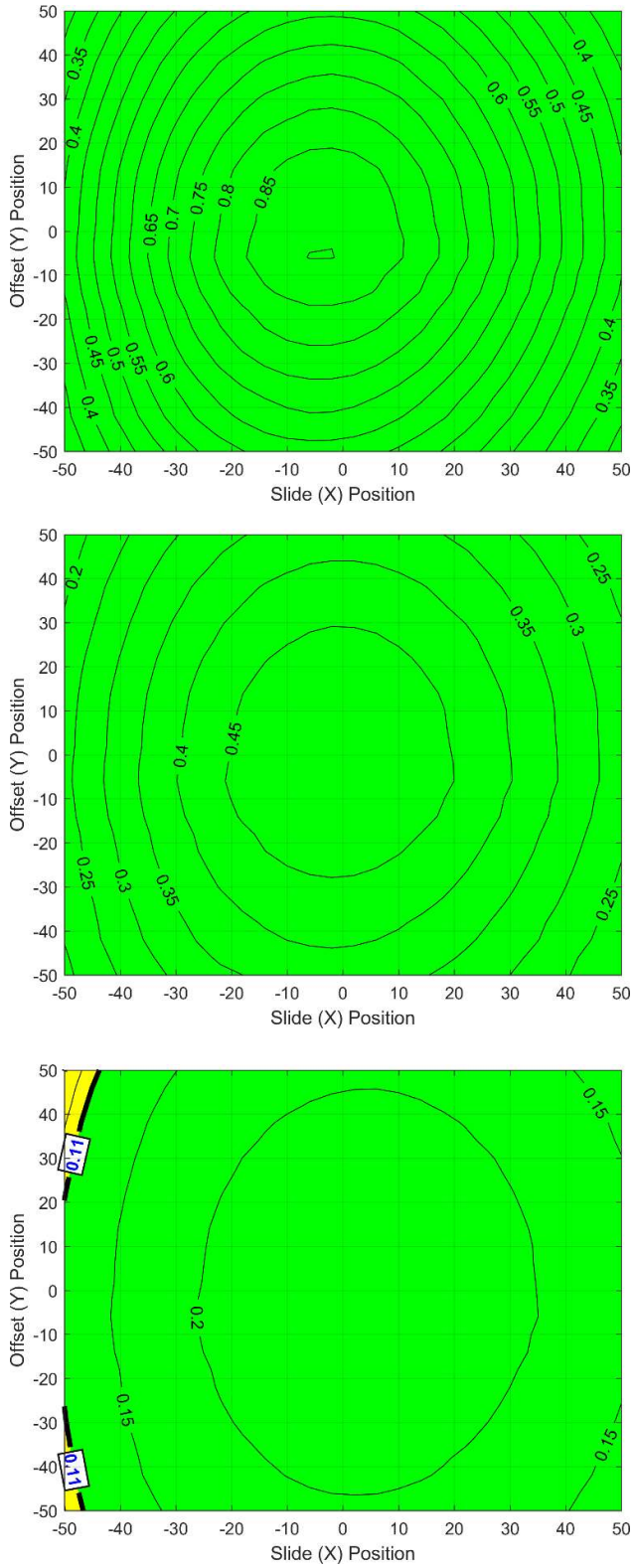

Figure 5.14: Experimental coupling values for the single coil operational mode at three Z positions, 25 mm (top), 45 mm (centre) and 75 mm (bottom). Coupling factor values are recorded on contours at 0.05 intervals. Colours indicate magnetic compatibility as discussed in section 5.2.

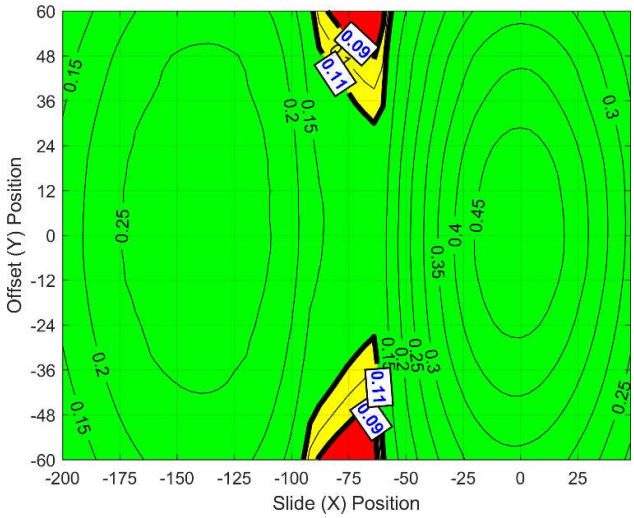

Figure 5.15: Experimental coupling values for the single coil operational mode at Z= 45 mm, showing coupling at an extreme X offset, as the second pickup coil becomes aligned with the first source coil.

5.5.4 Coupling Summary for the Three Modes

Figure 5.16 shows the histogram for the coupling values for all measurements taken in the ±50 mm in XY and 25-75 mm in Z region. It has been normalized to the number of samples in each mode and placed into 500 bins across the 0-1 range.

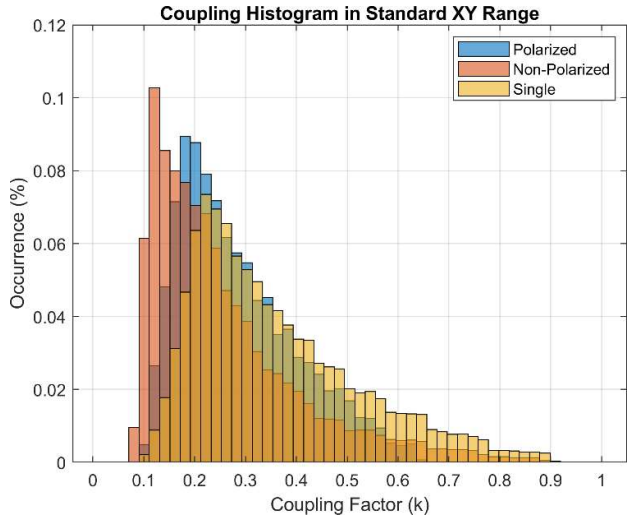

Figure 5.16: Histogram for the coupling factors recorded in the (±50, ±50, 25-75) range for the three operational modes.

This study shows the single coil operation mode has the highest average coupling, followed by the polarized mode. The non-polarized mode has the lowest average coupling.

5.5.5 Rotational Offsets

Having validated the DD coil FE simulation for all its operational modes. The rotational offsets were considered using FE simulation only. This found that the coupling values by up to 16% for the polarized

mode, up to 9% for the non-polarized mode and up to 38% for the single coil modes, compared to the non-rotated value. The rotational offset could increase or decrease the coupling factor.

5.5.6 Compatibility with J2954 TS Designs

Having validated the DD coil FE simulation for all its operational modes. A study of the interoperability of the DD coil with the TS coils could be performed that only uses FE simulations.

The first TS study is with the VA (single) coil from appendix A.1. The DD coil replaces the GA coil from appendix C.1, the VA was scaled to 0.35 of its original size. This model is shown in Fig.15 with contour plots for the coupling of the coils at 45 mm. This Z value would correspond to 190 mm at full scale, assuming the complete DD assembly is the same thickness as TS-C.1, 62 mm.

A natural offset of (-70, 0, 45) has also been applied to the final contour plot to demonstrate the effect of the J2954 solution (section 13.7) used for the operation of single coil VA with a dual coil GA. This is also shown in Figure 5.17.

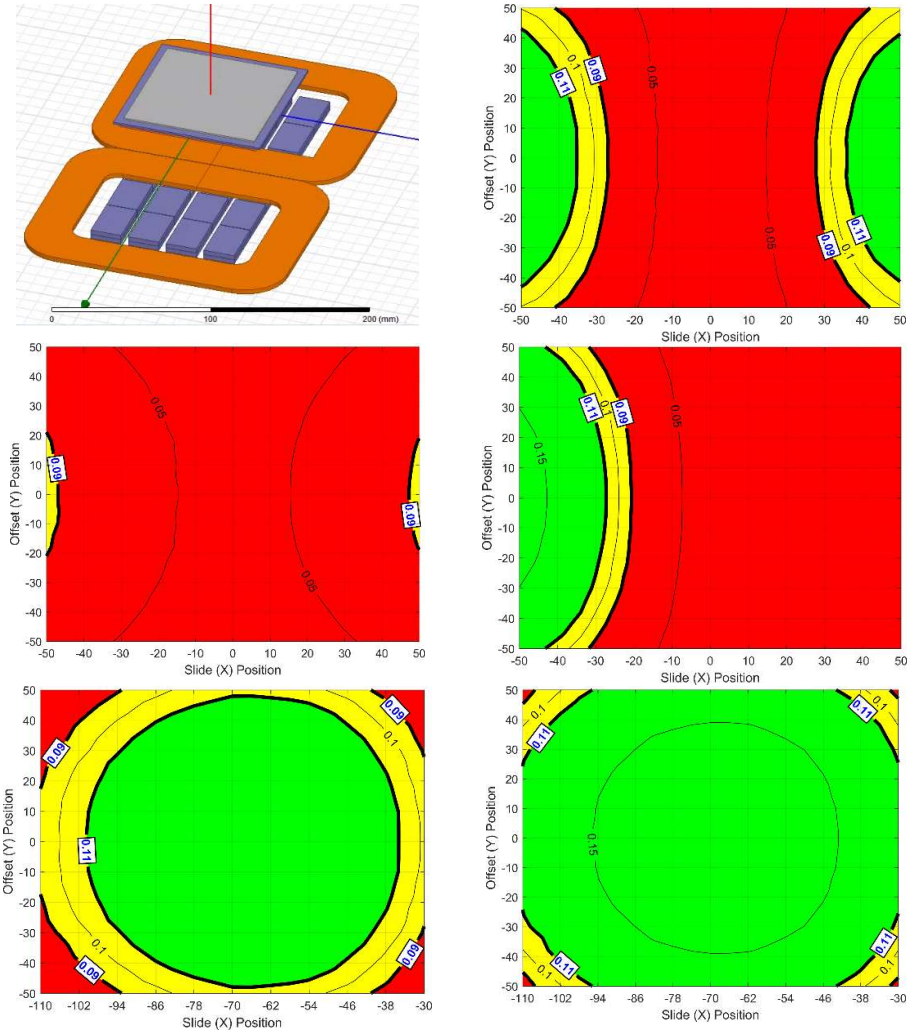

Figure 5.17: The finite element design used to test the operation of the DD coil design with the TS design from appendix A.1 (top left). The TS design is scaled to 0.35 its original size, and Z = 45 mm. Coupling for polarized mode (top right), non-polarized (mid left) and single coil (mid right). Coupling profiles with a natural offset of (-70, 0, 45) are shown for polarized (bottom left) and single (bottom right) operational modes.

The second TS study is with the (dual) VA coil from appendix B.3, shown in Figure 5.18. The DD coil replaces the GA coil from appendix D.1, and a scale of 0.35 was used. The contour plots for the coupling of the coils at 35 mm are shown. This Z value would correspond to 165 mm at full scale, assuming the complete DD assembly is the same thickness as TS-D.1, 65 mm.

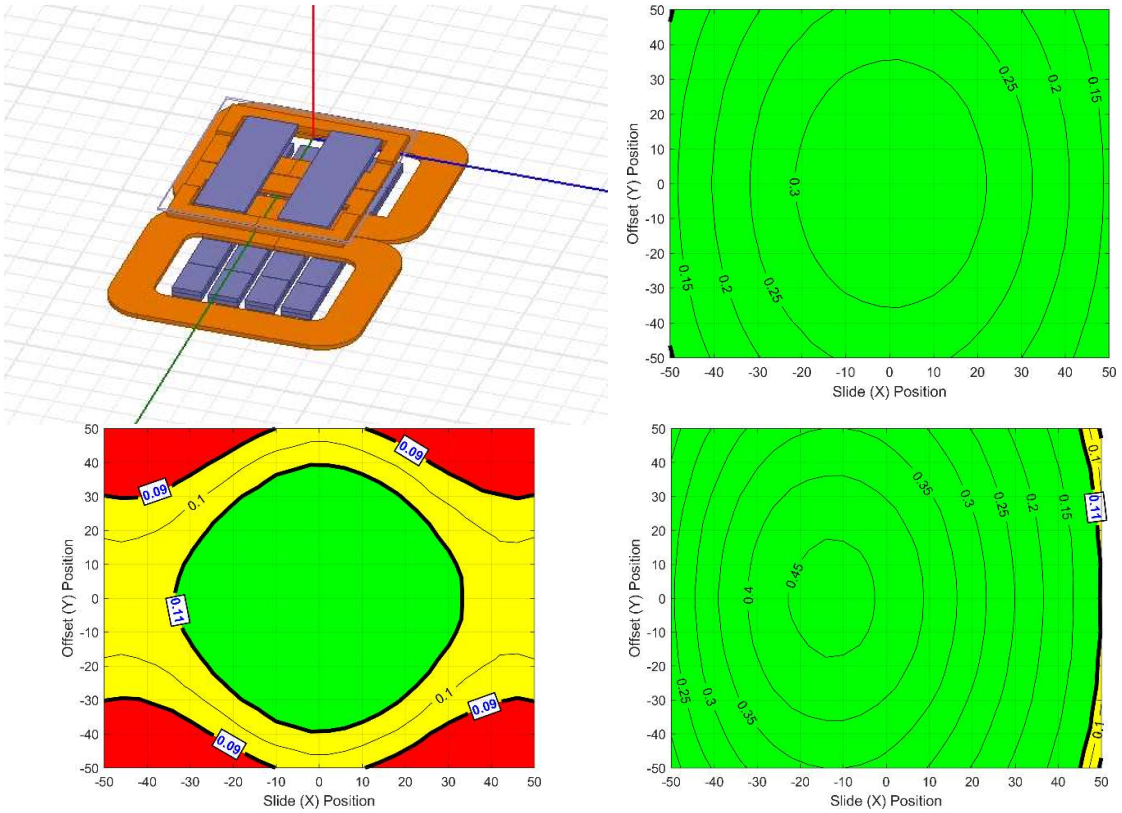

Figure 5.18: The finite element design used to test the operation of the DD coil design with the TS design from appendix B.3 (top left). The TS design is scaled to 0.35 its original size. Note: The VA's aluminium shield is shown in wireframe to show the coil structure. Coupling for polarized mode (top right), non-polarized mode (bottom left), single coil (bottom left).

The third TS study is with the (single) GA coil from appendix C.2. The TS VA coil being replaced is A.6, so a scale of 0.53 is used. The model is shown in Figure 5.19 with the contour plot for Z=75 mm. This corresponds to a J2954 Z value of 200 mm at full scale (assuming GA thickness of 62, and < 3mm packaging on bottom side of the VA). The pickup coils are operating in the same mode as they did for non-polarized source coil operation.

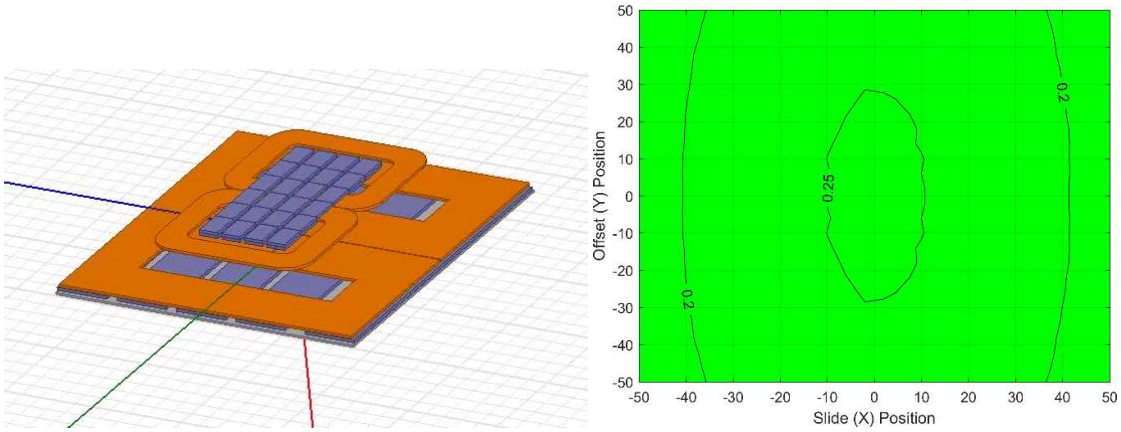

Figure 5.19: The finite element model used to test the operation of the DD coil design with the TS design from appendix E2.1.1 (left). The TS design is scaled to 0.56 its original size. Coupling factor for these coils (right). The DD VA coils are operating in the same way as they did for the polarized mode.

The fourth TS study is with the (dual) GA coil from appendix E.2.1.1. The TS VA coil being replaced is E.2.1.4, so a scale of 0.56 is used. The model is shown in Figure 5.20 with the contour plot for Z=75mm. This a J2954 Z value of 197 mm at full scale (assuming GA thickness of 62, and < 3mm packaging on bottom side of the VA). The pickup coils are operating in the same mode as they did for polarized source coil operation.

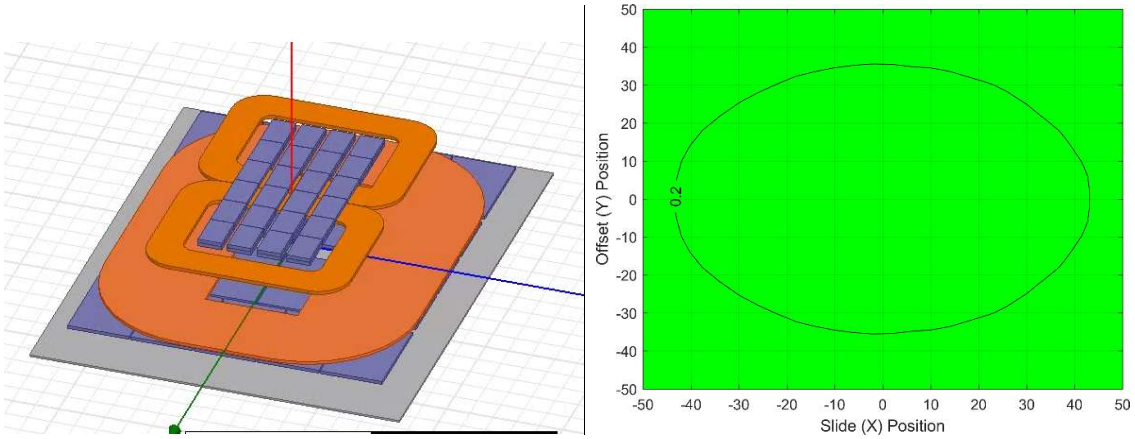

Figure 5.20: The finite element model used to test the operation of the DD coil design with the TS design from appendix C.2 (left). The TS design is scaled to 0.53 its original size. The coupling factor for the coils at Z = 75 (right). The DD VA coils are operating in the same way as they did for the non-polarized mode.

5.6 (Discussion) Inferred Coil Sizing and DD Operation Modes For J2954

5.6.1 Validation of FE Model

All the difference values between finite element and experimental measurements for the key parameters remain within the target ±10%. Therefore, the FE simulations for the example DD coils can be considered validated. Remaining differences, and the trends seen across the Z slices are due to

approximations made in both experiments and simulations. These approximations include the use of a fixed self-inductance for coils when they differ less than 10%, and simplifications used in the finite element model. These approximations are necessary to ensure that simulations and experimental measurements can be completed within the target timeframe of 72 hours (discussed in 5.4). In future work, it may be desirable to increase the complexity of the simulations to reduce this validation target further.

The FE simulations incorporating TS designs are yet to be validated. This is because experimental prototypes of the TS coils are not yet available. For this reason, the interoperability study is not used for assessment of coil sizing. The methods used to develop the TS simulations are the same as used in the validated work. This means it is, however, suitable for consideration of different operational modes. As this just considers qualitatively if there are regions that the coupling requirements are satisfied, and does not consider the accurate positions and therefore sizing of coils.

5.6.2 DD Independent Operation

Here, Q2 and Q3 are considered:

Q2: How can the optimal GA-VA design/operational mode be identified for a particular operational region?

Q3: How can multi-dimensional coupling mapping of small scale prototype GA-VA coil pairs, be used to consider compliance with standards?

The polarized design has coupling that exceeds 0.1±0.01 across the standard range of operation. This would make it the preferred choice for a WPT designer to use as it is likely to be possible to develop electronics for this design, at full scale to be compliant to the efficiency requirements of J2954.

The non-polarized operational mode has a significantly lower operational range than the polarized mode, however it does have one advantage. This is that the self-inductance of the coils changes less than the polarized design. This may offer benefits, to the tuning of the resonant circuits that power the coils. With this mode, they will need to operate over a smaller range of inductances.

The single coil operational mode also satisfies the coupling limit. It has the highest coupling average from the histogram. It also offers a unique opportunity for coupling when the coils are at a very large misalignment in the X direction. This occurs when the second pickup coil is above the first source coil. The option to use this mode may be considered by WPT designers, however, it comes with the caveat that the power rating of the coils may need to be reduced to account for the fact that only half the GA coil is being used.

Considering the point at which the coupling drops below the 0.1 threshold, the sizing of the coils can be considered. This assumes the DD coil is sized as a GA coil for SAE J2954.

For this configuration, coupling factor falls below 0.1 at (50, 50, 65), with the coils operating in polarized mode. This implies the scaled range (scale up from 0.34) would be ±147 mm in X and Y and 191 mm in Z (magnetic gap). This exceeds the J2954 ranges of ±100 mm in Y, ±75 mm in X. As J2954 considers Z, measured as VA ground clearance, to be 250 mm (for Z3 class), this would mean if the GA thickness (minus the packaging below the coil on the VA) is >59 mm then the DD coil can be classified as Z3. Therefore, it should be possible to build the DD design into a full-scale system that satisfies J2954 efficiency requirements to operate as a Z3 class GA. The dimensions of the GA DD coils for this full-scale system should be a minimum of 800x500x59 mm.

It is not practical to assess the symmetrical DD coil design for sizing as a VA coil. This is because the GA/VA designs proposed in J2954 are asymmetrical, the DD design is symmetrical. Typically, the VAs is much smaller in size than their corresponding GAs. Further investigation is needed to assess how the sizing of VAs affects the coupling values.

Rotational offsets have been shown to have a substantial effect on the DD coil coupling values. It is unclear if this result is directly from the rotation or a result of relative positional change. The relative positional change occurs as DD coil rotates around the Z axis, when this happens one of the two coils in the VA moves closer to the GA. Further work is needed with a VA design with a single coil to investigate this effect further. Care must therefore be taken at the extremes of the positional range of operation regarding the impact of these rotations.

5.6.3 DD Interoperability with TS Coils

This considers research question Q4:

Q4: How can multi-dimensional coupling mapping be used to consider the operation of a new coil design (GA or VA) with reference coil designs (such as the TS coils in SAE J2954)?

The interoperability of the DD coil with the TS designs of J2954 has also been considered in finite element simulations.

With the DD coil design acting as a GA coil, it requires a natural offset to operate with single coil VA designs. This is shown by the fact that the combined coupling factor does not exceed 0.1 for the standard range. With a natural offset of X = -70 mm (or 200 mm at full scale), although the coupling factor remains low, it can exceed 0.1 with the DD operating in single coil mode.

The DD coil design operates well with the dual coil TS-VA in both polarized and single coil operational modes, with coupling that appears to remain above 0.1 over the total range of operation. This range, when scaled would be ±142 mm in X and Y and therefore would suggest the DD coils could be developed as a GA to meet J2954's requirements.

With the DD coil design acting as a VA coil, the results show coupling remains above 0.1 over the entire range for both single and dual coil GAs. To do this, however, the operational mode of the pickup needs to change to adapt to both. With the dual coil TS-GA, the DD coils operate in polarized mode, with the single coil TS-GA the DD operates in non-polarized mode. Therefore, this should be considered in the design of the VA electronics.

Further work is needed to validate the TS coil FE models. Once the validation is completed, sizing of the DD design for operation with each of the TS coils can be considered.

5.7 Impact on WPT Development Process

This section considers Q5:

Q5: How can multi-dimensional coupling mapping be integrated into the WPT development process for a new coil design?

For WPT designers starting from the beginning, performing tests with the SAE J2954 TS method is a significant challenge. Not only must GA/VA coil designs be designed and constructed to full scale, but all the electronics that power them and a full-size test rig must be developed. The complete range of TS GA/VAs must also be built with their electronic designs. This would require significant resources to get to this point.

Using the MDCM method proposed in this work, issues with magnetic compatibility can be identified at an earlier stage of coil development. This method only needs a coil design concept and a small-scale prototype to begin assessment. The method itself is low cost. The experimental equipment to automatically position the coils cost less than £300 and small-scale prototypes of coil designs are vastly cheaper to make than full sized designs. This means developers can easily trial their coil designs both experimentally, and in simulations, for the ability of a coil design to satisfy the operational ranges of J2954. This can then be used to identify the minimum dimensions needed for a full-sized coil to meet the operation range. The method has also outlined how interoperability with the Test Stand (TS) designs can be assessed at this early stage.

The need for GA/VA electronics is avoided in this assessment. This means that the assessment focuses solely on the magnetic compatibility of the coils, ignoring any effects the electronics may have on the GA/VA compatibility.

Once FE models have been validated, it is possible to perform parameter optimization sweeps. These could consider how changing parameters of the coil design, such as the spacing between the ferrite bars, will affect the coupling between GA/VA pairs. Ultimately it may be possible to use genetic algorithms or similar methods to develop new coil designs that are optimized for coupling at the design stage.

Recent work from Bertoluzzo, Buja and Dashora (Bertoluzzo, Buja and Dashora, 2019) has also highlighted the potential opportunities in having independent coil operation of DD system designs. In their work they used the non-polarized operational mode to overcome the "null point" of the coupling of the polarised operational mode. It is foreseeable MDCM methods could be used to characterise generic GA-VA pairings to work out when operational mode switching like this should occur.

5.7.1 Coil Development Process Flow

The process a WPT developer may follow to bring a new coil concept GA-VA coil pair through development is shown as a flowchart in Figure 5.21.

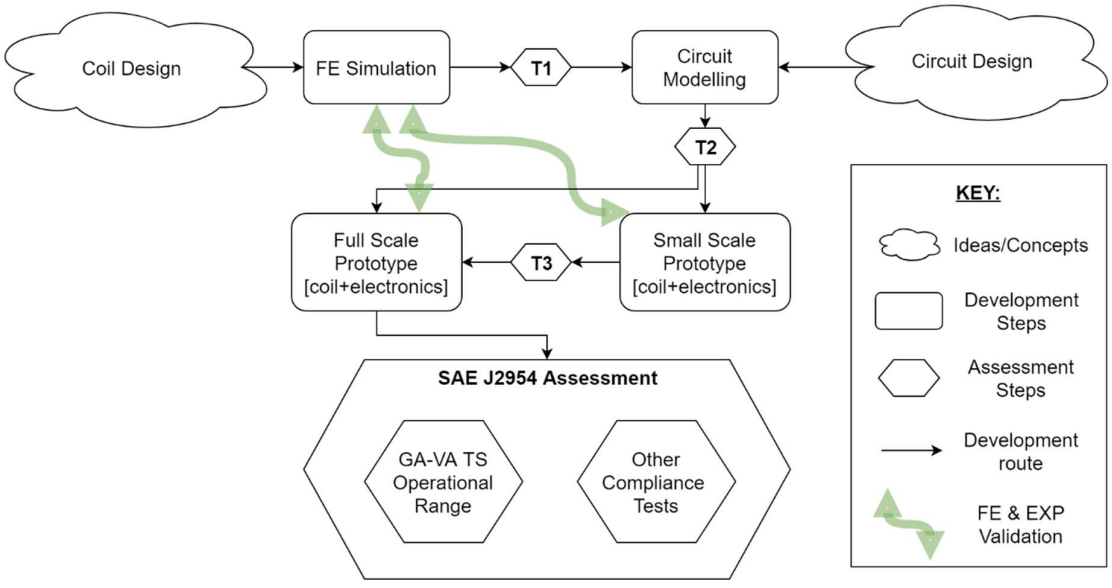

Figure 5.21: Development process to create a SAE J2954 compliant coil set from a coil concept design.

Here the ideas and concepts are provided by the developer for both a coil design as well as a circuit design. These ideas could be inspired from a range of sources, the TS designs in J2954 for instance.

The first step developers would perform next is FE simulation of the coil design. A CAD of the concept coils would be created and modelled in the developer's preferred simulation package. This is how the author approached developing a WPT system for a radio controlled car.

The first assessment step, T1, is then met. Here if the results from the simulation pass the developer's requirements, the concept can be considered further. These requirements could be based around factors like inductances, coupling factors and the range of operation. It is up to the developer to identify what factors the concept must meet.

Circuit modelling can then be performed with the range of coupling and inductances found from the FE simulation results. This may only include values from the developer's chosen nominal position, or it may include numerous positions in the operational range.

The second assessment step is now met, T2, and requirements again are chosen by the developer. At this point simulated power transfers and efficiencies could be considered.

Depending on the experience and confidence of the developer, they could either now develop full scale coils or develop a small scale prototype. Full scale coils are more expensive to manufacture both the coils themselves and the powering electronics. At full scale, more space is needed and safety considerations must be made for securely mounting and moving the coils. If the developer is confident in their design and their assessment to this point, they could go directly to this step and begin J2954 assessment.

If the developer is less confident, the option of creating a small scale prototype exists. The electronic design and control strategy can be assessed, as can the coupling profile over a range of positions. This culminates in assessment in T3, which again has its requirements set by the developer. Assuming the developer is satisfied they can continue on to develop the full size coils.

Once either small-scale or full-sized prototypes exist, it is possible to perform validation of the FE simulations. With a validated FE simulation, certain tests become easier to perform such as field analysis and positional sweeps. The reasons for validation were further discussed in section 4.1.8 so are not repeated here.

The SAE J2954 assessment methods were also discussed earlier on, in section 5.1, so will not be considered again here. It is worth noting, however, that this is the first point in the process flow that assessments are performed that are not designed by the developer. These are standard tests set by the SAE that all coil designs must meet.

If at any point, the concept designs fail the tests in T1, T2, T3 or the SAE J2954 Assessment, then the concept must be modified. At the worst case, this means the developer must start again with a new concept coil design. Alternatively, the developer will need to perform modifications to the existing concept in some way to ensure the tests are passed. These modifications have a chance of nullifying previous work, leading to the loss of sunk time and resources. Therefore, it is beneficial to find out if a concept will fail as soon as possible in the development process to limit the losses in development.

With multi-dimensional coupling mapping MDCM, the development process flow can be modified. This modified process flow is shown in Figure 5.22.

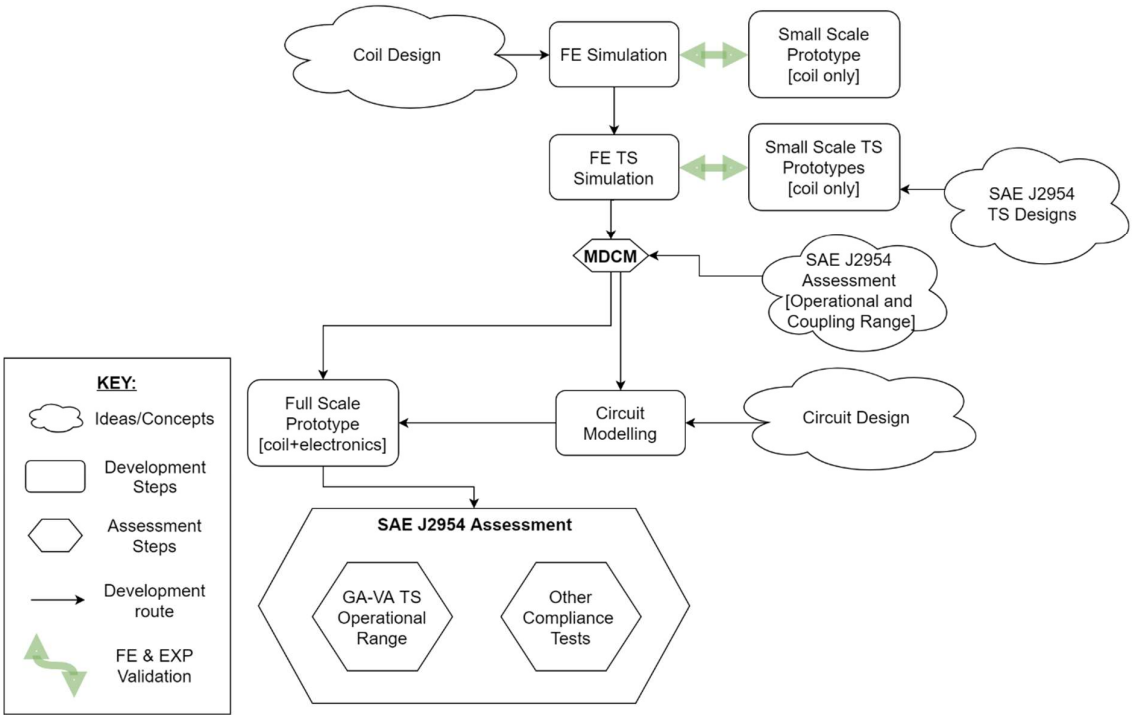

Figure 5.22: Modified process flow using the multi-dimensional coupling mapping methods.

As before, a coil concept is introduced from the developer, and an FE simulation is created from a CAD of the concept coils. These processes are not changed from the standard development steps.

Small scale prototypes of the coils (in isolation from electronics) are now developed alongside the FE simulations and used for direct validation. FE simulations and small-scale EXP prototypes are also made to assess interoperation with the TS coils in J2954.

At this point the Multi-Dimensional Coupling Mapping (MDCM) method is performed. This assessment would be similar to the one performed in this chapter (but also include prototypes TS coils analysis, which was not available for this study). This differs from the various tests in T1-3 which were chosen

by the developer, as the MDCM method has the requirements set from the operational range and coupling factors used in J2954 (but scaled down to the size of the coils).

MDCM will also provide guidance in aspects of the circuit modelling. In the standard development steps, the FE simulations may be used to provide the range of tolerances but this depends on what simulations were performed by the developer. As the MDCM method follows a standard set of tests over the complete range of operation, the coupling factor and inductance range will be known, just inductance vales will need to be scaled.

With the confidence from MDCM results, the need for small scale electronics to test the concept coils should not be necessary. Of course it is still possible, if the developer prefers to test the electronics on the existing small scale prototypes it could be easily performed.

The benefits of the process using MDCM over the existing process is realised from the integration of SAE J2954 testing considerations in the early stages of development. Test stand coil designs and the operational ranges from J2954 are used to develop the MDCM tests. This means when the final assessment steps are performed, the risk of failing J2954's assessment should be reduced. This is because the final assessment requirements are now considered very early on in the development process.

The MDCM process is also less reliant on the developer of the WPT system to create suitable testing steps. This would be highly useful for inexperienced developers, whom may not know what the requirements should be set to at each test stage. The author himself found this an issue during the early work on developing a WPT system (discussed in section 4.3.2).

The MDCM method does not replace the testing processes which exist in J2954, nor is it limited to only testing to J2954. It is a generic method for assessing the coupling between GA and VA coils at the component level. The criteria that sets whether coils are compatible or not can be changed to suit the application being considered.

5.8 Future Standards

As the J2954 standard is still in draft form there is potential for the test parameters to change. It is also possible that as WPT technologies mature, new standards will emerge. If this happens it may be necessary to alter the coupling factor range used for the magnetic compatibility criteria. The underlying method, however, would still be valid.

As discussed in Chapter 3, coupling factor is a variable that considers a wide range of factors associated with magnetic compatibility and these will inevitably be included in some way for any future standards

considering WPT technologies. This is because there is always a need to consider the magnetic fields, and therefore coupling, for a WPT system to work. The range of positions may change though for certain applications. For instance, in WPT standards for rail applications, there is likely to be a significant reduction in lateral range of motion. For dynamic WPT standards, the longitudinal tolerances (along the roadway) will be infinite.

5.9 Chapter 5 Summary

Four research questions were considered in this chapter, these are:

Q2: How can the optimal GA-VA design/operational mode be identified for a particular operational region?

Q3: How can multi-dimensional coupling mapping of small scale prototype GA-VA coil pairs, be used to consider compliance with standards?

Q4: How can multi-dimensional coupling mapping be used to consider the operation of a new coil design (GA or VA) with reference coil designs (such as the TS coils in SAE J2954)?

Q5: How can multi-dimensional coupling mapping be integrated into the WPT development process for a new coil design?

The process of assessment of the DD coil example showed how the optimal operational mode of the coils could be chosen based on the coupling measured over the operational range. This is relevant to Q2 which considered the optimal operational mode. The coil design itself was not considered for optimisation, for this consideration section 4.6 of the previous chapter should be consulted.

Q3 and Q4 were considered in section 5.6. Looking at the point at which the coupling fell below 0.1, the position was found using the high resolution coupling map. This was then scaled to the required operational range of J2954 to find the sizing of the coils. This makes use of the H2 hypothesis. In FE studies the operation of the DD coil example was considered with the TS designs from J2954, which showed how various operational modes performed.

Q5 was considered in section 5.7. This discussed how the methods could be applied in the development process, and how the process flow could be modified. This modified process flow should reduce the risk of late stage compliance issues in J2954's assessment. This is due to incorporating consideration of the standard in the early stages of development.

6 DISCUSSION

In this chapter the work presented is going to be considered for its significance in the published literature. It will explain the new findings and how the understanding of WPT technologies have been moved forward. It will also identify the value for industry that the solutions provide, particularly the benefits for developers of WPT systems.

This chapter is split into 6 sections, each corresponding to an area of findings or innovation.

1. **COUPLING FACTOR FOR MAGNETIC COMPATIBILITY ASSESSMENT:** Coupling factor as a value to assess the magnetic compatibility of coils.
2. **MULTI DIMENSIONAL COUPLING MAPPING (MDCM):** Advantages realised from producing high resolution maps of coupling factor.
3. **EARLY STAGE ASSESSMENTS TO STANDARDS:** The methods and how they can be incorporated into the development processes of WPT coil design,
4. **COIL DESIGN OPTIMIZATION:** How the assessment results can be used to cross-compare different coil designs and optimise future designs.
5. **IMPACT ON STANDARDS:** Ways this work could feed back into the standard.
6. **NEXT STEPS/FUTURE WORK:** Areas that should be investigated in subsequent work.

6.1 COUPLING FACTOR FOR MAGNETIC COMPATIBILITY ASSESSMENT

The work of Lin, Covic and Boys (Lin, Covic and Boys, 2015) demonstrated that the compatibility between different coil designs could be assessed using Finite Element (FE) analysis software, and they showed that some coil combinations are magnetically incompatible. Lin et al. used a coupling factor of $k > 0.1$ to consider if a coil combination is compatible, however, they dismissed practical validations as being unfeasible. Others have also published work to support the idea that the coupling factor threshold close to this value is key to magnetic compatibility. Zaheer et al. (Zaheer *et al.*, 2015) discussed the implication of coupling threshold on multi-coil designs. Miller et al. (Miller *et al.*, 2016) also considered that a coupling factor above a minimum threshold is needed. This is discussed in section 3.1.

The range of coupling factors typical in WPT was surveyed but the information available was limited. The average of the factors was a minimum of 0.106 and a maximum of 0.404 (section 3.2.3). Further investigation of what happens outside this range was performed. It has shown that when the coupling factor is below 0.1 the fundamental magnetic efficiency of WPT drops, and it is not possible with the coils typically used in WPT to increase efficiency further (section 3.2.4). Above the coupling factor

range, the electronics typically used for WPT may become inefficient or cease to function, as discussed in section 3.2.5. However, this is a limitation of the electronics rather than a fundamental issue, as at high coupling factors the WPT system becomes tightly coupled and therefore acts as a conventional transformer. Power transfer across a conventional transformer is trivial with the right electronic design.

The coupling factor parameter includes the assessment all aspects of the coil geometry and magnetic fields in a WPT system. It has been shown, in section 3.2.2, that the ratio of inductances that make up the coupling factor is based around integrals of both the magnetic fields and geometry of the coils. These values, and the integration over closed loops, will account for the field strength, field direction/polarity, coil shape, and the materials in use in the WPT system geometry.

Coupling factor has been shown in this work to also be independent of the scale of the system, this is considered in section 3.3. Analytical methods and a FE simulation were employed to demonstrate this case for both simple and complex coil geometries. Because of this property, results from small scale prototypes are valid for the assessment of magnetic compatibility of full scale coil designs.

For WPT developers, these findings can simplify the design and optimisation of coils. Only one parameter needs to be considered that will tell the developer if a GA-VA pairing is compatible. Maximising coupling factor can also be used as an optimisation target in the design process. The finding that coupling factor is independent of scale is also a benefit to developers, whom can use small scale prototypes to consider coupling of full scale designs.

The author is aware that these findings may appear trivial to some researchers working on WPT technologies. Indeed, he himself wondered if these were trivial findings, and spent some time investigating if there was any published work that identified these findings elsewhere. As no relevant published work was found, and through discussion with other WPT developers, it was decided that these findings should be identified and highlighted in this work.

6.2 Multi-Dimensional Coupling Mapping (MDCM)

The key differentiator to methods before this, is the ability to take high resolution readings, experimentally, in three-dimensional space. Work before this, considered three dimensional experimental measurements unfeasible or impractical (Lin, Covic and Boys, 2015). Published work would therefore, typically only show values for a single dimension at a time, and at a low resolution (Lin, Covic and Boys, 2015; Su Y Choi *et al.*, 2015; Zaheer *et al.*, 2017). These measurements are suitable for finding general trends of the coupling, and the coupling values at pre-defined limit points, but they are typically limited to one or two positions along the other axes. Therefore, it is possible that

the profiles could miss key characteristics of the actual coil coupling (further motivation is in section **Error! Reference source not found.**). It is also not possible to visualise the coupling profile without having to manually take potentially 100s of positional measurements.

This work has shown that it is feasible to perform multi-dimensional high resolution experimental mapping, by using the experimental rig that has been developed in section 4.3. The example DD coils assessed in Chapter 5, had been designed with holes in the casing to perform two dimensional offset studies. The coil designer, Alex Ridge, had placed 10 mm interspaced holes on the side of the casing to position the coils for alignment measurements. At best, this would have taken 100 measurements per Z-slice in the ±50 mm XY range. The experimental rig, however, took 2704 readings in the same region, at 2 mm intervals, and measured this for 11 Z-slices at a time, a total of 29,744 positional points. The rate of positional measurements was 720 per hour, meaning this particular study could be completed in less than 42 hours. This type of high resolution mapping gives a high degree of confidence that the profiles show all measurable characteristics in the three-dimensional region.

Efficient FE multi-dimensional simulations have also been developed in section 4.2. The advantages of FE simulations include the ability to measure features not possible experimentally, and to perform sweeps of parameters that would otherwise be difficult to consider with real coils (such as the sizing of ferrite bars). These simulations are validated against the EXP measurements to ensure simulation accuracy (section 4.1.8). Once validated, they can then be used for assessments alongside experimental work (to increase confidence in results) as well as to perform studies not yet possible with the available experimental equipment (such as the rotational study in section 5.5.5 and the TS interoperability study in section 5.5.6).

One of the unique benefits from the high resolution of the maps is that the point at which the coupling factor falls below a designated threshold is accurately known in 3D space. Therefore, the size of the coils needed to satisfy a position range can be quantified. This fact was used in the study for the coil sizing of the DD coil design for J2954's requirements. By setting the threshold at a coupling value of 0.1, the points at which this value is met is known to an accuracy of (±2, ±2, ±1) mm in 3D space. This could then be used to work out the scaling needed to meet the requirement of the J2954 standard.

These methods would be of interest to developers of WPT systems. They can be used as a method to assess and validate new coil designs without having to develop full sized prototypes and the power electronics for the coils. The MDCM equipment is currently working at 200 FE and 720 EXP measurement/simulations per hour, an order of magnitude faster than previous simulation and manual experimental methods. The cost of the test rig is less than £300 so it highly accessible to WPT

developers with a small budget[2]. To support these developers all the scripts and code for control of the rig and data processing have been made available with the open source MIT licence on GitHub (Abbott, 2018b, 2018a). This means that future researchers can freely use and build on this work to adapt and add application specific features.

The experimental rig also has other applications outside coil coupling measurements. Recently it was used to measure the magnetic field from an iPhone wireless charger. It has also been taken to several shows and conferences with the HVM Catapult as a demonstration piece.

6.3 Early Stage Assessments to Standards

Ensuring the coils for WPT, which may have been designed by different groups, work together, is of utmost importance to the uptake of WPT as a mainstream technology. Users of WPT systems want to ensure the coils on their vehicles (VA) are compatible with all the coils that are available on the roads or at home in their parking spaces (GA) (Transport Research Laboratory, 2015).

Recently, the J2954 draft standard has been released from SAE International (SAE International, 2017). This standard currently considers static WPT for light duty vehicles. To assess interoperability between GA and VA designs, several "test stand" (TS) designs are provided for some of the power and Z-gap classifications. The idea behind this, is that if a new GA or VA design transfers power above the required efficiency limit to the TS-GA/VA designs, they are interoperable (and therefore magnetically compatible). This requires the developers of WPT systems to test their full-sized coil designs and all the necessary power electronics, together with a set of TS coil designs and their associated electronics.

By applying the MDCM assessment methods developed in this work, the author has shown it is possible to perform preliminary compliance testing of magnetic compatibility at a much earlier stage. This has been demonstrated on a GA-VA symmetrical DD coil pair. The assessment can both work out the sizing of the coils to ensure compliance to J2954's operational range as well as assessment of how the coils should wired to work with a selection of TS-GA and TS-VA coil designs.

Developers of WPT systems will now be able to use this MDCM assessment in the process of creating new coil designs. It provides a way of testing if a coil design is likely to satisfy the standard without the need, and the commitment, to developing a full-sized prototype of the coils and all their electronics. The assessment outlined here can be performed with minimal standard laboratory equipment and

[2] Considering that taking a measurement over 50 positional points, could take a researcher 2 hours at £15 an hour, the rig would have paid for itself in less than 1000 positional points, or just under 1.4 hours of operation.

tools. If applied in the development process of new WPT designs, it should reduce the risk of late stage compliance issues.

6.4 Coil Design Optimization

There are several research groups whom have developed WPT solutions, each have chosen different coil design ideas to solve the issues they see as the most pressing. The University of Auckland, have focused largely on the issue of misalignment and coupling for automotive static WPT applications (Boys and Covic, 2015). To solve these issues they have investigated a number of multi-coil designs, such as the DD, BPP, DDQ, Solenoid and Tri-Polar layouts (Kim *et al.*, 2014; Lin, Covic and Boys, 2015; Zaheer *et al.*, 2015). KAIST's work has focused on dynamic WPT coils, and they have developed numerous track GA designs that have a focus on minimizing flux leakage as well as very high current power electronics (Rim, 2014). Others, such as Primove have developed three phase coil designs (Dickson, 2013), and ORNL have looked at the grid impact of WPT (Miller *et al.*, 2015).

All these solutions have their merits, however, as the focus of these works are different, the results they present are not typically comparable. For instance, Auckland present a coupling value, whereas KAIST uses normalised power output. One of the reasons for this difference arises because Auckland choose to compensate for poor coupling by increasing the input power, to maintain a fixed output power, whereas KAIST chooses to de-rate the output power. This makes comparison of the coil designs, and therefore selection of an optimal coil design, difficult.

The methods performed in this work, involve direct assessment of coupling between a GA and VA, using a standardized process. It is independent of all factors within the coil electronics, such as, operating frequency, compensation topology, frequency tuning and any other steps used to increase the efficiency or power level of WPT systems. It is scale independent too, requiring only the ranges to be modified to suit the application of interest. Therefore, by testing coil designs with the MDCM method it is possible to perform direct coil design comparison, and therefore selection of the optimal design for a given application (this is shown in section 4.6).

Direct comparison between two coil designs is the first step towards optimization of coil designs. It has been demonstrated here for the both or operational mode and three different coil designs. In the future it could be used for other factors, such as geometric optimisation, where, for instance, the ferrite size is chosen to maximize coupling with the minimum ferrite volume. Taking this idea to the nth degree, computer algorithms could be used to generate coil designs themselves, which could then be tested with the methods here. This could be used to find optimal coil designs for given application constraints.

6.5 Impact on Standards

The standards to govern WPT systems are still in development, and thus far only one draft standard has been released, this is J2954 from SAE International (SAE International, 2016, 2017). This only covers static WPT systems for light duty vehicles. Equivalent standards will be needed for heavy duty vehicles, dynamic and opportunistic charging, as well as other sectors such as rail. These standards will all need to consider the magnetic compatibility of the coils used in WPT.

This work has contributed a complementary method of assessing compatibility of different coil designs that differs from the test methods used in J2954 in a few ways. Firstly, measurements in J2954 are only taken at intervals of 25 mm or more. The MDCM method takes measurements at a higher resolution. This difference has little impact if the coupling profile is reasonably uniform, if there was an unusual coupling factor profile, the J2954 method may not identify this (further discussion is made in section **Error! Reference source not found.**).

A second difference between the methods is that the coils and coil electronics are paired together in J2954. In the MDCM method, the coils are independent of their electronics. This means coils can be assessed at a component level, which is not currently possible in J2954. The SAE discusses support for component testing and being able to separate GA coils from the GA electronics (in appendix R.2.1), however, they note further development work is needed. There does not appear to be any development in separating VA coils from their electronics in the current version of J2954.

The MDCM method introduced here could be used to support further development of component level testing in J2954. It provides evidence that the coils can be tested for compatibility in isolation to their electronics. There may be ways to incorporate these findings into later revisions of J2954 as well as the any other WPT standards that are currently in development.

6.6 Next Steps/Future Work

The validation between finite element (FE) and experimental (EXP) work has been performed for the symmetrical DD coil design studied in Chapter 5. Extending this validation to more coil designs will increase the range of FE models available for benchmarking future coil concepts. Validation of the TS designs is of particular interest as this will enable quantification of coil sizing when considering the interoperability requirements in SAE J2954.

Although this work has demonstrated that the coupling factor is independent of the scale of the system, there is likely to be some quantifiable differences that occurs when scaling up a coil design to full size. This is not a fundamental issue with the scaling of the coupling factor, it arises from

unavoidable manufacturing differences in things like magnetic materials, coil packaging and small changes in the coil construction. Therefore, developing a small-scale and full-scale prototype pair could quantify this error and show the typical expected differences between small and large scale coil designs.

There is substantial scope to contribute to the development of J2954 and other WPT standards in the future. The standards are currently in draft form and there are many areas still looking for information and validation before they can be finalized. These areas include component level testing and the magnetic field assessment method discussed in section 5.1.5. The MDCM method could be employed within the component testing process to separate out GA/VA electronics from the assessment of the coil designs. Contribution to the standard would demonstrate experience and expertise and would help shape the way WPT technologies are commercialised. To maximise contribution at this level, a full-scale test rig is likely to be needed, so that the actual TS-GA and TS-VA coils can be assessed with their associated electronics.

Considering the scaling up of the test rig to full scale, there will be a need to replace substantial parts of the current rig. The control system used in the current test rig and the measurement method could be used in the scaled up test rig. It would not be wise to continue to use the current mounting system on larger coils. There was already a risk in mounting the DD coils on the rig due to their mass and the twisting force on the horizontal (X-direction) aluminium bar. The stepper motors are also only rated to lift masses much less than those proposed for full scale VA coils (8 kg vs approximately 50-100 kg). Therefore, if the rig is to be scaled up it would be best to replace the complete frame and motors in use with another Arduino compatible system.

A detailed study of the effect of rotation using the MDCM method should also be considered. A large change in the coupling factor of the DD coils with rotation was reported in section 5.6.2. It is not clear if this effect is due to the relative position change of the coils with the yaw rotation, or if it is due to the rotation itself. An FE study (possibly with EXP validation) should be performed to assess this further and identify the effect that rotation will have on the compliance to J2954's operational range.

7 CONCLUSION

The aim of this work was to investigate Wireless Power Transfer (WPT) technologies for automotive applications. Through this work, a number of research questions and hypotheses have been raised as topics of interest.

H1: The coupling factor can be used as a key variable to evaluate if the fields between the GA/VA are magnetically compatible.

Q1: What is the typical range of coupling factor and what happens outside this range to the operation of the WPT system?

H2: Coupling factor is independent of the scale of the WPT system.

H3: Multi-dimensional mapping of coupling factor at a high resolution is feasible for both FE and EXP studies.

Q2: How can the optimal GA-VA design/operational mode be identified for a particular operational region?

Q3: How can multi-dimensional coupling mapping of small scale prototype GA-VA coil pairs, be used to consider compliance with standards?

Q4: How can multi-dimensional coupling mapping be used to consider the operation of a new coil design (GA or VA) with reference coil designs (such as the TS coils in SAE J2954)?

Q5: How can multi-dimensional coupling mapping be integrated into the WPT development process for a new coil design?

When the vehicle side (VA) and road side (GA) of a WPT system are developed by different groups, they should be designed to operate together, this is called interoperability. Many parameters must be considered to ensure the GA-VA work together and the parameter of interest considered in this work is the magnetic compatibility. Magnetic compatibility is the assessment of the suitability of the electromagnetic flux field between GA-VA coils.

To investigate magnetic compatibility, the published work that considers coupling factor has been reviewed. Through consideration of these, and consideration of how coupling factor relates to magnetic fields. Coupling factor has been shown to be suitable a suitable parameter to assess the magnetic compatibility of a GA-VA coil pair (H1).

It has been shown that when the coupling factor is below 0.1 the efficiency of typical WPT systems becomes significantly reduced and the power output can be de-rated (Q1). This is due to a combination of electronic limitations (the need to avoid excessive currents in the GA coil) as well as the fundamental magnetic efficiency reduction. There is also an upper limit to coupling factor for typical WPT systems, but this arises from limitations in the electronic circuits rather than any fundamental limit. At high coupling the WPT system acts like a conventional transformer.

The coupling factor has also been demonstrated to be independent of the scale of the GA/VA coils being studied (H2). Both analytical calculation and FE simulations have been performed to show this. Therefore, small scale prototypes of coil designs can be used to consider the magnetic compatibility of the fully sized designs. This finding also means that once the "magnetically compatible" region for a GA-VA pairing is known, the GA-VA designs can be resized to ensure they are suitable for a given application[3].

Through finite element (FE) simulations and an experimental (EXP) test rig, a method of measuring coupling factor across multiple dimensions at a high resolution has been produced (H3). With this Multi-Dimensional Coupling Mapping (MDCM) method, up to 200 FE simulations per hour (per computer) can be completed, and 720 EXP positional points per hour, can be measured. This enables studies of over 10,000 positional points in less than 72 hours. This can be used to measure coupling factor between the GA-VA, as well as to find out the tolerance to misalignment of new coil designs. By maximising coupling values or maximising the operational position range that the coupling limit is met the optimisation of coil designs and operational modes can be considered (Q2).

The MDCM method has been applied to the draft SAE J2954 standard. This has shown that the assessments can be used to demonstrate whether coil combinations are compatible (Q3). It can also be used to work out the size that prototype coils must be made to achieve the standard's requirements (Q3). The mode that multi-coil designs must operate in with the Test Stand (TS) designs has also been considered (Q4).

Through analysis of the development process of creating a new coil design, improvements in the process have been identified which, by using the MDCM method, reduce the risk of late stage compliance issues which could save significant development costs (Q5).

[3] An example: a GA-VA pairing is considered compatible to a tolerance of 30 mm offset from the centre. If the GA-VA design were scaled up three times, the offset tolerance is now 90 mm using the independence property.

References

Abbott, M. D. (2018a) 'PostProcessing_MATLAB'. GitHub.

Abbott, M. D. (2018b) 'TestRigControl_MATLAB'. GitHub.

Abbott, M. D., Yang, C. P. and Jennings, P. A. (2017) 'Investigation of the Interoperability of a Dynamic WPT Pickup with Multiple Source Track Designs', in *2017 IEEE Vehicle Power and Propulsion Conference (VPPC)*.

Aldhaher, S., Luk, P. C.-K. and Whidborne, J. F. (2014) 'Electronic Tuning of Misaligned Coils in Wireless Power Transfer Systems', *IEEE Transactions on Power Electronics*, 29(11), pp. 5975–5982. doi: 10.1109/tpel.2014.2297993.

Armstrong, J. H. (2008) *The Railroad What It Is, What It Does*. 5th Editio. Edited by W. C. Vantuono. Simmons-Boardman Books, Inc.

Aspencore (2018) *Mutual Inductance of Two Adjacent Inductive Coils*. Available at: https://www.electronics-tutorials.ws/inductor/mutual-inductance.html (Accessed: 29 May 2018).

Automotive Council UK and Advanced Propulsion Centre UK (2017) 'Lightweight Vehicle and Powertrain Structures Roadmap - Presentation'. Available at: https://www.apcuk.co.uk/app/uploads/2018/02/LW_Full_Pack.pdf.

Babic, S. and Akyel, C. (2017) 'Calculation of mutual inductance and magnetic force between two thick coaxial Bitter coils of rectangular cross section', *IET Electric Power Applications*, 11(3), pp. 441–446. doi: 10.1049/iet-epa.2016.0628.

Babic, S., Salon, S. and Akyel, C. (2004) 'The mutual inductance of two thin coaxial disk coils in air', *IEEE Transactions on Magnetics*, 40(2 II), pp. 822–825. doi: 10.1109/TMAG.2004.824810.

Bandyopadhyay, S. *et al.* (2016) 'Multi-Objective Optimisation of a 1-kW Wireless IPT Systems for Charging of Electric vehicles'.

Bertoluzzo, M., Buja, G. and Dashora, H. (2019) 'Avoiding Null Power Point in DD coils', in *WIreless Power Week*.

Bertoluzzo, M., Buja, G. and Dashora, H. K. (2017) 'Design of DWC system track with unequal DD coil set', *IEEE Transactions on Transportation Electrification*, 7782(c), pp. 1–1. doi: 10.1109/TTE.2016.2646740.

Bi, Z. *et al.* (2016) 'A review of wireless power transfer for electric vehicles: Prospects to enhance

sustainable mobility', *Applied Energy*. Elsevier Ltd, 179, pp. 413–425. doi: 10.1016/j.apenergy.2016.07.003.

Birrell, S. A. *et al.* (2014) 'How driver behaviour and parking alignment affects inductive charging systems for electric vehicles', *Transportation Research Part C: Emerging Technologies*. Elsevier Ltd, 58, pp. 721–731. doi: 10.1016/j.trc.2015.04.011.

Bolger, J. G. (1978) 'INDUCTIVE POWER COUPLING FOR AN ELECTRIC HIGHWAY SYSTEM', in *28th IEEE Vehicular Technology Conference, Denver, CO, March 22-24,*. Denver.

Bolger, J. G. *et al.* (1978) *TESTS OF THE PERFORMANCE AND CHARACTERISTICS OFA PROTOTYPE INDUCTIVE POWER COUPLING FOR ELECTRIC HIGHWAY SYSTEMS*. Berkeley.

Bowdler, N. (2014) *Wirelessly charged electric buses set for Milton Keynes*, *BBC News*. Available at: http://www.bbc.co.uk/news/technology-25621426 (Accessed: 1 April 2016).

Boys, J. T. and Covic, G. A. (2013a) 'Inductive power transfer systems (IPT) Fact Sheet: No . 1 – Basic Concepts', *Https://Www.Qualcomm.Com/Documents/Inductive-Power-Transfer-Systems-Ipt-Fact-Sheet-No-1-Basic-Concepts*, (1).

Boys, J. T. and Covic, G. A. (2013b) *IPT Fact Sheet Series : No . 2 Magnetic Circuits for Powering Electric Vehicles*.

Boys, J. T. and Covic, G. A. (2015) 'The Inductive Power Transfer Story at the University of Auckland', *IEEE Circuits and Systems Magazine*, 15(2), pp. 6–27. doi: 10.1109/MCAS.2015.2418972.

Brook Lyndhurst Ltd. (2015) *Uptake of Ultra Low Emission Vehicles in the UK*.

Budhia, M. *et al.* (2013) 'Development of a single-sided flux magnetic coupler for electric vehicle IPT charging systems', *IEEE Transactions on Industrial Electronics*, 60(1). doi: 10.1109/TIE.2011.2179274.

Budhia, M., Covic, G. and Boys, J. (2010) 'A new IPT magnetic coupler for electric vehicle charging systems', *IECON Proceedings (Industrial Electronics Conference)*, pp. 2487–2492. doi: 10.1109/IECON.2010.5675350.

California PATH Program (1994) 'Roadway Powered Electric Vehicle Project Track Construction And Testing Program Phase 3D', *Traffic*. Available at: http://www.escholarship.org/uc/item/1jr98590.

Campi, T., Cruciani, S. and Feliziani, M. (2014) 'Magnetic Shielding of Wireless Power Transfer Systems', 10(1), pp. 422–425.

Carlson, R. W. and Normann, B. (2014) *Test Results of the PLUGLESS™ Inductive Charging System from*

Evatran Group, Inc. SAE Technical Paper.

Chan, H. (2000) 'A simplified Neumann's formula for calculation of inductance of spiral coil', *8th International Conference on Power Electronics and Variable Speed Drives*, 2000(475), pp. 69–73. doi: 10.1049/cp:20000222.

Choi, S Y *et al.* (2014) 'Asymmetric Coil Sets for Wireless Stationary EV Chargers With Large Lateral Tolerance by Dominant Field Analysis', *Ieee Transactions on Power Electronics*, 29(12), pp. 6406–6420. doi: 10.1109/tpel.2014.2305172.

Choi, Su Y. *et al.* (2014) 'Trends of Wireless Power Transfer Systems for Roadway Powered Electric Vehicles', in *2014 IEEE 79th Vehicular Technology Conference (VTC Spring)*. IEEE, pp. 1–5. doi: 10.1109/VTCSpring.2014.7023175.

Choi, Su Y. *et al.* (2015) 'Advances in Wireless Power Transfer Systems for Roadway-Powered Electric Vehicles', *IEEE Journal of Emerging and Selected Topics in Power Electronics*, 3(1), pp. 18–36. doi: 10.1109/JESTPE.2014.2343674.

Choi, Su Y *et al.* (2015) 'Ultraslim S-Type Power Supply Rails for Roadway-Powered Electric Vehicles', *IEEE Transactions on Power Electronics*, 30(11), pp. 6456–6468.

Cirimele, V., Freschi, F. and Mitolo, M. (2016) 'Inductive power transfer for automotive applications: State-of-the-art and future trends', *2016 IEEE Industry Applications Society Annual Meeting*, pp. 1–8. doi: 10.1109/IAS.2016.7731966.

Conductix-Wampfler GmbH (2013) 'Charging electric buses quickly and efficiently: bus stops fitted with modular components make "Charge & Go" simple to implement', *Press Release*, pp. 1–7.

Covic, G. a. and Boys, J. T. (2013) 'Modern Trends in Inductive Power Transfer for Transportation Applications', *IEEE Journal of Emerging and Selected Topics in Power Electronics*, 1(1), pp. 28–41. doi: 10.1109/JESTPE.2013.2264473.

Dai, J. and Ludois, D. C. (2015) 'A Survey of Wireless Power Transfer and a Critical Comparison of Inductive and Capacitive Coupling for Small Gap Applications', *IEEE Transactions on Power Electronics*, 30(11). doi: 10.1109/TPEL.2015.2415253.

Dashora, H. K. *et al.* (2017) 'Analysis and design of DD coupler for dynamic wireless charging of electric vehicles', *Journal of Electromagnetic Waves and Applications*. Taylor & Francis, 5071, pp. 1–20. doi: 10.1080/09205071.2017.1373036.

Degraeuwe, B. *et al.* (2017) 'Impact of passenger car NOX emissions on urban NO2 pollution – Scenario

analysis for 8 European cities', *Atmospheric Environment*. Elsevier, 171(2), pp. 330–337. doi: 10.1016/j.atmosenv.2017.10.040.

Dickson, T. (2013) 'Wireless Electrification', in *Eighth International Hydrail Conference*.

Diekhans, T. and De Doncker, R. W. (2015) 'A Dual-Side Controlled Inductive Power Transfer System Optimized for Large Coupling Factor Variations and Partial Load', *IEEE Transactions on Power Electronics*, 30(11), pp. 6320–6328. doi: 10.1109/TPEL.2015.2393912.

EE Times (2011) *Qualcomm acquires wireless EV charging firm | EE Times*, *EE Times*. Available at: http://www.eetimes.com/document.asp?doc_id=1260563 (Accessed: 16 February 2015).

FABRIC Consortium (2014) *Fabric*. Available at: http://www.fabric-project.eu/ (Accessed: 28 January 2016).

FABRIC Consortium (2015) *Interoperability considerations*.

Ford UK (2018) *Ford EcoBoost Engine Technology*. Available at: https://www.ford.co.uk/shop/research/technology/performance-and-efficiency/ford-ecoboost (Accessed: 16 August 2018).

Guo, Y. *et al.* (2016) 'Switch-On Modeling and Analysis of Dynamic Wireless Charging System Used', *Ieee Transactions on Industrial Electronics*, 63(10), pp. 6568–6579.

Ibrahim, M. *et al.* (2016) 'Inductive Charger for Electric Vehicle: Advanced Modeling and Interoperability Analysis', *IEEE Transactions on Power Electronics*, 31(12), pp. 8096–8114. doi: 10.1109/TPEL.2016.2516344.

International Commission on Non-Ionizing Radiation Protection (1998) 'ICNIRP Guidelines for Limiting Exposure To Time-Varying Guidelines for Limiting Exposure To Time-Varying Electric, Magnetic and Electromagnetic fields', *Health Physics*, 74, p. 494-522. doi: 10.1097/HP.0b013e3181f06c86.

International Commission on Non-Ionizing Radiation Protection (2010) 'ICNIRP STATEMENT — GUIDELINES FOR LIMITING EXPOSURE TO TIME-VARYING ELECTRIC AND MAGNETIC FIELDS (1 HZ TO 100 KHZ)', *Health Physics*, 99(6), pp. 818–836. doi: 10.1097/HP.0b013e3181f06c86.

INTIS GmbH (2016a) *INTIS - Integrated Infrastructure Solutions*. Available at: http://www.intis.de/intis/mobility.html (Accessed: 22 June 2016).

INTIS GmbH (2016b) 'Presenting a test centre for electric vehicle inductive energy transfer systems', pp. 1–4.

INTIS GmbH (2016c) 'The Future is Wireless'.

INTIS GmbH (2016d) 'The Future is Wireless Wireless Power 30 kW coil system for stationary charging VW T5 Transporter A conversion to electric drive and inductive charging , carried out by INTIS'.

Jones, P. T. and Onar, O. (2014) 'Impact of Wireless Power Transfer in transportation: Future transportation enabler, or near term distraction', in *2014 IEEE International Electric Vehicle Conference (IEVC)*. IEEE, pp. 1–7. doi: 10.1109/IEVC.2014.7056203.

Joy, E. R., Dalal, A. and Kumar, P. (2014) 'Accurate computation of mutual inductance of two air core square coils with lateral and angular misalignments in a flat planar surface', *IEEE Transactions on Magnetics*, 50(1). doi: 10.1109/TMAG.2013.2279130.

Kalwar, K. A., Aamir, M. and Mekhilef, S. (2015) 'Inductively coupled power transfer (ICPT) for electric vehicle charging - A review', *Renewable and Sustainable Energy Reviews*. Elsevier, 47, pp. 462–475. doi: 10.1016/j.rser.2015.03.040.

Kamineni, A. *et al.* (2015) 'Analysis of Coplanar Intermediate Coil Structures in Inductive Power Transfer Systems', *IEEE Transactions on Power Electronics*, 30(11), pp. 6141–6154.

Kamineni, A., Covic, G. A. and Boys, J. T. (2016) 'Self-Tuning Power Supply for Inductive Charging', *IEEE Transactions on Power Electronics*, XX(X), pp. 1–1. doi: 10.1109/TPEL.2016.2590571.

Kim, S. *et al.* (2014) 'Tripolar Pad for Inductive Power Transfer Systems', 8993(c), pp. 3066–3072. doi: 10.1109/TPEL.2016.2606893.

Lee, H. and Cho, D. H. (2015) 'Economic Analysis Based on the Interrelationships of the OLEV System Components', *2015 IEEE 18th International Conference on Intelligent Transportation Systems*, pp. 2677–2682. doi: 10.1109/ITSC.2015.430.

Lin, F. Y., Covic, G. A. and Boys, J. T. (2015) 'Evaluation of Magnetic Pad Sizes and Topologies for Electric Vehicle Charging', *IEEE Transactions on Power Electronics*, 30(11), pp. 6391–6407.

Lin, F. Y., Covic, G. A. and Boys, J. T. (2016) 'Leakage flux control of mismatched IPT systems', *IEEE Transactions on Transportation Electrification*, 7782(c), pp. 1–1. doi: 10.1109/TTE.2016.2630922.

Machura, P. and Li, Q. (2019) 'A critical review on wireless charging for electric vehicles', *Renewable and Sustainable Energy Reviews*. Elsevier Ltd, 104(May 2018), pp. 209–234. doi: 10.1016/j.rser.2019.01.027.

Maykuth, A. (2018) *Malvern start-up imagines a world where electric vehicles are recharged wirelessly*, *The Inquirer Philly.com*. Available at: http://www.philly.com/philly/business/energy/malvern-startup-

imagines-a-world-where-electric-vehicles-are-recharged-wirelessly-20180427.html?arc404=true (Accessed: 13 August 2018).

McDonough, M. and Fahimi, B. (2012) 'A study on the effects of motion in inductively coupled vehicular charging applications', *2012 IEEE Transportation Electrification Conference and Expo, ITEC 2012*. doi: 10.1109/ITEC.2012.6243467.

Miller, J. and Daga, A. (2015) 'Elements of Wireless Power Transfer Essential to High Power Charging of Heavy Duty Vehicles', *IEEE Transactions on Transportation Electrification*, 7782(c), pp. 1–1. doi: 10.1109/TTE.2015.2426500.

Miller, J. M. *et al.* (2015) 'ORNL Experience and Challenges Facing Dynamic Wireless Power Charging of EV's', *IEEE Circuits and Systems Magazine*, 15(2), pp. 40–53. doi: 10.1109/MCAS.2015.2419012.

Miller, J. M. *et al.* (2016) 'The WPT Dilemma - High K or High Q?', in *2016 IEEE PELS Workshop on Emerging Technologies: Wireless Power Transfer (WoW)*.

Miller, J. M. *et al.* (2017) 'Electric Fuel Pumps for Wireless Power Transfer', *IEEE POWER ELECTRONICS MAGAZINE*, pp. 24–35.

Miller, J. M. and Chinthavali, M. (2014) 'ORNL Developments in Stationary and Dynamic Wireless Charging Applications'.

Mock, P. (2014) *EU CO2 standards for passenger cars and light-commercial vehicles*, *ICCT*. Available at: http://www.theicct.org/eu-co2-standards-passenger-cars-and-lcvs.

Mohamed, A. A. S. and Mohammed, O. (2018) 'Physics-based co-simulation platform with analytical and experimental verification for bidirectional IPT system in EV applications', *IEEE Transactions on Vehicular Technology*, 67(1), pp. 275–284. doi: 10.1109/TVT.2017.2763422.

Momentum Dynamics Corporation (no date) *Shift to Electric Transit Buses Continues as Momentum Dynamics Installs America's Second 200 kW Wireless Charging System*, *CISON*. Available at: https://www.prnewswire.com/news-releases/shift-to-electric-transit-buses-continues-as-momentum-dynamics-installs-americas-second-200-kw-wireless-charging-system-300677782.html (Accessed: 30 July 2018).

Naberezhnykh, D. *et al.* (2014) 'Operational requirements for dynamic wireless power transfer systems for electric vehicles', in *2014 IEEE International Electric Vehicle Conference (IEVC)*. IEEE, pp. 1–8. doi: 10.1109/IEVC.2014.7056236.

Ning, P. *et al.* (2013) 'A compact wireless charging system development', *Conference Proceedings -*

IEEE Applied Power Electronics Conference and Exposition - APEC, pp. 3045–3050. doi: 10.1109/APEC.2013.6520733.

Obayashi, S. and Ev, P. (2014) 'EMC Issues on Wireless Power Transfer', pp. 601–604.

Park, C. *et al.* (2015) 'Uniform Power I-Type Inductive Power Transfer System With DQ -Power Supply Rails for On-Line Electric Vehicles', *IEEE TRANSACTIONS ON POWER ELECTRONICS*, 30(11), pp. 6446–6455.

Patil, D. *et al.* (2017) 'Wireless Power Transfer for Vehicular Applications: Overview and Challenges', *IEEE Transactions on Transportation Electrification*, 4(1), pp. 1–1. doi: 10.1109/TTE.2017.2780627.

Patrick McGee (2018) *Bosch claims breakthrough in cleaning up diesel fuel*, *Financial Times*. Available at: https://www.ft.com/content/95d990c8-4887-11e8-8ee8-cae73aab7ccb (Accessed: 16 August 2018).

Plugless (2016) *Tech Specs - Gen 2 | Plugless Power*. Available at: https://www.pluglesspower.com/gen2-tech-specs/ (Accessed: 15 December 2016).

Plugless Power (2017) *Corded Charging Problems*, *Plugless Power Blog*. Available at: https://www.pluglesspower.com/learn/corded-charging-problems/ (Accessed: 16 August 2018).

Prasanth, V. and Bauer, P. (2013) 'Study of misalignment for on Road Charging', *2013 IEEE Transportation Electrification Conference and Expo: Components, Systems, and Power Electronics - From Technology to Business and Public Policy, ITEC 2013*, (1). doi: 10.1109/ITEC.2013.6573478.

Prasanth, V. and Bauer, P. (2014) 'Distributed IPT Systems for Dynamic Powering: Misalignment Analysis', *Ieee Transactions on Industrial Electronics*, 61(11), pp. 6013–6021. doi: 10.1109/tie.2014.2311380.

Prasanth, V., Bauer, P. and Ferreira, J. A. (2015) 'A Sectional Matrix Method for IPT Coil Shape Optimization', (1), pp. 1684–1691.

Qualcomm (2012) *Qualcomm Halo: Frequently Asked Questions*.

Rakouth, H. *et al.* (2013) 'EV Charging Through Wireless Power Transfer: Analysis of Efficiency Optimization and Technology Trends', in *Proceedings of the FISITA 2012 World Automotive Congress*. Springer Berlin Heidelberg, pp. 871–884. doi: 10.1007/978-3-642-33741-3_14.

Rim, C. T. (2014) 'The R & D History of On-Line Electric Vehicles (OLEV) - Presentation', in.

Rim, C. T. and Mi, C. (2017) 'History of RPEVs □ . □ Introduction'.

SAE International (2016) *Surface Vehicle Information Report - J2954 - May 2016*.

SAE International (2017) *Surface Vehicle Information Report - J2954 - November 2017*.

Schneider, J. (2012) *SAE J2954 OVERVIEW AND PATH FORWARD :* Available at: http://www.sae.org/smartgrid/sae-j2954-status_1-2012.pdf.

Sorrentino, G. (2014) *Wireless Charging : What is the Future ?*

Suh, I. S. (2015) *Wireless Charging Technology and the Future of Electric Transportation*.

Suh, I. S. and Kim, J. (2013) 'Electric vehicle on-road dynamic charging system with wireless power transfer technology', *Proceedings of the 2013 IEEE International Electric Machines and Drives Conference, IEMDC 2013*, pp. 234–240. doi: 10.1109/IEMDC.2013.6556258.

Tavakoli, R. and Pantic, Z. (2017) 'Analysis, Design and Demonstration of a 25-kW Dynamic Wireless Charging System for Roadway Electric Vehicles', *IEEE Journal of Emerging and Selected Topics in Power Electronics*, 6777(c), pp. 1–16. doi: 10.1109/JESTPE.2017.2761763.

Technology, I. (2018) *IPT Charge*.

TechRadar (2018) *BMW is making a massive charging pad for its electric cars | TechRadar*. Available at: https://www.techradar.com/news/bmw-is-making-a-massive-charging-pad-for-its-electric-cars (Accessed: 21 May 2018).

Tejeda, A. *et al.* (2016) 'Core-less Circular Pad with Controlled Flux Cancellation for EV Wireless Charging', *IEEE Transactions on Power Electronics*, 8993(c), pp. 1–1. doi: 10.1109/TPEL.2016.2642192.

Thai, V. X. *et al.* (2015) 'Coreless Power Supply Rails Compatible with Both Stationary and Dynamic Charging of Electric Vehicles'.

Transport Research Laboratory (2015) *Feasibility study : Powering electric vehicles on England ' s major roads*.

UNPLUGGED Project (2014) *Deliverable D2.3 – Interoperability WP2*.

UNPLUGGED Project (2016) *UNPLUGGED: The Project*. Available at: http://unplugged-project.eu/wordpress/?page_id=44 (Accessed: 31 March 2016).

ZABER (2018) *X-LHM-E Series: Motorized linear stages with built-in controllers and motor encoders*.

Zaheer, A. *et al.* (2015) 'Investigation of multiple decoupled coil primary pad topologies in lumped IPT systems for interoperable electric vehicle charging', *IEEE Transactions on Power Electronics*, 30(4), pp. 1937–1955. doi: 10.1109/TPEL.2014.2329693.

Zaheer, A. *et al.* (2016) 'A Dynamic EV Charging System for Slow Moving Traffic Applications', *IEEE Transactions on Transportation Electrification*, 7782(c), pp. 1–1. doi: 10.1109/TTE.2016.2628796.

Zaheer, A. *et al.* (2017) 'A Dynamic EV Charging System for Slow Moving Traffic Applications', *IEEE Transactions on Transportation Electrification*, 3(2), pp. 354–369. doi: 10.1109/TTE.2016.2628796.

Zell, C. E. and Bolger, J. G. (1982) 'Development of an engineering prototype of a roadway powered electric transit vehicle system: A public/private sector program', *Vehicular Technology Conference, 1982. 32nd IEEE*, 32, pp. 35–38. doi: 10.1109/VTC.1982.1623054.

Zhang, W. *et al.* (2015) 'Loosely Coupled Transformer Structure and Interoperability Study for EV Wireless Charging Systems', *IEEE Transactions on Power Electronics*, 30(11). doi: 10.1109/TPEL.2015.2433678.

Zhang, X. *et al.* (2016) 'Coil Design and Efficiency Analysis for Dynamic Wireless Charging System for Electric Vehicles', *IEEE Transactions on Magnetics*, 9464(c), pp. 1–1. doi: 10.1109/TMAG.2016.2529682.

Zhao, L. and Mieee, S. (2017) 'A Hybrid Wireless Charging System with DDQ Pads for Dynamic Charging of EVs'.

Zhu, Q. *et al.* (2016) 'Applying LCC Compensation Network to Dynamic Wireless EV Charging System', *IEEE Transactions on Industrial Electronics*, 0046(c), pp. 1–1. doi: 10.1109/TIE.2016.2529561.